

Integrated Chemical Effects Test Project: Test #3 Data Report

Los Alamos National Laboratory

**U.S. Nuclear Regulatory Commission
Office of Nuclear Regulatory Research
Washington, DC 20555-0001**



Integrated Chemical Effects Test Project: Test #3 Data Report

Manuscript Completed: September 2005
Date Published: October 2005

Principal Investigator: Jack Dallman

Prepared by
J. Dallman, B. Letellier, J. Garcia, J. Madrid, W. Roesch
Los Alamos National Laboratory
Los Alamos, NM 87545

D. Chen, K. Howe
University of New Mexico

L. Archuleta, F. Sciacca
OMICRON

B. P. Jain, NRC Project Manager

Prepared for
Division of Engineering Technology
Office of Nuclear Regulatory Research
U.S. Nuclear Regulatory Commission
Washington, DC 20555-0001



INTEGRATED CHEMICAL EFFECTS TEST PROJECT: TEST #3 DATA REPORT

ABSTRACT

A 30-day test was conducted in the Integrated Chemical Effects Test (ICET) project test apparatus. The test simulated the chemical environment present inside a pressurized water reactor containment water pool after a loss-of-coolant-accident. The initial chemical environment contained 14.54 kg of boric acid and 0.663 g of lithium hydroxide. Trisodium phosphate (3.786 kg), hydrochloric acid (211 mL), and additional boric acid (600 g) were added beginning at 30 minutes and lasting until 4 hours into the test. The test was conducted for 30 days at a constant temperature of 60°C (140°F). The materials tested within this environment included representative amounts of submerged and unsubmerged aluminum, copper, concrete, zinc, carbon steel, and insulation samples (80% calcium silicate and 20% fiberglass). Representative amounts of concrete dust and latent debris were also added to the test solution. Water was circulated through the bottom portion of the test chamber during the entire test to achieve representative flow rates over the submerged specimens. The test solution reached a pH of 7.9 by Day 3, and the test solution turbidity decreased to less than 1 NTU after 24 hours. During the introduction of trisodium phosphate at the beginning of the test, a white flocculence was observed through the submerged observation window. This flocculence was accompanied by a rise in turbidity and total suspended solids (TSS). Turbidity and TSS dropped after chemical addition was complete, and the white flocculence was no longer visible in the water after the first day. Observations of the test solution indicated similar behavior of the solution at both room temperature and test temperature. After the initial flocculence had settled out of solution, no chemical byproducts were visible in the water and no precipitation occurred as samples cooled from test temperature to room temperature. Large amounts of white deposits of varying size were observed on the submerged galvanized steel, aluminum, copper, and inorganic zinc coated steel coupons. The bottom of the tank was filled with sediment that had a pinkish-white deposit on top. The test solution remained clearly Newtonian for the entire test. Aluminum was detectable in the solution, but only in trace amounts.

CONTENTS

ABSTRACT.....	i
EXECUTIVE SUMMARY	x
ACKNOWLEDGMENTS	xii
ACRONYMS AND ABBREVIATIONS	xiii
1 INTRODUCTION	1
1.1. Objective and Test Conditions.....	1
1.2. Information Presented in This Report.....	2
2 TEST PROCEDURES	3
2.1 Chemical Test Apparatus Functional Description	3
2.2 Pre-Test Preparation.....	4
2.2.1. Test Loop Cleaning.....	4
2.2.2. Test Coupons and Samples	5
2.2.3. Quality Assurance Program	10
2.2.4. Test Parameters.....	10
2.3 Test Operation.....	12
2.3.1. Description.....	12
2.3.2 Process Control	13
2.4 Analytical Methods.....	13
2.4.1. Data Compilation and Nomenclature.....	13
3 TEST RESULTS.....	21
3.1 General Observations.....	21
3.1.1. Control of Test Parameters	22
3.1.2. Hydrogen Generation.....	24
3.2 Water Samples	25
3.2.1. Wet Chemistry	25
3.2.2. Metal Ion Concentration	28
3.2.3. Optical/TEM Images from Filtered and Unfiltered Samples.....	33
3.3 Insulation.....	33
3.3.1 Deposits in Fiberglass Samples	33
3.3.2 Calcium Silicate Samples	70
3.4 Metallic and Concrete Samples	70
3.4.1 Weights and Visual Descriptions.....	70
3.4.2 SEM Analyses.....	80
3.5 Sedimentation	81
3.6 Precipitates.....	87
3.7 Corrosion Products.....	87
3.8 Gel Analysis.....	89
3.8.1 Visual Description	89
3.8.2 ESEM and SEM/EDS Analyses.....	90
4 SUMMARY OF KEY OBSERVATIONS	97
REFERENCES	98

Appendices

- Appendix A SEM and ESEM/EDS Data for Test #3 Day-4 Fiberglass in Low-Flow Zone
- Appendix B ESEM and SEM Day-15 Fiberglass
 - B1. ESEM/EDS and SEM/EDS Data for Test #3 Day-15 Fiberglass in High-Flow Zones
 - B2. ESEM/EDS and SEM/EDS Data for Test #3 Day-15 Fiberglass in Low-Flow Zones
- Appendix C ESEM and SEM Day-30 Fiberglass
 - C1. ESEM/EDS Data for Test #3 Day-30 Fiberglass in High-Flow Zones
 - C2. ESEM Data for Test #3 Day-30 Fiberglass in Low-Flow Zones
 - C3. ESEM/EDS Data for Test #3 Day-30 Drain Collar Fiberglass
 - C4. SEM/EDS and ESEM/EDS Data for Test #3 Day-30 Birdcage Fiberglass
- Appendix D ESEM and SEM/EDS Data for Test #3 Day-30 Corrosion Products
- Appendix E SEM Day-30 Coupons
 - E1. SEM/EDS Data for Test #3 Day-30 Aluminum Coupons
 - E2. SEM/EDS Data for Test #3 Day-30 Copper Coupons
 - E3. SEM/EDS Data for Test #3 Day-30 Galvanized Steel Coupons
 - E4. SEM/EDS Data for Test #3 Day-30 Steel Coupons
- Appendix F SEM/EDS Data for Test #3 Day-30 Flow Meter
- Appendix G SEM/EDS and ESEM/EDS Data for Test #3 Day-30 Gel
- Appendix H SEM/EDS and ESEM/EDS Data for Test #3 Day-30 Cal-sil
- Appendix I ESEM/EDS Data for Test #3 Day-30 Sediment
- Appendix J TEM Data for Test #3 Solution Samples
- Appendix K UV Absorbance Spectrum – Day-30 Solution Samples
- Appendix L ICET Test #3: Pre-Test, Test, and Post-Test Project Instructions

FIGURES

Figure 2-1. Test loop process flow diagram.	4
Figure 2-2. Coupon rack configuration in the ICET tank. The blue line represents the surface of the test solution.	6
Figure 2-3. A loaded coupon rack in the ICET tank.	7
Figure 2-4. Fiberglass samples attached to coupon rack.	8
Figure 2-5. Solid pieces of cal-sil samples in SS mesh.	9
Figure 2-6. Cal-sil dust.	9
Figure 3-1. In-line pH measurements.	23
Figure 3-2. Bench-top pH meter results.	24
Figure 3-3. Hydrogen generation.	24
Figure 3-4. Day 1 turbidity results.	25
Figure 3-5. Daily turbidity results.	26
Figure 3-6. Test #3 TSS results.	27
Figure 3-7. Viscosity at 60°C and 23°C.	28
Figure 3-8. Aluminum concentration.	29
Figure 3-9. Calcium concentration.	29
Figure 3-10. Copper concentration.	30
Figure 3-11. Iron concentration.	30
Figure 3-12. Magnesium concentration.	31
Figure 3-13. Silica concentration.	31
Figure 3-14. Sodium concentration.	32
Figure 3-15. Zinc concentration.	32
Figure 3-16. Phosphate concentration.	33
Figure 3-17. ESEM image of a Test #3 Day 4 low-flow exterior fiberglass sample, magnified 150 times. (T3D4FX1, 4/12/05)	36
Figure 3-18. ESEM image for a Test #3 Day 4 low-flow exterior fiberglass sample, magnified 1000 times. (T3D4FX2, 4/12/05)	36
Figure 3-19. EDS counting spectrum (after calibration) for the deposits between the fibers on the ESEM image shown in Figure 3-18. (T3D4FX4, 4/12/05)	37
Figure 3-20. SEM image of a Test #3 Day 4 low-flow exterior fiberglass sample, magnified 150 times. (T3D4FibGlsEX001, 4/12/05)	37
Figure 3-21. SEM image of a Test #3 Day 4 low-flow exterior fiberglass sample, magnified 300 times. (T3D4FibGlsEX003, 4/12/05)	38
Figure 3-22. ESEM image of a Test #3 Day 4 low-flow interior fiberglass sample, magnified 150 times. (T3D4FI6, 4/12/05)	38
Figure 3-23. ESEM image of a Test #3 Day 4 low-flow interior fiberglass sample, magnified 1000 times. (T3D4FI7, 4/12/05)	39

Figure 3-24. EDS counting spectrum (after calibration) for the deposits between the fibers on the ESEM image shown in Figure 3-23. (T3D4FI8, 4/12/05) 39

Figure 3-25. SEM image of a Test #3 Day 4 low-flow interior fiberglass sample, magnified 50 times. (T3D4FibGlsIN001, 4/12/05) 40

Figure 3-26. SEM image for a Test #3 Day 4 low-flow interior fiberglass sample, magnified 150 times. (T3D4FibGlsIN002, 4/12/05) 40

Figure 3-27. SEM image of a Test #3 Day 4 low-flow interior fiberglass sample, magnified 400 times. (T3D4FibGlsIN003, 4/12/05) 41

Figure 3-28. ESEM image of a Test #3 Day 15 low-flow exterior fiberglass sample, magnified 110 times. (T3D15LX9) 42

Figure 3-29. ESEM image of a Test #3 Day 15 low-flow exterior fiberglass sample, magnified 1000 times. (T3D15LX0) 42

Figure 3-30. EDS counting spectrum for the deposits between the fibers on the ESEM image shown in Figure 3-29. (T3D15LXD)..... 43

Figure 3-31. SEM image of a Test #3 Day 15 low-flow exterior fiberglass sample, magnified 100 times. (T3D15LowFlowExt011)..... 43

Figure 3-32. SEM image of a Test #3 Day 15 low-flow exterior fiberglass sample, magnified 1000 times. (T3D15LowFlowExt013)..... 44

Figure 3-33. EDS counting spectrum for the flocculent deposits between the fibers on the SEM image shown in Figure 3-32. (T3D15LowFlowExtEDS3)..... 44

Figure 3-34. ESEM image of a Test #3 Day 15 low-flow interior fiberglass sample, magnified 100 times. (T3D15LI6)..... 45

Figure 3-35. ESEM image of a Test# 3 Day 15 low-flow interior fiberglass sample, magnified 1000 times. (T3D15LI8)..... 45

Figure 3-36. EDS counting spectrum for the flocculent deposits between the fibers on the ESEM image shown in Figure 3-35. (T3D15LIC) 46

Figure 3-37. SEM image of a Test #3 Day 15 low-flow interior fiberglass sample, magnified 100 times. (T3D15LowFlowInt008)..... 46

Figure 3-38. SEM image of a Test #3 Day 15 low-flow interior fiberglass sample, magnified 1000 times. (T3D15LowFlowInt010)..... 47

Figure 3-39. ESEM image of a Test #3 Day 15 high-flow exterior fiberglass sample, magnified 110 times. (T3D15HX4, 4/22/05)..... 48

Figure 3-40. ESEM image of a Test #3 Day 15 high-flow exterior fiberglass sample, magnified 1000 times. (T3D15HX5, 4/22/05)..... 48

Figure 3-41. EDS counting spectrum for the deposits between the fibers on the ESEM image shown in Figure 3-40. (T3D15HIB, 4/22/05) 49

Figure 3-42. SEM image of a Test #3 Day 15 high-flow exterior fiberglass sample, magnified 100 times. (T3D15HiFlowExt005, 4/22/05) 49

Figure 3-43. SEM image of a Test #3 Day 15 high-flow exterior fiberglass sample, magnified 500 times. (T3D15HiFlowExt007, 4/22/05) 50

Figure 3-44. EDS counting spectrum for the flocculent deposits between the fibers on the SEM image shown in Figure 3-43. (T3D15HiFlowExtEDS2, 4//22/05)..... 50

Figure 3-45. ESEM image of a Test #3 Day 15 high-flow interior fiberglass sample, magnified 100 times. (T3D15HI1, 4/22/05) 51

Figure 3-46. ESEM image of a Test #3 Day 15 high-flow interior fiberglass sample, magnified 2000 times. (T3D15HI3, 4/22/05) 51

Figure 3-47. EDS counting spectrum for the flocculent deposits between the fibers on the ESEM image shown in Figure 3-46. (T3D15HIA, 4/22/05)..... 52

Figure 3-48. SEM image of a Test #3 Day 15 high-flow interior fiberglass sample, magnified 100 times. (T3D15HIFlowInt002, 4/22/05)..... 52

Figure 3-49. SEM image of a Test #3 Day 15 high-flow interior fiberglass sample, magnified 1000 times. (T3D15HIFlowInt004, 4/22/05)..... 53

Figure 3-50. EDS counting spectrum for the flocculent deposits between the fibers on the SEM image shown in Figure 3-49. (T3D15HiFlowIntEDS1, 4/22/05)..... 53

Figure 3-51. ESEM image of a Test #3 Day 30 exterior low-flow fiberglass sample, magnified 70 times. (t3lfex09, 5/6/05) 54

Figure 3-52. ESEM image of a Test #3 Day 30 exterior low-low fiberglass sample, magnified 1000 times. (t3lfex11, 5/6/05) 54

Figure 3-53. ESEM image of a Test #3 Day 30 interior low-flow fiberglass sample, magnified 70 times. (t3lfin12, 5/6/05) 55

Figure 3-54. ESEM image of a Test #3 Day 30 interior low-flow fiberglass sample, magnified 1000 times. (t3lfin13, 5/6/05) 55

Figure 3-55. ESEM image of a Test #3 Day 30 exterior high- flow fiberglass sample, magnified 100 times. (t3hifx33, 5/11/05) 56

Figure 3-56. EDS counting spectrum for the large masses of particulate deposits shown in Figure 3-55. (t3hifx34, 5/11/05) 57

Figure 3-57. ESEM image of a Test #3 Day 30 exterior high-flow fiberglass sample, magnified 600 times. (t3hifx35, 5/11/05) 57

Figure 3-58. ESEM image of a Test #3 Day 30 interior high-flow fiberglass sample, magnified 100 times. (T3HiFI36, 5/11/05)..... 58

Figure 3-59. ESEM image of a Test #3 Day 30 interior high-flow fiberglass sample, magnified 1000 times. (t3hifi37, 5/11/05) 58

Figure 3-60. Drain screen collar removed from the tank..... 59

Figure 3-61. ESEM image of a Test #3 Day 30 exterior fiberglass sample on the drain collar (away from the drain screen), magnified 100 times. (t3dcex25, 5/6/05) 60

Figure 3-62. ESEM image of a Test #3 Day 30 exterior fiberglass sample on the drain collar (away from the drain screen, magnified 1000 times. (t3dcex21, 5/6/05) 60

Figure 3-63. EDS counting spectrum for the light particulate deposits (EDS1) shown in Figure 3-62. (t3dcex22, 5/6/05) 61

Figure 3-64. EDS counting spectrum for the dark deposits (EDS2) shown in Figure 3-62. (t3dcex23, 5/6/05) 61

Figure 3-65. Comparison of EDS counting spectra between Figure 3-63 (yellow) and Figure 3-64 (red). (t3dcex24, 5/6/05) 62

Figure 3-66. ESEM image of a Test #3 Day 30 exterior fiberglass sample on the drain collar (adjacent to the drain screen, magnified 100 times. (t3DCSC16, 5/6/05) 62

Figure 3-67. ESEM image of a Test #3 Day 30 exterior fiberglass sample on the drain collar (adjacent to the drain screen, magnified 1000 times. (t3dcsc17, 5/6/05) 63

Figure 3-68. EDS counting spectrum for the particulate deposits shown in Figure 3-67. (t3dcsc18, 5/6/05) 63

Figure 3-69. ESEM image of a Test #3 Day 30 interior fiberglass sample on the drain collar, magnified 100 times. (t3dcin28, 5/6/05)..... 64

Figure 3-70. ESEM image of a Test #3 Day 30 interior fiberglass sample on the drain collar, magnified 1000 times. (t3dcin27, 5/6/05)..... 64

Figure 3-71. Tank bottom after the test fluid was drained..... 65

Figure 3-72. ESEM image of a Test #3 Day 30 exterior fiberglass sample within the birdcage, magnified 80 times. (T3BCEX01, 5/6/05) 66

Figure 3-73. EDS counting spectrum for the large deposits shown in Figure 3-72. (t3bcexe2, 5/6/05) 66

Figure 3-74. ESEM image of a Test #3 Day 30 exterior fiberglass sample within the birdcage, magnified 80 times. (t3bcex02, 5/6/05) 67

Figure 3-75. ESEM image of a Test #3 Day 30 exterior fiberglass sample within the birdcage, magnified 500 times. (t3bcex03, 5/6/05) 67

Figure 3-76. EDS counting spectrum for the deposits shown in Figure 3-75. (T3BCExE1, 5/6/05) 68

Figure 3-77. Comparison of EDS counting spectra of Figure 3-76 (red) and Figure 3-73 (yellow). (t3bcexe3, 5/6/05)..... 68

Figure 3-78. ESEM image of a Test #3 Day 30 interior fiberglass sample within the birdcage, magnified 80 times. (t3bcin05, 5/6/05) 69

Figure 3-79. ESEM image of a Test #3 Day 30 interior fiberglass sample within the birdcage, magnified 1000 times. (t3bcin07, 5/6/05) 69

Figure 3-80. Al-155, submerged, pre-test 71

Figure 3-81. Al-155, submerged, post-test. 71

Figure 3-82. Al-156, submerged, pre-test. 71

Figure 3-83. Al-156 submerged, post-test. 71

Figure 3-84. Al-157, submerged, pre-test. 72

Figure 3-85. Al-157, submerged, post-test. 72

Figure 3-86. GS-468, submerged, pre-test. 72

Figure 3-87. GS-468, submerged, post-test. 72

Figure 3-88. IOZ-156, submerged, pre-test. 73

Figure 3-89. IOZ-156, submerged, post-test. 73

Figure 3-90. CU-207 submerged, pre-test. 74

Figure 3-91. CU-207, submerged, post-test. 74

Figure 3-92. CU-225, submerged, pre-test. 74

Figure 3-93. CU-225, submerged, post-test. 74

Figure 3-94. US-11, submerged, pre-test. 75

Figure 3-95. US-11, submerged, post-test. 75

Figure 3-96. Conc-005, submerged, pre-test. 75

Figure 3-97. Conc-005, submerged, post-test. 75

Figure 3-98. Al-159, unsubmerged, pre-test. 77

Figure 3-99. Al-159, unsubmerged, post-test. 77

Figure 3-100. GS-503, unsubmerged, pre-test. 77

Figure 3-101. GS-503, unsubmerged, post-test. 77

Figure 3-102. CU-228, unsubmerged, pre-test. 78

Figure 3-103. CU-228 unsubmerged, post-test. 78

Figure 3-104. IOZ-187, unsubmerged, pre-test. 78

Figure 3-105. IOZ-187, unsubmerged, post-test. 78

Figure 3-106. US-13, unsubmerged, pre-test. 79

Figure 3-107. US-13, unsubmerged, post-test. 79

Figure 3-108. Sediment removed from the tank. Some gel appears on the top..... 82

Figure 3-109. Samples removed from tank bottom 82

Figure 3-110. ESEM image of a Test #3 Day 30 pink sediment, magnified 100 times
(t3pnkp31, 5/6/05)..... 83

Figure 3-111. ESEM image of a Test #3 Day 30 pink sediment, magnified 1000 times.
(t3PNKP29, 5/6/05) 83

Figure 3-112. EDS counting spectrum for the sediment shown in Figure 3-111.
(t3pnkp30, 5/6/05)..... 84

Figure 3-113. ESEM image of a Test #3 Day 30 yellow sediment, magnified 100 times.
(t3ylwp33, 5/6/05)..... 84

Figure 3-114. ESEM image of a Test #3 Day 30 yellow sediment, magnified 100 times.
(t3ylwp34, 5/6/05)..... 85

Figure 3-115. EDS counting spectrum for the particles shown in Figure 3-114.
(t3ylwp35, 5/6/05)..... 85

Figure 3-116. Comparison of EDS counting spectra for pink sediment
(yellow, t3pnkp30) and yellow sediment (red, t3ylwp35). (t3ylwp36, 5/6/05)..... 86

Figure 3-117. XRD results for Test-#3 Day 30 mixed sediment. 86

Figure 3-118. Gel-like material covering stainless steel mesh on the bottom
of the test tank. 89

Figure 3-119. Gel-like material recovered from the bottom of the test tank. 90

Figure 3-120. SEM image of a Test #3 Day 30 white gel-like material from the top
of the birdcage, magnified 100 times. (T3D30GelMaterial003, 5/9/05) 91

Figure 3-121. SEM image of a Test #3 Day 30 white gel-like material from the top of the
birdcage, magnified 1000 times. (T3D30GelMaterial004, 5/9/05) 92

Figure 3-122. EDS counting spectrum for the white gel-like material (whole image) shown in Figure 3-121. (T3D30Gel02, 5/9/05)..... 92

Figure 3-123. ESEM image of a Test #3 Day 30 white gel-like material from the top of the birdcage, magnified 1000 times. (t3Gel08, 5/6/05)..... 94

Figure 3-124. Another EDS counting spectrum for the white gel-like material shown in Figure 3-123. (t3geled6, 5/6/05)..... 94

Figure 3-125. Comparison of EDS counting spectra for Figure 124 (yellow: the gel-like materials shown in Figure 3-123) and Figure 3-73 (red: the large deposits taken from the birdcage exterior shown in Figure 3-72). (t3geled7, 5/6/05) 95

Figure 3-126. XRD results for a Test #3 Day 30 white gel-like sample. 95

TABLES

Table 1-1. Test Series Parameters..... 2

Table 2-1. Quantity of Each Coupon Type in Test #3..... 5

Table 2-2. Material Quantity/Sump Water Volume Ratios for the ICET Tests 11

Table 3-1. ICP Results for Selected Elements 28

Table 3-2. Weight Data for Submerged Coupons..... 76

Table 3-3. Mean Weight Gain/Loss (g) Data for Submerged Coupons 76

Table 3-4. Weight Data for Unsubmerged Coupons 79

Table 3-5. Mean Gain/Loss (g) Data for Unsubmerged Coupons 79

Table 3-6. Dry Mass Compositions of Test #3 Day 30 Sediment by XRF Analysis 87

Table 3-7. The Chemical Compositions for Figure 3-122..... 93

Table 3-8. XRF Results for a Test #3 Day-30 White Gel-like Sample 96

INTEGRATED CHEMICAL EFFECTS TEST PROJECT: TEST #3 DATA REPORT

EXECUTIVE SUMMARY

The U.S. Nuclear Regulatory Commission (NRC) Office of Nuclear Regulatory Research has developed a comprehensive research program to support resolution of Generic Safety Issue (GSI)-191. GSI-191 addresses the potential for debris accumulation on pressurized-water-reactor (PWR) sump screens with the consequent loss of net-positive-suction-head margin in the emergency-core-cooling-system (ECCS) pump. Among the GSI-191 research program tasks is the experimental investigation of chemical effects that may exacerbate sump-screen clogging.

The Integrated Chemical Effects Test (ICET) project represents a joint effort by the U.S. NRC and the nuclear utility industry, undertaken through the Memorandum of Understanding on Cooperative Nuclear Safety between NRC and Electrical Power Research Institute (EPRI), Addendum on Integral Chemical Effects Testing for PWR ECCS Recirculation. The ICET project simulates the chemical environment present inside a containment water pool after a loss-of-coolant accident (LOCA) and monitors the chemical system for an extended time to identify the presence, composition, and physical characteristics of chemical products that form during the test. The ICET test series is being conducted by Los Alamos National Laboratory at the University of New Mexico, with the assistance of professors and students in the civil engineering department.

This report describes the ICET experimental apparatus and surveys the principal findings of Test #3. As an interim data report compiled during preparation for subsequent ICET tests, this description summarizes both primary and representative findings that were available at the time the report was prepared. The NRC and the nuclear power industry may conduct additional analyses to enhance the understandings obtained from this test.

All of the ICET tests are being conducted in an environment that simulates expected containment pool conditions during recirculation. The initial chemical environment contains 2800 mg/L of boron, 100 mg/L of hydrochloric acid, and 0.7 mg/L of lithium hydroxide. (The hydrochloric acid and a small portion of the boron were added during the spray phase) The tests are conducted for 30 days at a constant temperature of 60°C (140°F). The materials tested within this environment include representative amounts of submerged and unsubmerged aluminum, copper, concrete, zinc, carbon steel, and insulation samples. Representative amounts of concrete dust and latent debris are also added to the test solution. Tests consist of an initial 4-hour spray phase to simulate containment spray interaction with the unsubmerged samples. Water is circulated through the bottom portion of the test chamber during the entire test to achieve representative flow rates over the submerged specimens.

ICET Test #3 was conducted using trisodium phosphate (TSP) to control pH, with a target pH of 7. (TSP was added during the spray phase.) Insulation samples consisted of scaled amounts of NUKON™ fiberglass and calcium silicate (cal-sil) material. In addition, the test apparatus contained 373 metal coupon samples and 1 concrete sample. Process control consisted of

monitoring online measurements of recirculation flow rate, test solution temperature, and pH. Flow rate and temperature were controlled to maintain the desired values of 25 gpm and 140°F. Daily water samples were obtained for measurements of pH, turbidity, total suspended solids, kinematic viscosity, and shear-dependent viscosity and for analytical laboratory evaluations of the chemical elements present. In addition, microscopic evaluations were conducted on water sample filtrates, fiberglass, cal-sil, coupons, and sediment.

Before time zero, 14.54 kg of boric acid and 0.663 g of LiOH were dissolved into the ICET tank. The measured in-line probe pH was 4.2, which was the expected value obtained from analytical predictions. TSP Batch 1 (300 g of boric acid, 1893 g of TSP) and Batch 2 (300 g of boric acid, 1893 g of TSP, 211 mL of 12.29 N HCl) were added into the recirculation line from 30 minutes until 4 hours into the test. When these prepared batches were added, the pH began to rise until it reached a pH of 7.32 (bench-top reading) 4 hours after the initiation of TSP addition. The test ran uninterrupted for 30 days, and the conditions were maintained within the accepted flow and temperature ranges.

During the introduction of TSP at the beginning of the test, a white flocculence was observed through the submerged observation window. This flocculence was accompanied by a rise in turbidity and total suspended solids (TSS). Turbidity and TSS dropped after chemical addition was complete, and the white flocculence was no longer visible in the water after the first day. Observations of the test solution indicated similar behavior of the solution at both room temperature and test temperature. After the initial flocculence had settled out of solution, no chemical byproducts were visible in the water and no precipitation occurred as samples cooled from test temperature to room temperature.

Analyses of the test solution revealed aluminum in the solution, but only at trace amounts. Calcium, silica, and sodium were prevalent in the solution.

Examinations of fiberglass taken from the test apparatus after 15 days revealed chemical products and a web-like material that spanned individual fibers. After 30 days of testing, the web-like material was more prevalent, and contiguous webbing appeared to span multiple fibers.

Daily measurements of the constant-shear kinematic viscosity revealed an approximately constant value at both test temperature and room temperature for both filtered and unfiltered samples. Shear-dependent viscosity measurements indicated that the test solution was representative of a Newtonian fluid.

The ICET series is being conducted under an approved quality assurance (QA) program, and QA procedures and project instructions were reviewed and approved by the project sponsors. Analytical laboratory results are generated under a quality control program approved by the Environmental Protection Agency, and other laboratory analyses were performed using standard practices as referenced in the body of this report.

ACKNOWLEDGMENTS

The principal authors of this report gratefully acknowledge the assistance of the following persons, without whom successful completion of the third Integrated Chemical Effects Test could not have been accomplished. Mr. John Gisclon, representing the Electric Power Research Institute, contributed much practical, timely advice on preparation of the QA experimental project instructions and the preparation of calcium silicate. Mr. Michael Niehaus from Sandia National Laboratories provided a characterization of time-dependent strain-rate viscosity measurements for the circulating solution. Mr. Luke Bartlein, of Los Alamos National Laboratory's Nuclear Design and Risk Analysis group (D-5), provided timely tagging of all test pictures and analytical images. Mr. Jim Young, of group PS-1, provided valuable reviews and inputs to QA documentation and practices. The authors also express their gratitude for the contributions and continued participation of numerous NRC staff members who reviewed the project instructions and preliminary data to ensure relevance to plant safety, high-quality defensible results, and timely execution of this test. Dr. Alicia Aragon of Sandia National Laboratories provided a very thorough review of the report and many helpful suggestions.

The authors acknowledge Ms. Eileen Patterson of IM-1, Los Alamos National Laboratory, and Ms. Katsura Fujiike of OMICRON, for their editing support.

ACRONYMS AND ABBREVIATIONS

Al	Aluminum
Au	Gold
cal-sil	calcium silicate
CPVC	Chlorinated Polyvinyl Chloride
CS	Coated steel
Cu	Copper
DAS	Data Acquisition System
DHR	Decay Heat Removal
ECCS	Emergency Core-Cooling System
EDS	Energy-Dispersive Spectroscopy
EPA	Environmental Protection Agency
ESEM	Environmental Scanning Electron Microscopy
F	Filtered
GS	Galvanized Steel
GSI	Generic Safety Issue
HCl	Hydrochloric Acid
HI	High Flow Interior Fiberglass Sample
HX	High Flow Exterior Fiberglass Sample
ICET	Integrated Chemical Effects Tests
ICP	Inductively Coupled Plasma
ICP-AES	Inductively Coupled Plasma – Atomic Emission Spectroscopy
IOZ	Inorganic Zinc
LANL	Los Alamos National Laboratory
LI	Low Flow Interior Fiberglass Sample
LiOH	Lithium Hydroxide
LOCA	Loss-of-Coolant Accident
LX	Low Flow Exterior Fiberglass Sample
NIST	National Institute of Standards and Technology
NRC	Nuclear Regulatory Commission
NTU	Nephelometric Turbidity Unit
P	Phosphorous
Pd	Palladium
PI	Project Instruction

PVC	Polyvinyl Chloride
PWR	Pressurized Water Reactor
QA	Quality Assurance
RO	Reverse Osmosis
SEM	Scanning Electron Microscopy
SS	Stainless Steel
T1	ICET Test #1
T2	ICET Test #2
TEM	Transmissive Electron Microscopy
TOC	Total Organic Carbon
TSP	Trisodium Phosphate
TSS	Total Suspended Solids
U	Unfiltered
UNM	University of New Mexico
US	Uncoated steel
WD	Working Distance
XRD	X-Ray Diffraction
XRF	X-Ray Fluorescence

1 INTRODUCTION

The Integrated Chemical Effects Test (ICET) project represents a joint effort by the United States Nuclear Regulatory Commission (NRC) and the nuclear utility industry to simulate the chemical environment present inside a containment structure after a loss-of-coolant accident (LOCA) and to monitor the chemical system for an extended time to identify the presence, composition, and physical characteristics of chemical products that may form. The ICET series is being conducted by Los Alamos National Laboratory (LANL) at the University of New Mexico (UNM), with the assistance of professors and students in the civil engineering department.

1.1. Objective and Test Conditions

Containment buildings of pressurized water reactors (PWRs) are designed to accommodate the energy release following a postulated accident. They also permit recirculation of reactor coolant and emergency-core-cooling-system (ECCS) water to the decay heat removal (DHR) heat exchangers. The water collected in the sump from the reactor coolant system, the safety injection system, and the containment spray system is recirculated to the reactor core to remove residual heat. The sump contains a screen to protect system structures and components in the containment spray and emergency-core-cooling-system (ECCS) flow paths from the effects of debris that could be transported to the sump. Concerns have been raised that fibrous insulation material could form a mat on the screen, obstructing flow, and that chemical reaction products such as gelatinous or crystalline precipitants could migrate to the screen, causing further blockage and increased pressure-head losses across the debris bed. Another potential adverse chemical effect includes increased bulk fluid viscosity that could also increase head losses through a debris bed.

The primary objectives for the ICET series are (1) to determine, characterize, and quantify chemical reaction products that may develop in the containment sump under a representative post-LOCA environment and (2) to determine and quantify any gelatinous material that could be produced during the post-LOCA recirculation phase.

The ICET series was conceived as a limited-scope suite of five different 30-day tests with different constituents. The conditions selected for each test are shown in Table 1-1. As shown in this table, Test #3 of the ICET series was to be operated at a low pH level (~7) and included substantial quantities of calcium silicate insulation material as well as fiberglass. All tests in the series included metal coupons whose surface areas were scaled to those in representative PWR containment and sump systems.

Table 1-1. Test Series Parameters

Run	Temp	TSP	NaOH	pH	Boron	Note
	(°C)	Na ₃ PO ₄ ·12H ₂ O			(mg/L)	
1	60	N/A	Yes	10	2800	100% fiberglass insulation test. High pH, NaOH concentration as required by pH
2	60	Yes	N/A	7	2800	100% fiberglass insulation test. Low pH, TSP concentration as required by pH.
3	60	Yes	N/A	7	2800	80% calcium silicate/20% fiberglass insulation test. Low pH, TSP concentration as required by pH
4	60	N/A	Yes	10	2800	80% calcium silicate/20% fiberglass insulation test. High pH, NaOH concentration, as required by pH.
5	60	TBD	TBD	TBD	TBD	Confirmatory test; one of the above four tests will be repeated.

A complete rationale for the selection of these test conditions is provided in Ref. 1, but in brief, the ICET apparatus consists of a large stainless-steel (SS) tank with heating elements, spray nozzles, and associated recirculation pump and piping to simulate the post-LOCA chemical environment. Samples of structural metals, concrete, and insulation debris are scaled in proportion to their relative surface areas found in containment and in proportion to a maximum test dilution volume of 250 gal. of circulating fluid. Representative chemical additives, temperature, and material combinations are established in each test; the system is then monitored while corrosion and fluid circulation occur for a duration comparable to the ECCS recirculation mission time.

1.2. Information Presented in This Report

This report surveys the principal findings of ICET Test #3. As an interim data report compiled during preparation for subsequent ICET tests, this exposition summarizes both primary and representative findings, but it cannot be considered comprehensive. For example, only a small selection of photographs out of several hundred is presented here. In addition, this report presents observations and data without in-depth analyses or interpretations. However, trends and typical behaviors are noted where appropriate. Section 2 of this report reviews the test procedures followed for Test #3. Analytical techniques used in evaluating test results are also briefly reviewed in Section 2. Section 3 presents key test results for Test #3, including representative and noteworthy results of water sampling, insulation samples (cal-sil and fiberglass), metallic and concrete coupon samples, tank sediment, corrosion products, and gel. The results for Test #3 are presented in both graphical and narrative form. Section 4 presents a summary of key observations for Test #3. This report also includes several appendices that capture additional Test #3 images and information. The data presented in the appendices are largely qualitative,

consisting primarily of environmental scanning electron microscopy (ESEM), scanning electron microscopy (SEM) and transmissive electron microscopy (TEM) micrographs and energy-dispersive spectroscopy (EDS) spectra.

2 TEST PROCEDURES

The functional description and physical attributes of the ICET apparatus were presented in detail in the ICET Test #1 report (Ref. 2). The experimental apparatus is briefly described below, followed by a review of the test operation and analytical techniques used to evaluate the test results.

2.1 Chemical Test Apparatus Functional Description

The test apparatus was designed to meet the functional requirements of the Project Test Plan (Ref. 1). Functional aspects of the test apparatus are as follows:

1. The central component of the system is a test tank. The test apparatus was designed to prevent solids from settling in the test piping.
2. The test tank can maintain both a liquid and vapor environment, as would be expected in post-LOCA containment.
3. The test loop controls the liquid temperature at 140°F ($\pm 5^\circ\text{F}$).
4. The system circulates water at flow rates that simulate spray flow rates per unit area of containment cross section.
5. The test tank provides for water flow over submerged test coupons that is representative of containment pool fluid velocities expected at plants.
6. Piping and related isolation valves are provided such that a section of piping can be isolated without interrupting the test.
7. The pump discharge line is split in two, one branch directing the spray header in the tank's vapor space and the other returning to the liquid side of the tank. Each branch is provided with an isolation valve, and the spray line includes a flow meter.
8. The recirculation piping includes a flow meter.
9. The pump circulation flow rate is controlled at the pump discharge to be within $\pm 5\%$ of the flow required to simulate fluid velocities in the tank. Flow is controlled manually.
10. The tank accommodates a rack of immersed sample coupons, including the potential reaction constituents identified in the test plan.

11. The tank also accommodates six racks of sample coupons that are exposed to a spray of liquid that simulates the chemistry of a containment spray system. Provision is made for these racks to be visually inspected.
12. The coupon racks provide sufficient space between the test coupons to preclude galvanic interactions among the coupons. The different metallic test coupons are also electrically isolated from each other and the test stand to prevent galvanic effects resulting from metal-to-metal contact between specimens or between the test tank and the specimens.
13. The fluid volumes and sample surface areas are based on scaling considerations that relate the test conditions to actual plant conditions.
14. All components of the test loop are made of corrosion-resistant material (for example, SS for metallic components).

The as-built test loop consists of a test tank, a recirculation pump, 2 flow meters, 10 isolation valves, and pipes that connect the major components, as shown schematically in Figure 2-1. P, T, and pH represent pressure, temperature, and pH probes, respectively.

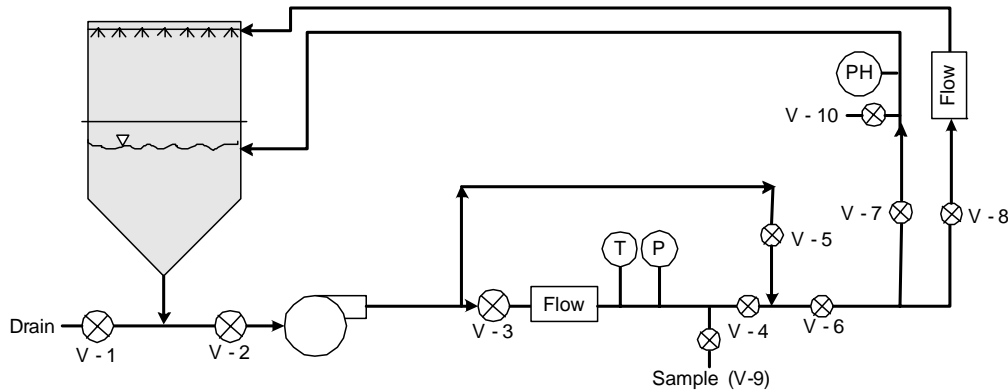


Figure 2-1. Test loop process flow diagram.

2.2 Pre-Test Preparation

2.2.1. Test Loop Cleaning

In preparation for Test #3, the experiment test loop was thoroughly cleaned to remove all Test #2 deposits and residues. In addition to visual inspections, the test apparatus was flushed and cleaned per the written direction given in the pre-test operations project instruction (PI) (Ref. 3). The system was flushed with ammonium hydroxide followed by ethanol until it was visually clean and the water conductivity was $<50 \mu\text{S}/\text{cm}$.

2.2.2. Test Coupons and Samples

Each ICET experiment exposes metallic and concrete coupons to anticipated post-LOCA environments. Each coupon is approximately 12 in. square. The metallic coupons are approximately 1/16 in. thick, except for the inorganic-coated steel coupons, which are approximately 3/32 in. thick. The concrete coupons (one per test) are approximately 1-1/2 in. thick. Insulation materials are also exposed. For Test #3, fiberglass insulation samples and calcium silicate samples were included in the test. As with Tests #1 and #2, Test #3 subjected seven racks of coupon to the specified environment, with one being submerged in the test tank and the remaining six being held in the tank's gas/vapor space. The Test #3 coupons of each type were as shown in Table 2-1.

Table 2-1. Quantity of Each Coupon Type in Test #3

Material	No. of Coupons
Coated Steel (CS)	77
Aluminum (Al)	59
Galvanized Steel (GS)	134
Copper (Cu)	100
Uncoated Steel (US)	3
Concrete	1

Note: Inorganic zinc (IOZ) coated steel and CS are the same coupon type.

The arrangement of the coupon racks in the test tank is schematically illustrated in Figure 2-2. The figure shows a side view of the ICET tank, with the ends of the seven CPVC racks illustrated. The normal water level is shown with the blue line in the figure. Rack #1 is the only submerged rack, and it sits on angle iron. It is centered in the tank, so that flow from the two headers reaches it equally. Racks #2-#4 are positioned above the water line, supported by angle iron in the tank. Racks #5-#7 are positioned at a higher level, also supported by angle iron. Racks #2-#7 are exposed to spray. In the figure, north is to the right, and south is to the left. Directions are used only to identify such things as rack locations and sediment locations.

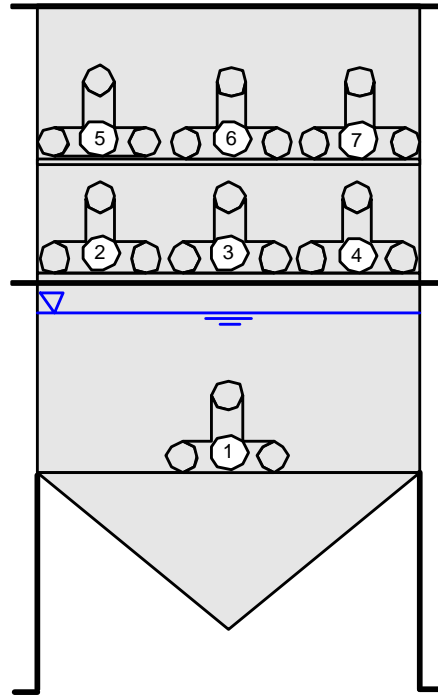


Figure 2-2. Coupon rack configuration in the ICET tank. The blue line represents the surface of the test solution.

Figure 2-3 shows the configuration of an unsubmerged coupon rack loaded with metal coupons in the ICET tank. The loading pattern of the racks was nearly identical, varying by only one or two coupons. Shown in the figure from left to right, the coupons are arranged as follows: 4 Cu, 4 Al, 4 inorganic zinc (IOZ), 7 GS, 4 Cu, 3 Al, 4 IOZ, 7 GS, 4 Cu, 3 Al, 4 IOZ, and 7 GS.



Figure 2-3. A loaded coupon rack in the ICET tank.

Several fiberglass samples were placed in the ICET tank. Samples were either submerged or held above the water level. The unsubmerged fiberglass samples were positioned so they would be exposed to sprays. The fiberglass samples were contained in SS wire mesh that allowed water flow while confining the fiberglass material. Both loosely-packed and more tightly-packed samples were used. In addition, some submerged fiberglass samples were located where they would be exposed to relatively high-flow conditions, and others were located in quiescent regions of the tank. Figure 2-4 shows the so-called “sacrificial” fiberglass samples in wire mesh pouches attached to the submerged coupon rack (rack 1 in Figure 2-2). Each pouch contains approximately 5 g of fiberglass. Those samples were attached with SS wire and removed from the tank on Days 4, 15, and 30, and examined. As shown in the figure, bigger insulation bags were wrapped around the sacrificial specimens during the test. See Subsection 2.4.1.1 for descriptions of other fiberglass samples.



Figure 2-4. Fiberglass samples attached to coupon rack.

Several cal-sil insulation samples were also placed in the ICET tank. Samples were either submerged or held above the water level. The unsubmerged cal-sil samples were positioned so they would be exposed to sprays. As with the fiberglass samples, all of the cal-sil samples (except for the dust) were contained in SS wire mesh that allowed water flow while confining the cal-sil material. In addition to solid pieces of cal-sil, cal-sil dust (approximately 43.5 lb) was placed in the tank solution before the test began. Both types of samples are shown in Figures 2-5 and 2-6.



Table 2-5. Solid pieces of cal-sil samples in SS mesh.



Figure 2-6. Cal-sil dust.

2.2.3. Quality Assurance (QA) Program

A project QA manual was developed to satisfy the contractual requirements that apply to the ICET project. Specifically, those requirements were to provide credible results by maintaining an appropriate level of QA in the areas of test loop design, sampling, chemicals, operation, and analysis. These requirements were summarized in the contract requirement that QA was to be consistent with the intent of the appropriate sections of 10CFR50, Appendix B.

The 18 criteria of 10CFR50, Appendix B, were addressed separately in the QA manual, and the extents to which they apply to the ICET project were delineated. A resultant set of QA procedures was developed. In addition, project-specific instructions were written to address specific operational topics that required detailed step-by-step guidance. PIs generally applicable to all tests were written for the following topics and were followed for Test #3:

- Data Acquisition System (DAS)
- Coupon Receipt, Preparation, Inspection, and Storage
- DAS Alarm Response
- Chemical Sampling and Analysis
- TEM Examination of Test Samples
- SEM Characterization of Test Samples
- Viscosity Measurements

Project instructions specific to Test #3 were written for the following:

- Pre-Test Operations
- Test Operations, Test #3 (cal-sil and fiberglass, with TSP)
- Post-Test Operations

The pre-test, test, and post-test operations PIs that were used in Test #3 are included in Appendix L.

2.2.4. Test Parameters

ICET test parameters were selected based on literature surveys and the results of surveys of United States nuclear power plants. Quantities of test materials were selected to preserve the scaling of representative ratios between material surface areas and total cooling-water volumes. Chemical additives also simulate the post-LOCA sump environment. The Project Test Plan (Ref. 1) is the basis for the following information in this section.

The materials included in the tests are zinc, aluminum, copper, carbon steel, concrete, and insulation materials such as fiberglass and calcium silicate. The amounts of each material are given in Table 2-2 in the form of ratios (material surface area to water volume), with three exceptions: concrete dust, which is presented as a ratio of mass to water volume, and fiberglass and calcium silicate, which are presented as a ratio of insulation volume to water volume. Also shown in the table are the percentages of material that are submerged and unsubmerged in the test chamber.

Table 2-2. Material Quantity/Sump Water Volume Ratios for the ICET Tests

Material	Value of Ratio for the Test (ratio units)	Percentage of Material Submerged (%)	Percentage of Material Unsubmerged (%)
Zinc in Galvanized Steel	8.0 (ft ² /ft ³)	5	95
Inorganic Zinc Primer Coating (non-top coated)	4.6 (ft ² /ft ³)	4	96
Inorganic Zinc Primer Coating (top coated)	0.0 (ft ² /ft ³)	–	–
Aluminum	3.5 (ft ² /ft ³)	5	95
Copper (including Cu-Ni alloys)	6.0 (ft ² /ft ³)	25	75
Carbon Steel	0.15 (ft ² /ft ³)	34	66
Concrete (surface)	0.045 (ft ² /ft ³)	34	66
Concrete (particulate)	0.0014 (lbm/ft ³)	100	0
Insulation Material (fiberglass or calcium silicate)	0.137 (ft ³ /ft ³)	75	25

The physical and chemical parameters which are critical for defining the tank environment and which have a significant effect on sump-flow blockage potential and gel formation, have been identified in Reference 1. These physical and chemical parameters are summarized as follows:

Physical Parameters

• Water volume in the test tank	949 L	250 gal.
• Circulation flow	0–200 L/min	0–50 gpm
• Spray flow	0–20 L/min	0–5 gpm
• Sump temperature	60°C	140°F

Chemistry Parameters

• H ₃ BO ₃ concentration	2800 mg/L as boron
• Na ₃ PO ₄ ·12H ₂ O concentration	As required to reach pH 7 in the simulated sump fluid
• NaOH concentration	As required to reach pH 10 in the simulated sump fluid
• HCl concentration	100 mg/L
• LiOH concentration	0.7 mg/L as Li

The parameters planned for each ICET test run were described in Table 1-1.

2.3 Test Operation

2.3.1. Description

Preparation of ICET Test #3 (Run 3 in Table 1-1) began with 240 gal. of reverse osmosis (RO) water being heated to 65°C. (Adding the metal coupons and insulation samples reduces the water temperature by approximately 5°C, so the water was heated initially to 65°C.) With 25 gpm circulating through the loop, the predetermined quantities of boric acid (14.54 kg) and LiOH (0.66 g) were added and dissolved in the ICET tank solution. After the chemicals were added and observed to be well mixed, a baseline grab sample and measurements of the test solution were taken. Then the premeasured latent debris and concrete dust were added to the tank solution. After the solution circulated for 10 minutes, the pump was stopped and the coupon racks and insulation samples were put into the tank (see Section 2.2.2).

The test commenced with initiation of the tank sprays. The sprays lasted for 4 hours, and they resulted in 3.5 gpm of solution being sprayed on the unsubmerged coupons, through the 4 flow nozzles. Beginning at 30 minutes into the test, Batch 1 of TSP (Na₃PO₄·12H₂O) solution was metered into the recirculation line. That batch consisted of 300 g of boric acid and 1893 g of TSP in 5 gal. of RO water. When that batch had been injected, after approximately 90 minutes, injection of Batch 2 began. Batch 2 consisted of 300 g of boric acid, 1893 g of TSP, and 211 mL of 12.29 N HCl in 5 gal. of RO water. That batch was injected over the remainder of the spray cycle. The sprays were terminated after 4 hours, and the test continued uninterrupted for the next 30 days.

The experiment commenced at 3:30 p.m. on Tuesday, April 5, 2005, and it ended on May 5, 2005. During the test, grab samples were taken daily for wet chemistry and inductively coupled plasma – atomic emission spectroscopy (ICP-AES) analyses. Water loss due to water sample removals and evaporation was made up with RO water. Water samples, insulation, and metal coupons were analyzed after the test. Sampling and analyses were conducted in accordance with approved project instructions (Refs. 3, 4, and 5).

2.3.2. Process Control

During the test, critical process control parameters were monitored to ensure that the test conditions met the functional test requirements. Recirculation flow rate and temperature were controlled throughout the test. The solution pH was initially targeted to reach the prescribed value of 7 after the spray phase ended. The pre-determined amounts of chemicals were added, and pH was not controlled.

Recirculation flow in the test loop was controlled by adjusting the pump speed. Fine tuning was achieved by manually adjusting a valve located downstream of the recirculation pump. In-line flow meters were used to measure the flow rate in the recirculation line and the spray line.

Titanium-jacketed immersion electric heaters controlled the water temperature. The heaters were thermostatically controlled to automatically maintain the desired temperature.

2.4 Analytical Methods

Data collected during Test #3 included the in-line measurements of temperature, pH, and loop flow rate. During the daily water grab sample analysis, bench-top measurements were obtained for temperature, pH, turbidity, total suspended solids (TSS), and kinematic viscosity. The concentration of hydrogen in the tank atmosphere was also measured and could be used as an indicator of chemical reactions taking place. Water, fiberglass, and metal coupon samples were taken to other laboratory locations for additional analyses. These analyses included strain-rate viscosity, ESEM, SEM, EDS, TEM, ICP-AES, x-ray fluorescence (XRF), and x-ray diffraction (XRD). EDS provided a semi-quantitative elemental analysis after calibration of the instrument's x-ray signal using an internal element standard. Descriptions of the principles of operation and limitations of these analytical methods were provided in the Test #1 report (Ref. 2).

2.4.1. Data Compilation and Nomenclature

This section provides a brief guide to assist the reader in interpreting the ICET Test #3 information and data presented in the following sections and in the appendices. Standardized nomenclature is defined first to clarify the origin of samples that are described in the data sets. The appendices are listed, and a description is provided of how they were compiled.

2.4.1.1. Nomenclature

Many spatially unique but physically similar sample types were collected in ICET Test #3. To ensure that consistent interpretations and comparisons of data sets are made, it is imperative that a standardized nomenclature be adopted when referring to each sample type. Many different qualitative descriptions of these samples might be equally suitable, but different adjectives convey different connotations to each observer. Therefore, the following definitions establish the convention used in this report when

making generic references to sample type. Every effort should be made to adhere to this standard when interpreting the data so that all future audiences will have a common understanding of sample origins from the ICET series.

- White Precipitate** The behavior of test solution at temperature and upon cooling is observed during testing. Precipitates and their prominence indicate chemical interactions occurring in the solution. White precipitate formed in Test #1 (T1) water solution samples drawn from the test loop. Upon cooling below the test temperature, T1 daily water samples extracted from the tank formed a visible white material that is referred to as a precipitate. This precipitate was absent in Test #3 (T3) water samples. One probable cause of the differences is the pH levels of the test solutions and their effects on the aluminum samples. T1 had a high pH of about 9.5, whereas the pH for T3 was about 8.0. Aluminum solubility is highly dependent on pH levels. There may be other causes that effect the corrosion of aluminum and cause precipitates to form.
- Latent Debris** Commercial power plant containments gradually accumulate dust, dirt, and fibrous lint that are generically referred to as latent debris. This classification distinguishes resident material from debris generated during an accident scenario. At the beginning of T3, measured quantities of crushed concrete and soil were added to simulate the latent debris present in containment. These materials were examined via SEM/EDS to establish a baseline composition for comparison with sediment samples (see “Sediment” below).
- Sediment** Surrogate latent debris particulates and fugitive fiberglass fragments that were initially suspended in water at the beginning of T3 gradually settled to the bottom of the tank. In addition, a large amount of cal-sil dust was added to the tank solution. Most of that dust ended up on the tank bottom. A deep layer of sediment formed, which was 8-in. deep in some places. During the course of the test, additional material may have been deposited in this layer. At the conclusion of the test, the sediment layer was recovered as completely as possible.
- White Residue** At the conclusion of T3, all water was drained slowly from the tank. Exposed metal surfaces that cooled rapidly collected a thin deposit of white residue or scale. Some of this material was scraped from internal piping surfaces and tank walls for comparison with other sample types. A similar residue was observed after Tests #1 and #2.

Powder	At the conclusion of T3, fine particulate deposits were found on the submerged CPVC coupon rack. They were referred to as powder and examined by SEM/EDS.
Fiberglass	One of the principal debris types introduced to T3 was shredded fiberglass insulation. This debris was bundled in 3-in.-thick bags (or blankets) of fiberglass confined in SS mesh to prevent ingestion through the pump and to better control the placement of debris in various flow regimes. Fiberglass samples are designated by their placement in high-flow and low-flow areas of the tank. Additional 4-in.-square envelopes of fiberglass were also prepared for extraction during the course of the test. These samples are referred to as “sacrificial” samples. One sample, called the “birdcage,” was constructed so that the fiberglass within was loose and not compacted. The birdcage fiberglass sat on the tank bottom and was removed on Day 30. Some amount of fiber, especially short-fiber fragments, escaped the mesh bags and was deposited in other locations within the tank. This material is referred to as “fugitive” fiberglass.
Cal-sil	The insulation samples used in T3 were 80% cal-sil. That amount was divided into 4 size categories, in pieces that were roughly cubes. Of the total cal-sil, 14% was over 3 in., 19% was 1–3 in., 5% was less than 1 in., and 62% was “dust.” The dust consisted of cal-sil pieces that were ground into a fine powder. With the exception of the dust, the cal-sil pieces were contained within SS mesh and apportioned into submerged and unsubmerged samples. The dust was put into the tank solution before the test started, and it became the primary constituent of the sediment.
Drain Screen	A 12-in.-tall screen made of coarse SS mesh (1/8-in. holes) wrapped into a 2-in.-diam cylinder was inserted into the outlet drain at the bottom of the tank to protect the pump from ingesting large debris items. Two inches of the screen were inserted into the tank outlet to provide a solid base and stability. A 6-in.-tall drain collar was installed around the drain screen. This drain collar was a cylinder of fiberglass held in SS mesh. The drain collar was exposed to higher-velocity water flow than other samples in the tank. The drain collar fiberglass was examined as a separate debris location to identify any apparent differences with other sample locations.
Gelatinous Material	This term generically refers to any observed sample constituent with amorphous, hydrated, or noncrystalline physical characteristics. When Test #3 was shut down, deposits of pinkish-

white gel-like precipitates were observed on the top of the birdcage and on other objects on the tank's bottom.

Water Sample

Daily water samples were extracted from the ICET tank for elemental concentration analyses. After the sample line was properly flushed, some of this water was extracted directly from the tap. An equal amount of water was also generally collected through a micropore filter. Thus, daily water samples were designated as filtered (F) and unfiltered (U), and a corresponding filter paper exists in the sample archive for each daily sample that was collected.

High-Volume Filter

If white precipitates are observed in the tests, larger quantities of test solution are periodically extracted for filtration to determine whether suspended chemical products are present in the test liquid under in situ conditions. The intent of this exercise is to maintain the liquid temperature while forcing the liquid through a micropore filter under vacuum. Because the precipitates were not present in T3, these high-volume filter samples were not obtained.

Filter Paper

Many different samples of tank solution were fractionated by micropore filtration into a liquid supernate and a solid filtrate that existed at the time and temperature conditions of the filtering process. These samples included (1) daily water samples filtered during extraction, (2) daily water samples filtered after cooling to room temperature, and (3) high-volume water samples.

Chemical Deposits

Sacrificial fiberglass samples that were extracted at Day 4, Day 15, and Day 30 showed evidence of chemical products forming on and between fiber strands. These products are referred to as "deposits," although the exact physical mechanism of formation is not well understood. The physical appearance suggests growth, agglomeration, or crystallization on and around the fiber strands over time rather than capture or impaction of particles from the bulk solution. This observation is supported by the fact that the small sacrificial fiberglass samples were located in a region of lower-velocity water flow (i.e., in the interior of larger blankets).

Concrete Sample

Several chips of concrete (1/4–3/4 in. diam) were broken from the primary slab of submerged concrete and introduced to the tank in a small SS envelope at the start of the test. Examinations of these chips were conducted to determine if concrete surfaces provide a preferential site for gel formation.

Although these terms have been defined, the reader may note minor inconsistencies in the caption labels used in this document. The caption labels use the same descriptions that were applied in laboratory notebooks to improve traceability of the data.

2.4.1.2. Usage

The twelve appendices listed below are provided to present data collected for the sample types and analysis methods listed below. In addition, an appendix is provided with pertinent Test #3 project instructions.

- A SEM and ESEM/EDS Data for Test #3 Day-4 Fiberglass in Low-Flow Zone
- B ESEM and SEM Day-15 Fiberglass
- C ESEM and SEM Day-30 Fiberglass
- D ESEM and SEM/EDS Data for Test #3 Day-30 Corrosion Products
- E SEM Day-30 Coupons
- F SEM/EDS Data for Test #3 Day-30 Flow Meter
- G SEM/EDS and ESEM/EDS Data for Test #3 Day-30 Gel
- H SEM/EDS and ESEM/EDS Data for Test #3 Day-30 Cal-sil
- I ESEM/EDS Data for Test #3 Day-30 Sediment
- J TEM Data for Test #3 Solution Samples
- K UV Absorbance Spectrum—Day-30 Solution Samples
- L ICET Test #3: Pre-Test, Test, and Post-Test Project Instructions

These data are largely qualitative in nature, consisting primarily of ESEM, SEM, TEM micrographs, and EDS spectra. Each appendix represents a separate session of laboratory work that can be traced to a batch of samples that were processed in chronological order. This organizational scheme preserves the connection with laboratory notebooks and timelines that naturally developed during operation; however, in a few cases, results for a given sample type may be mixed across two or more appendices because of the order in which the individual samples were analyzed.

ESEM analyses were added to the ICET diagnostic suite for the first time during Test #2 as a means of examining hydrated chemical products. This equipment operates as an electron microscope, but it does not require a high-vacuum condition in the sample chamber. Thus, a sample need only be thoroughly drained of free water content before examination rather than fully desiccated, making the ESEM ideal for examinations of biological and environmental specimens. The complementary EDS capability that is often found with equipment of this type is not presently functional at UNM, so duplicate examinations are often performed on the same ICET sample using ESEM to obtain images of hydrated structural details and SEM/EDS to obtain representative elemental compositions. Throughout the report, ESEM analyses are also indicated by the descriptions of “hydrated” and “low-vacuum” findings.

Transcriptions of the logbooks are provided for each appendix to better document commonalities that existed among the samples at the time of analysis. Interpretation and understanding of the images and their accompanying EDS spectra will be greatly improved by frequent reference to the logbook sample descriptions and sequences. Typically, a relatively large quantity of a test sample was delivered for SEM or TEM analysis, and then several small sub-samples of each item were examined. Note that each sub-sample was assigned a sequential reference number during the laboratory session. These reference numbers have been cited in the figure captions whenever possible to preserve the connection between the micrographs and the notebook descriptions. Electronic file names have also been stamped on the images to permit retrieval of the original data files that are archived elsewhere. Individual data sets for a given sample item have been collated into a typical sequence of (1) visual image, (2) EDS spectra, and (3) semi-quantitative mass composition.

For most of the EDS spectra, semi-quantitative mass compositions are also presented. These results are obtained from a commercial algorithm that decomposes the spectra into the separate contributions of each element. Several caveats should be considered when interpreting the numeric compositions thus obtained; however, despite these caveats, semi-quantitative EDS analysis offers a natural complement to micrographic examination as a survey technique for identifying trends in composition.

1. The spectral deconvolution algorithm is based on a library of unique signatures of each element that were obtained for pure samples using a standard beam setting that may not identically match the conditions applied for the test item.
2. The operator must select a limited number of elements to be used in the proportional mass balance. These candidates are chosen from among the peaks that are observed in the spectrum; however, the composition percentages can vary, depending on which elements are included in the list. In a few cases, two or more alternative compositions have been generated by selecting a different set of elements from the same spectrum to illustrate the sensitivity of this technique to operator input.
3. The spectral unfolding algorithm is a statistical technique having a precision that depends on the relative quality of the data in each peak. Compositions with high R^2 correlation coefficients and total-mass normalization factors closer to unity represent the more-reliable estimates. The precision obtained in the fit depends on the duration of the scan and the number of counts received in each energy bin.
4. All sub-samples examined in the SEM microprobe facility are coated with a thin layer of either carbon or gold/palladium alloy to prevent the sub-samples from accumulating a charge from the impinging electron beam. Spectral peaks visible for gold (Au) and palladium (Pd) are not indigenous to the samples.
5. The EDS spectral analysis software contains a peak-recognition algorithm and an automated cursor that scans across the spectrum to locate each peak. An accompanying library of elemental energy signatures is also provided to suggest

what constituents might be contributing to a given energy bin, but the operator must judge what label to assign to the spectral image. It is possible that some peaks near closely neighboring elements have been mislabeled in these images. However, every effort was made to choose from candidate elements that were most likely to be present in the test material. In a few cases, the spectral peaks were not labeled by the SEM operator. These spectra should be viewed as corroborating evidence for similar samples that are definitively labeled. Careful comparisons of the energy scales in combination with a library of electron-scattering energies can also be used to infer the origin of the more-prominent peaks that are present in unlabeled spectra.

6. Unless an obvious spatial heterogeneity is being examined, the exact location of an EDS spectrum is not always relevant because the operator chooses arbitrary sites that are visually judged to be representative. It is not possible to sample a surface comprehensively on a microscopic basis and compute average compositions. In many cases, two or three replicate spectra are provided for this purpose, but SEM/EDS is most effective as a survey diagnostic.
7. EDS analysis is not particularly sensitive to the presence of boron for several reasons: (a) boron has a low atomic mass that does not interact well with electrons in the beam, (b) the emission lines are very close to those of carbon, and (c) the beam-port material has a high absorption cross section for these emission energies. Therefore, the correction factors used in the semi-quantitative composition analysis are quite large, as are the uncertainties in the estimated percentage of total composition for this element. There may be spectra presented in the appendices in which the lowest energy peaks are labeled as either B (boron) and/or C (carbon).

EDS locations were chosen manually at regions of specific interest. In many cases, multiple spectra were collected from a single sample and an annotated image is provided to identify the specific location. These annotated images are not generally noted in the laboratory logbook entries, but they are provided in proper sequence within the appendices.

Appendix J presents TEM data for water samples extracted from the ICET solution at Day 4, Day 15, and Day 30. The purpose of this examination was to determine whether the physical structure of any suspended products exhibits crystalline or amorphous characteristics. These data are also qualitative in nature, consisting generally of a set of high-resolution micrographs followed by companion electron diffraction images. The TEM sample holder consists of a carbon grid that is "lacey," or filamentary, in nature. This grid is visible as a relatively large-scale structure in the background of most images. Surface tension in a droplet of liquid suspends the particulates of interest across the grid so that the electron beam can illuminate the sample through the holes without interference from a substrate. Crystalline material will exhibit diffraction patterns unique to the molecular arrangement. Amorphous material that is diffuse or disorganized in structure will not exhibit regular diffraction patterns that can be identified.

Water samples submitted for TEM analysis are not temperature controlled because the temperature cannot be maintained during the examination.

In a few cases, data file names that were noted by the operator in the laboratory log were not successfully saved in electronic form. These cases are noted in the transcribed log sheets, but the corresponding images are unavailable and therefore cannot be presented in the data sequence.

3 TEST RESULTS

This section describes the results obtained from Test #3. An overview is first presented in the form of general observations. This overview is followed by more-detailed information organized by the type of samples/data collected. Data and photographs are provided here for the (1) water samples, (2) insulation [NUKON™ fiberglass samples and cal-sil materials] (3) metallic and concrete samples, (4) sediment, and (5) gel. Precipitates and corrosion products are also discussed.

3.1 General Observations

Twenty minutes after Batch 1 chemicals were introduced, white flocculence was observed through the submerged observation window. The entire tank solution, as viewed through the window, exhibited a large secondary circulating flow, and the particulates appeared to be neutrally buoyant. Approximately 2-1/2 hours later, the white flocculence was smaller than before, but were very fine and dense. Flow was not evident through the view window at that time.

At the 24-hour test point, a white deposit was observed on the submerged SS insulation mesh. This deposit was also observed on the submerged GS coupons. On Day 2, a very light scale was observed on the lower observation view window. Irregular vertical patterns were also observed on the lower view window. These appeared to be related to observed Day 1 bubble formation. (On Day 1, bubbles were observed to be released from the deposits on the interior of the lower view window.)

Five gallons of RO make-up water were added to the tank on Day 3. This caused some agitation of the particulates on the bottom of the tank and resulted in an increase in water cloudiness. Less than 1 day after the make-up water was added, the water clarity returned. From then on, the observed conditions of the coupons, insulation baskets, and other submerged items remained largely unchanged.

On Day 8, 5 gallons of RO water were added to the tank through the valve on the bottom of the tank. Even though the RO water was added in a fashion that should not have disturbed the settled particulates, the water became cloudy. Again, in less than 1 day's time, the water returned to normal test clarity.

On Day 9, about 3 gallons of test solution were lost when the flow meter was removed and then replaced after being cleaned. On Day 13, 5 more gallons of RO water had to be added. Again, the water was added through the bottom of the tank. This time, the particulate matter did not appear to be disturbed, and the tank solution did not appear cloudy.

The water clarity on Day 15 decreased somewhat. This also corresponded to an increase in TSS (Figure 5) but was 2 days after RO water was added.

On Day 22, 5 gallons of RO water were added to the tank through the totalizing flow meter that was attached just upstream of the valve at the bottom of the tank. Despite this fact, water clarity was unaffected on this day and on Day 23. This trend continued through Day 27.

On Day 27, 4 more gallons of RO water were added to the tank. Agitation of the deposits on the tank bottom was not observed.

Although the conditions in the tank remained relatively steady beginning on Day 3, a few exceptions have been observed. What appeared to be dissolution of white particulate was observed from Day 7 through Day 9. The white particulate that was observed on the bottom of the tank was nearly absent on Day 9. In addition to the perturbations caused by the addition of water, that could be an indication of continuing chemical interactions.

3.1.1. Control of Test Parameters

Recirculation flow rate: On Day 8 of the test, the flow meter output was lost. The problem appeared to be with the internals of the instrument. The following day, the flow meter was taken out of service and cleaned. Scale and precipitation deposits had accumulated on the turbine inside the flow meter, preventing the turbine from moving. The deposits were white and were observed to be coating the inside of the removed piping as well. They were solid, but could be removed easily with light scraping. The flow meter was flushed with RO water, which removed the scale on the turbine. After cleaning, the flow meter was re-installed and the measured flow rate was steady as before. While the flow meter was not operating, regular observations of the line pressure indicated that no flow perturbations occurred. Excluding the time that the flow meter was out of service and during the spray cycle, the average recirculation flow rate was 95.9 L/min (25.3 gpm). The recirculation flow rate had a standard deviation of 1.1 L/min, with a range of 93.3 to 99.1 L/min (24.6 to 26.2 gpm).

Temperature: Temperature is recorded at three submerged locations in the ICET tank. On Day 12 of Test #3, one of the three thermocouples began giving an erroneous reading. To reset the high-temperature alarm, the bad thermocouple within the DAS was replaced with a thermocouple that measured room temperature. Thus, temperature 1 on the DAS display panel became the room temperature. This temperature was factored into the average temperature displayed on the DAS panel. Neglecting the deactivated thermocouple, the average recorded temperature at the two valid locations was 60.4°C and 60.6°C (140.8°F and 141.0°F). The standard deviation in temperature recorded by the two thermocouples was within $\pm 0.27^\circ\text{C}$ ($\pm 0.49^\circ\text{F}$), with a maximum range of 58.0°C to 61.7°C (136.3°F to 143°F).

pH: Before time zero, 15.45 kg of boric acid and 0.663 g of LiOH were dissolved in the ICET tank. The measured bench-top pH was 4.24, which was similar to the expected value obtained from analytical predictions. Following the addition of the premixed TSP batches, the pH was 7.32. The pH then continued to rise through Day 3 of testing to 7.9. After Day 3, the pH varied in the range of 7.8–8.0.

The in-line pH probe tracked the overall bench-top pH readings, but the results have noise and a slight offset. Due to the noise within the raw data, the bench-top pH readings are more reliable. Figure 3-1 shows results from the in-line pH probe.

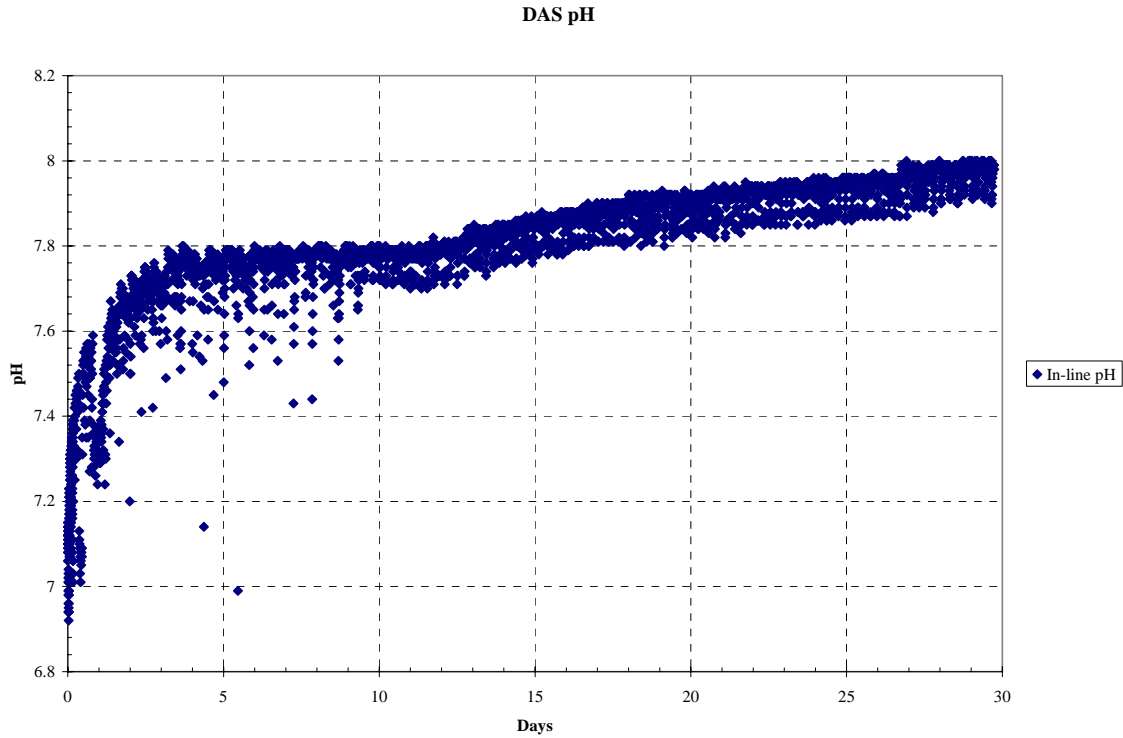


Figure 3-1. In-line pH measurements.

Four hours into the test, the in-line pH measurement was 7.37, and at Day 30 the pH measurement was 7.92. Figure 3-2 presents the bench-top pH readings. Four hours into the test, the bench-top pH measurement was 7.32, and at Day 30 the pH measurement was 8.05.

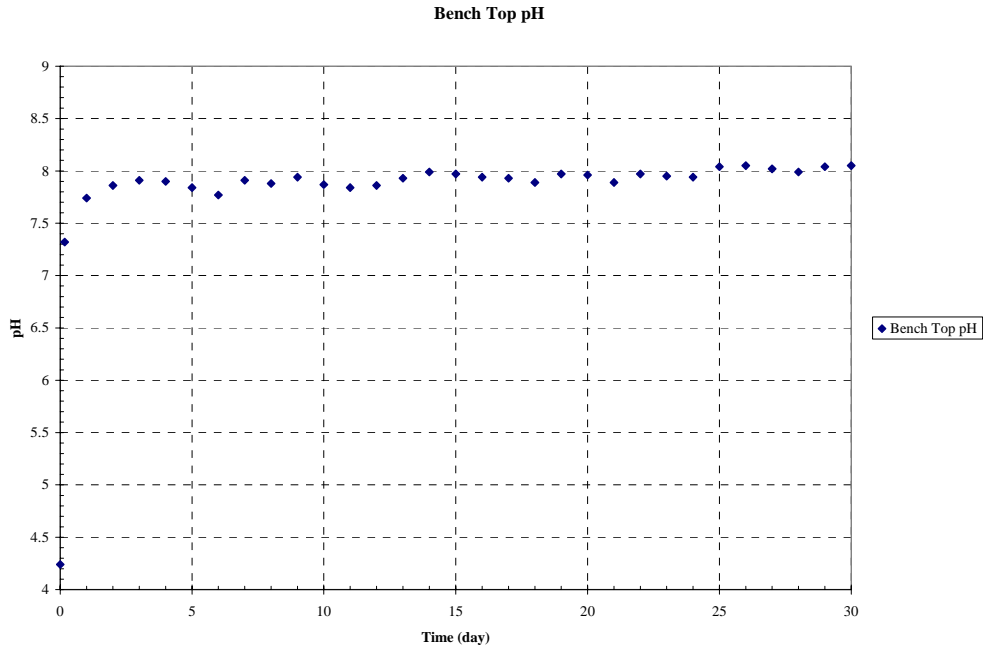


Figure 3-2. Bench-top pH meter results.

3.1.2. Hydrogen Generation

Hydrogen remained at or below 0.05% for Test #3. Figure 3-3 displays the evolution of hydrogen generation throughout the test. A general trend line has been superimposed upon the hydrogen generation data set. Each of the measured values is well below the hydrogen safety action threshold of 0.4%.

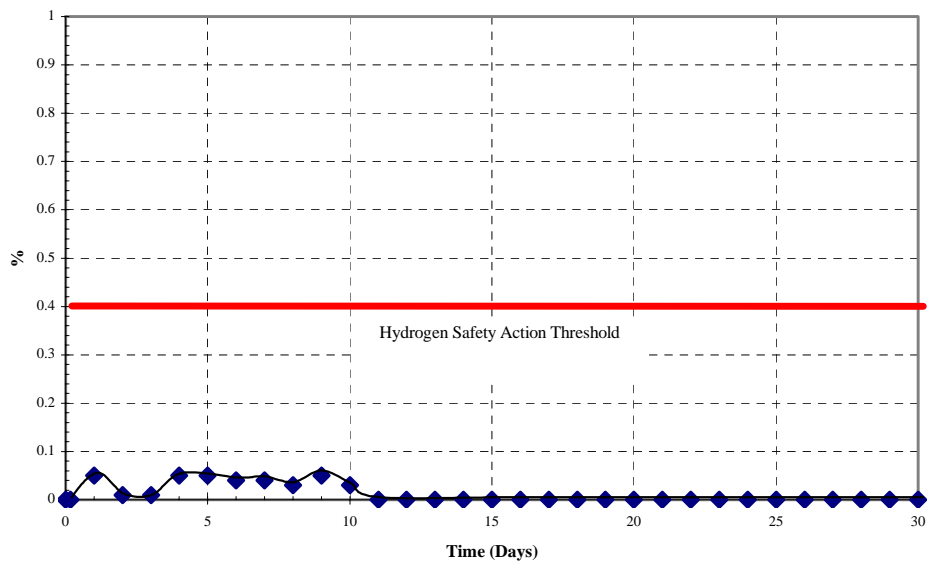


Figure 3-3. Hydrogen generation.

3.2 Water Samples

3.2.1. Wet Chemistry

Wet chemistry analyses included turbidity, TSS, and kinematic viscosity.

Turbidity: For the 23°C and 60°C water samples, the baseline turbidity values, which were taken after the latent debris and crushed concrete were added, were 7.3 NTU and 7.5 NTU, respectively. After the addition of cal-sil, the tank solution was observed to become much more turbid. Then with time, the turbidity decreased. Upon the addition of Batch 1 and Batch 2 chemicals, particulates were suspended in solution, and the solution was noticeably cloudier. Figure 3-4 presents the daily turbidity results.

Due to the cloudy nature of the water in the tank after the circulation pump was turned on, additional turbidity values were measured at 60°C over a 9-hour time period, in addition to the regular daily monitoring. Figure 3-4 depicts the evolution of turbidity during that time period. The x-axis on the graph represents the time in hours after the circulation pump was turned on, following cal-sil addition and while the system was heating up. As can be seen, the turbidity gradually decreased from 192 NTU at the 7-minute point to 54 NTU at the 5.9-hour point. Note that the 5.23-hour point on the graph corresponds to the time-zero test point. The spray nozzles were activated at that time. At the 6.4-hour point, the turbidity peaked above 200 NTU. The turbidity decreased to 79 NTU by the end of the spray phase. (Note that the Batch 1 addition began at approximately 5.8 hours on Figure 3-4, and Batch 2 addition began at 7.5 hours.)

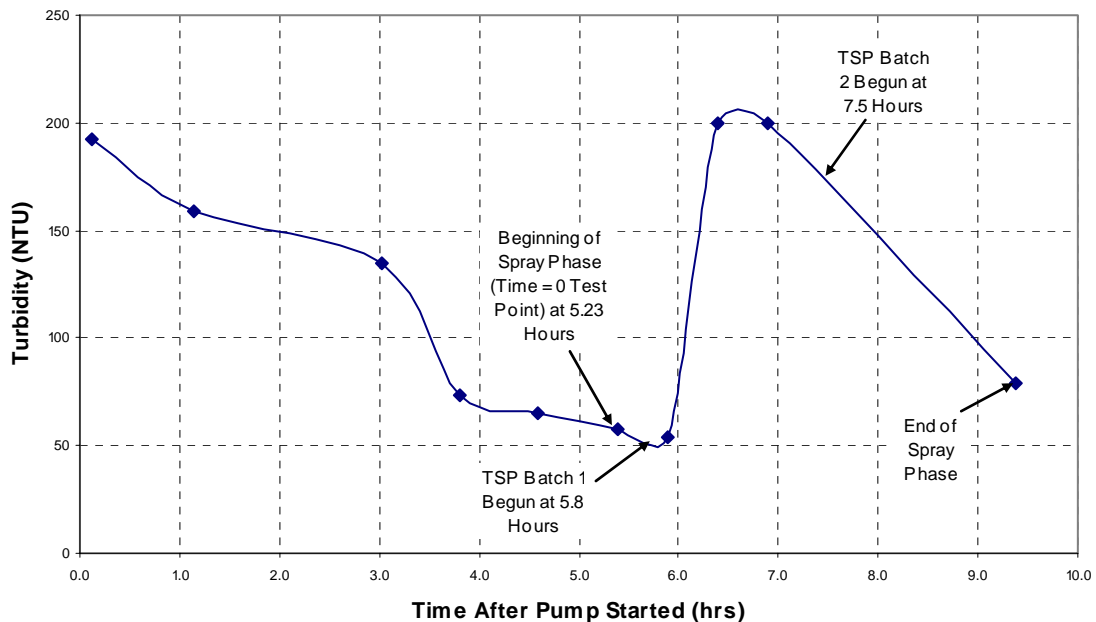


Figure 3-4. Day 1 turbidity results.

Figure 3-5 depicts the evolution of turbidity at 23°C and 60°C throughout Test #3. The trend of each curve exhibits an initial spike during the addition of Batch 1 chemicals,

followed by a sharp decline to the Day 1 test point and steady behavior from then on. The turbidity values on Day 15 were slightly higher, but no direct cause has been identified. The Day 15 values were 3.9 NTU and 3.5 NTU for the 60°C and 23°C samples, respectively. Thereafter, the turbidity values decreased and remained steady.

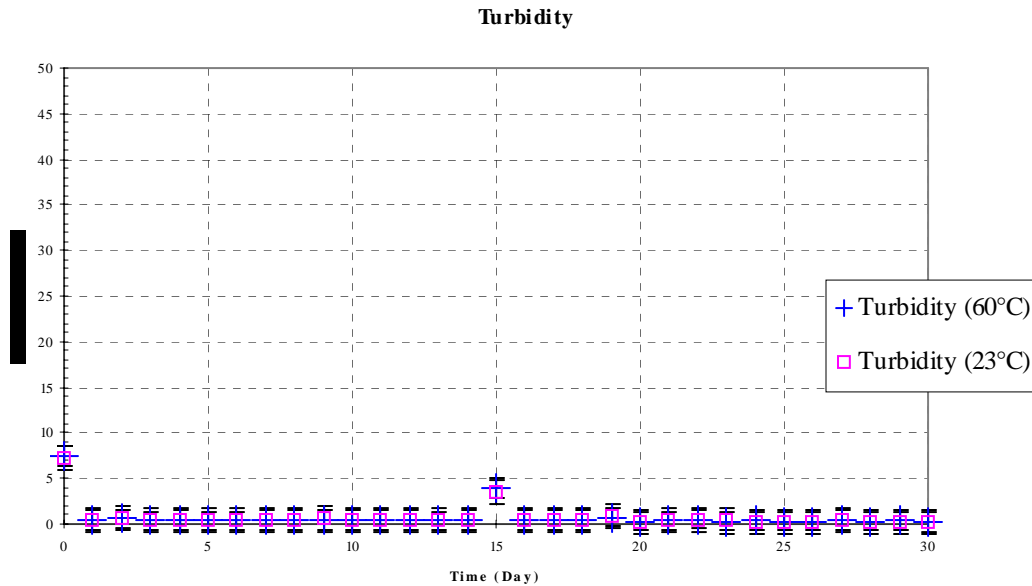


Figure 3-5. Daily turbidity results.

Total Suspended Solids: TSS are measured by filtering a volume of approximately 500 mL through an in-line filter directly at the sample tap. The selected equipment ensures that TSS measurements are not affected by temperature-dependent or time-dependent precipitation reactions that may occur once the process solution is removed from the tank. Figure 3-6 presents Test #3 TSS data as the experiment progressed. The baseline TSS measurement was taken after the addition of latent debris but prior to the Batches 1 and 2 chemical additions. After the addition of the Batch 1 chemicals but prior to the addition of Batch 2 chemicals, a second TSS measurement (not shown on the graph) was taken, and the value was 268 mg/L. Although very high, it appeared to be a reasonable measurement because a large amount of particles was suspended in solution at that time. Four hours into the test, another TSS measurement was taken, and that value was 73.2 mg/L. At that time, fewer particles were seen suspended in solution. After 24 hours, the TSS measurement dropped to 13.9 mg/L, where it leveled out for the rest the test.

Although TSS remained fairly stable over the entirety of the test, TSS measurements from six different days deviated from the trend. The Day 6 TSS measurement was slightly higher at 20.6 mg/L, which was not unexpected because the sample was taken right after the return of excess test solution to the tank. The return of the excess test solution caused some of the particles that were sitting at the bottom of the tank to be become resuspended in the solution, a situation that was reflected in the final measurement. The Day 15 and Days 24–27 measurements were higher than the test

average of approximately 13.4 mg/L that was observed for the majority of the test. The TSS filter weights for these days were confirmed, and there is no direct explanation for these higher values.

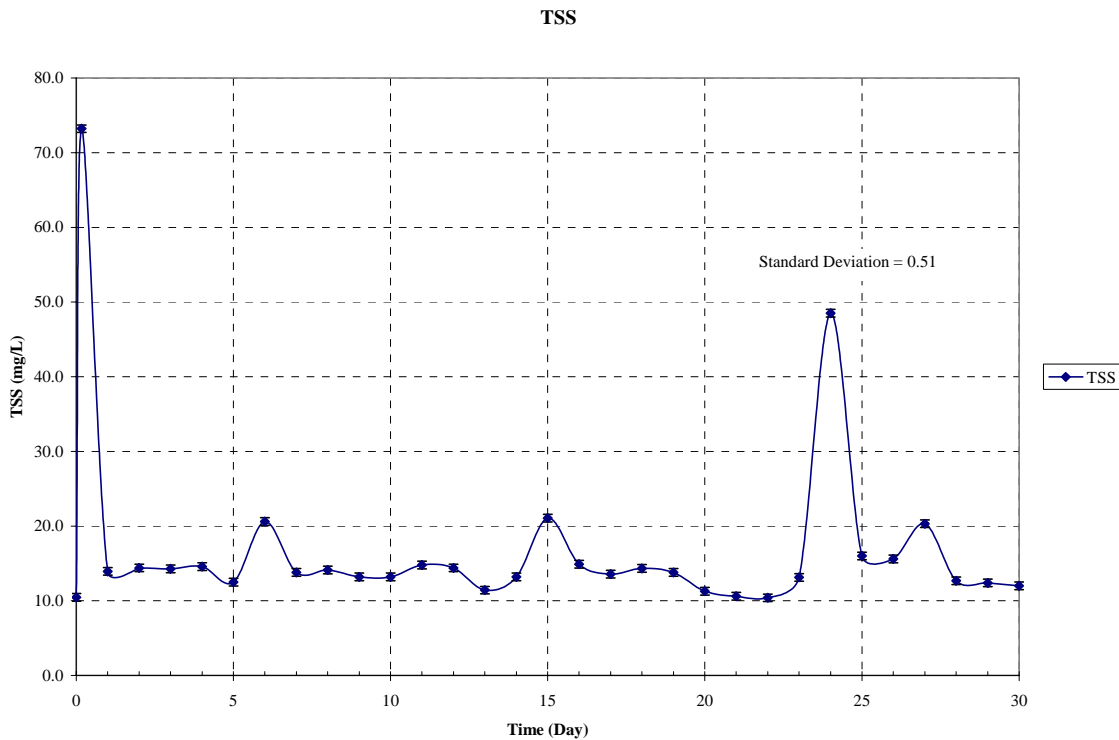


Figure 3-6. Test #3 TSS results.

Kinematic Viscosity: Kinematic viscosity was measured with a Cannon-Fenske capillary viscometer. Viscosity was measured on unfiltered samples, each at a temperature of 60°C ± 1.0°C (140°F ± 1.8°F) and 23°C ± 2.0°C (73.4°F ± 3.6°F). Figure 3-7 shows the viscosity results. Water’s viscosity is highly sensitive to temperature, and the allowed temperature range results in a variation of viscosity of 2.9% between 59°C (138.2°F) and 60°C (141.8°F) and 9.3% between 21°C (69.8°F) and 25°C (77.0°F). For this reason, temperature was measured to a 0.1°C accuracy with a National Institute of Standards and Technology (NIST)-traceable thermometer for all viscosity measurements. Also, the measured viscosity values were corrected to common temperatures to facilitate comparisons. The corrected temperatures were 60.0°C (140°F) and 23.0°C (73.4°F).

Viscosity remained relatively constant throughout Test #3. The viscosity at 60.0°C (140°F) remained at a value of approximately 0.49 mm²/s, and the 23.0°C (73.4°F) measurements remained around 0.95 mm²/s. These constant viscosity values are consistent with the steady water conditions in the test. Figure 3-7 shows the viscosity values through the course of the test.

Viscosity 60°C and 23°C

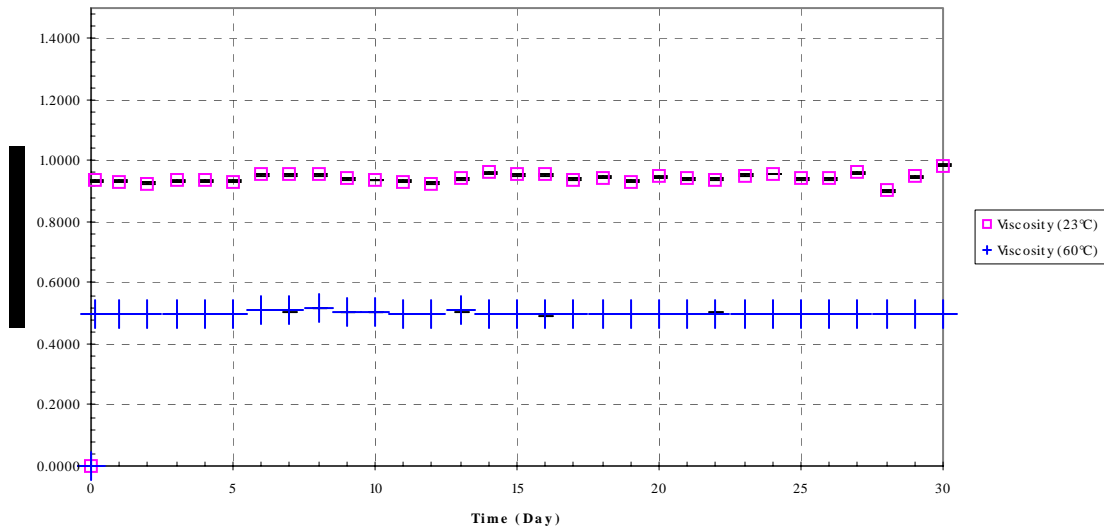


Figure 3-7. Viscosity at 60°C and 23°C.

3.2.2. Metal Ion Concentration

ICP results for Test #3 are displayed in Figures 3-8 through 3-16, which are daily sample results. Table 3-1 contains ICP results for elements that were analyzed on Days 1, 4, 15, and 30. Table 3-1 shows that chloride, boron, lead, lithium, and potassium concentrations remained relatively constant throughout the test. An examination of the figures reveals that phosphate, copper, iron, aluminum, and zinc are present in trace amounts, below 1 mg/L. It also can be seen that calcium, silica, sodium, and magnesium are present in higher concentrations.

Table 3-1. ICP Results for Selected Elements

Unfiltered Samples					
Sample Time	Chloride	Boron	Lead	Lithium	Potassium
	mg/L				
Baseline	No data	2090	0.05	0.22	No data
4 Hours	111	2180	No data	0.26	17.3
Day 1	105	2160	0.04	0.250	19.8
Day 15	113	No data	0.03	0.23	27.1
Day 30	110	2550	0.03	0.18	25.7

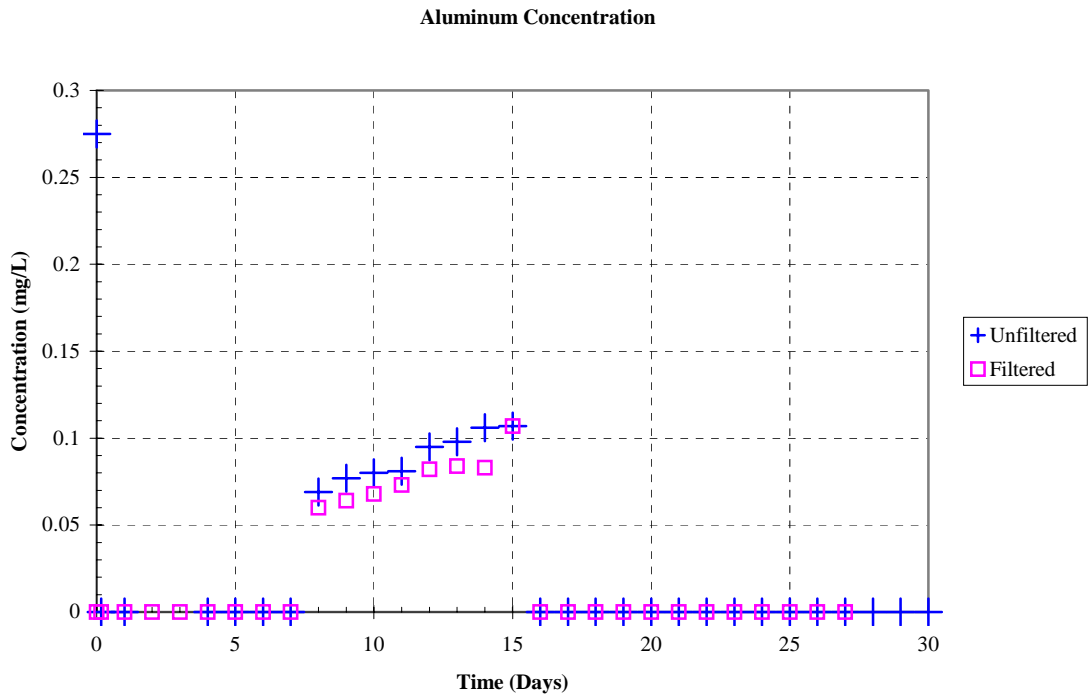


Figure 3-8. Aluminum concentration.

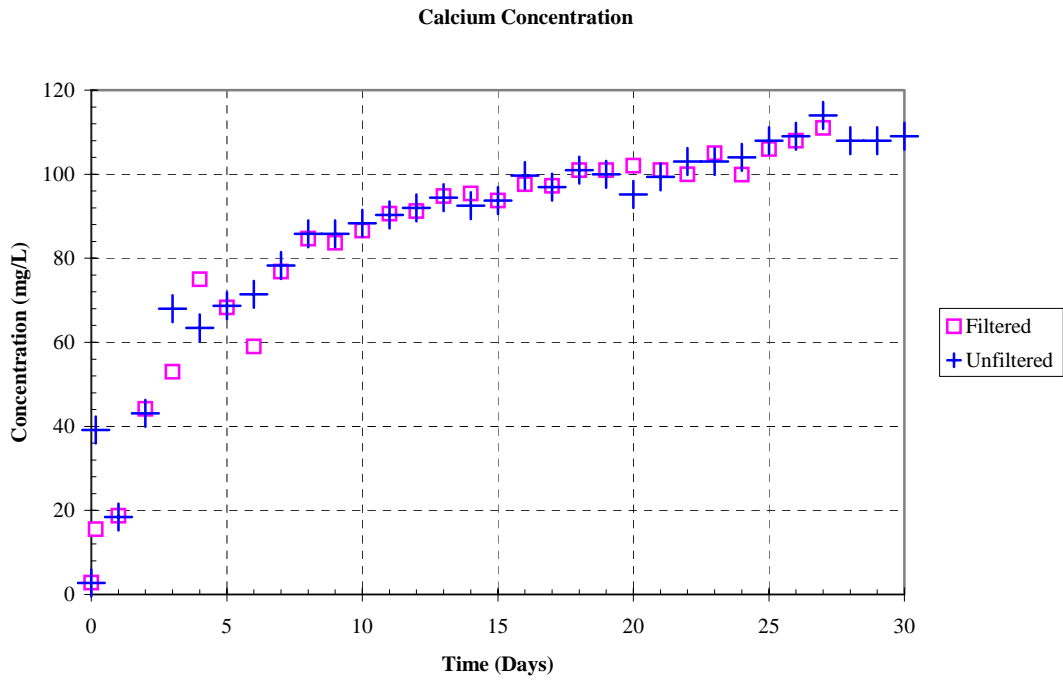


Figure 3-9. Calcium concentration.

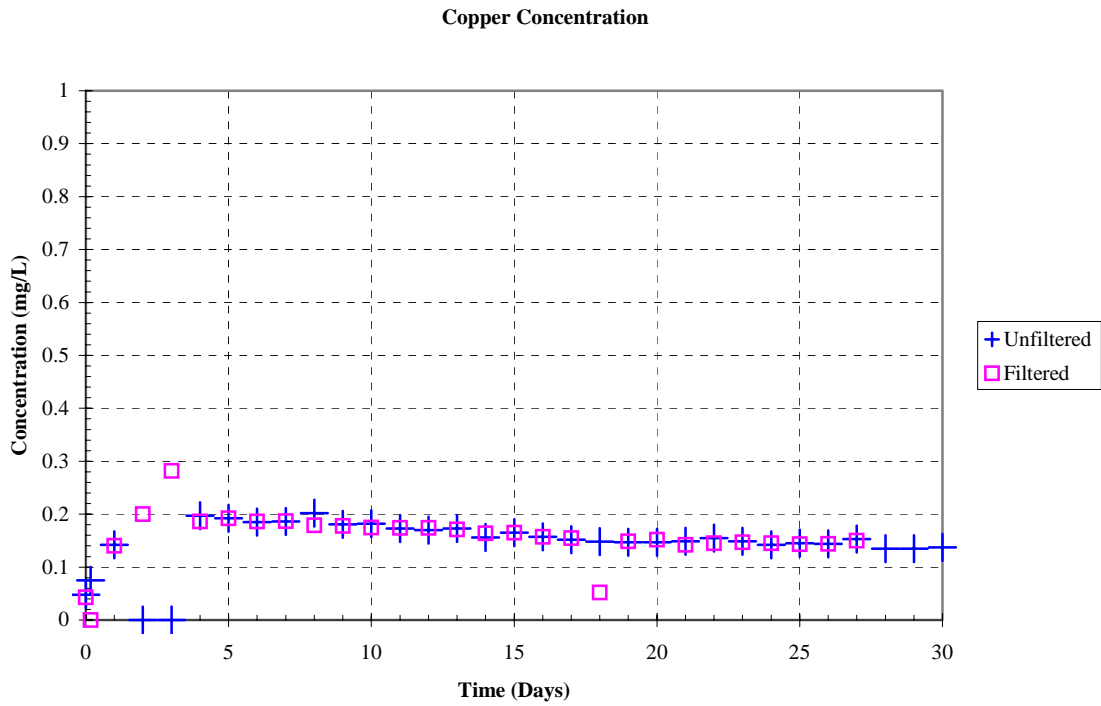


Figure 3-10. Copper concentration.

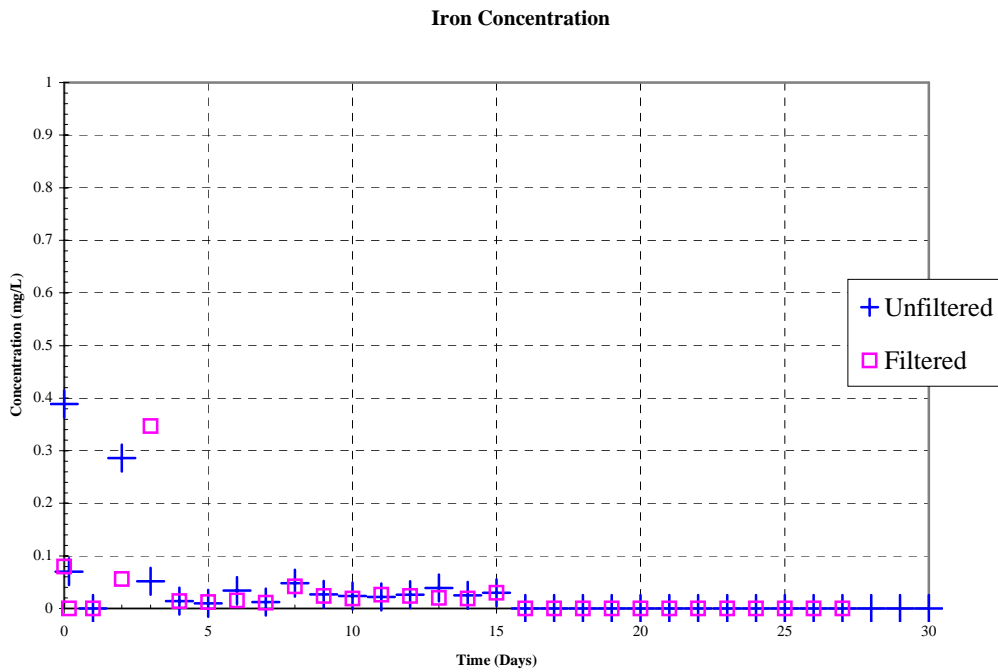


Figure 3-11. Iron concentration.

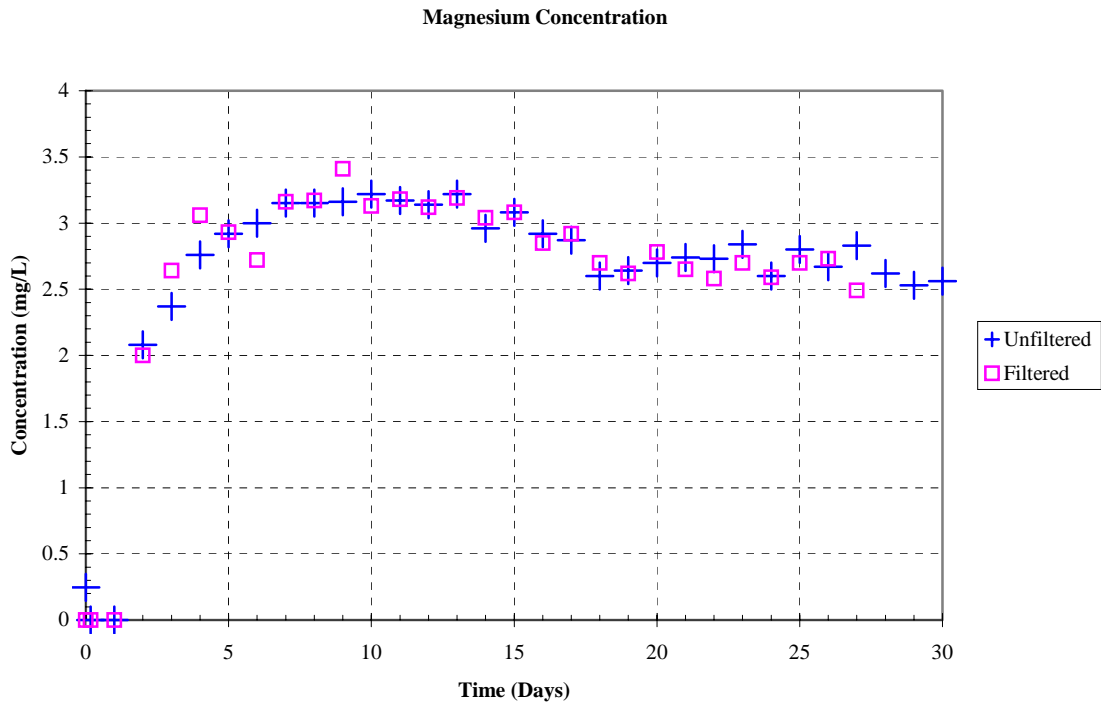


Figure 3-12. Magnesium concentration.

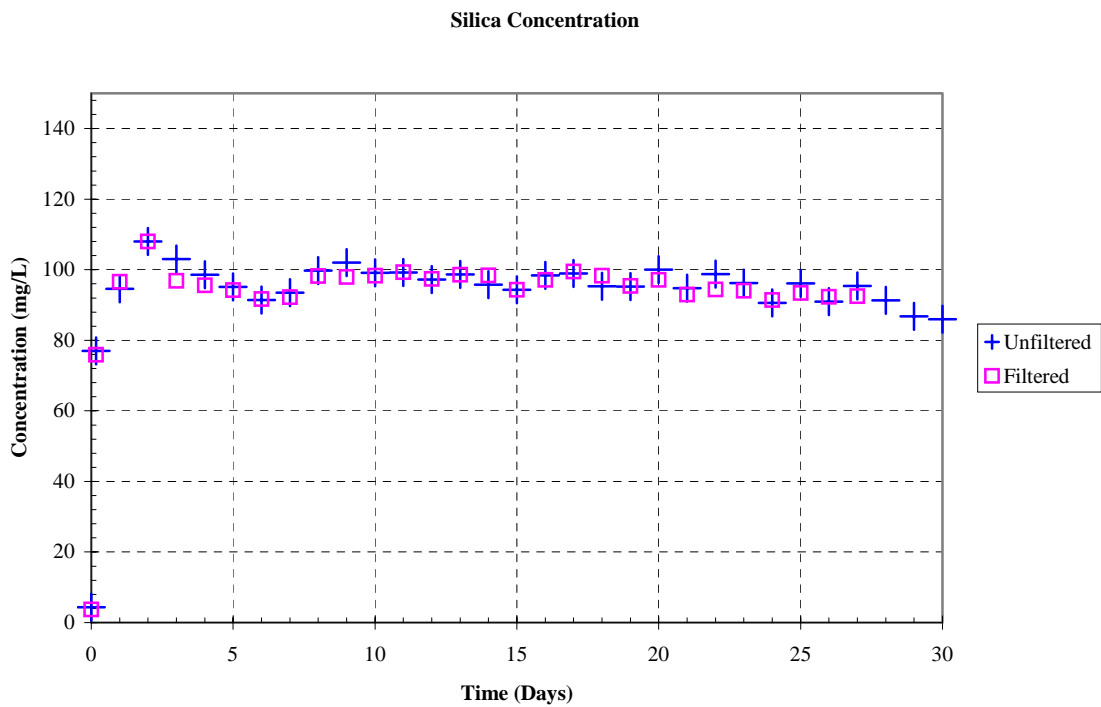


Figure 3-13. Silica concentration.

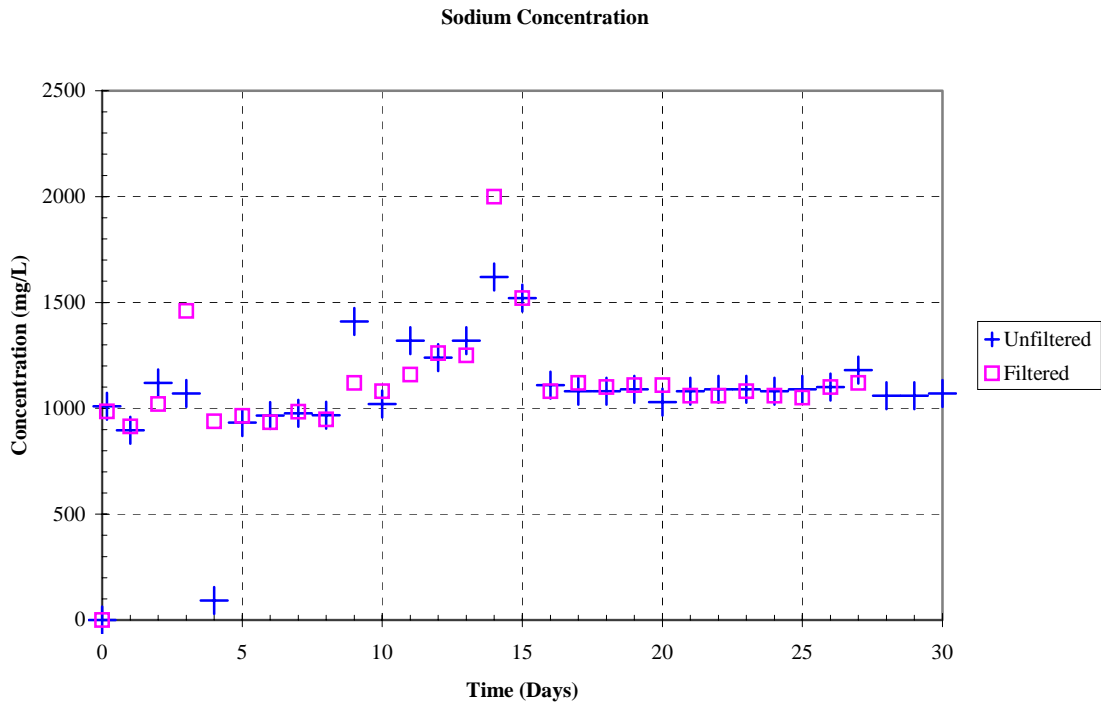


Figure 3-14. Sodium concentration.

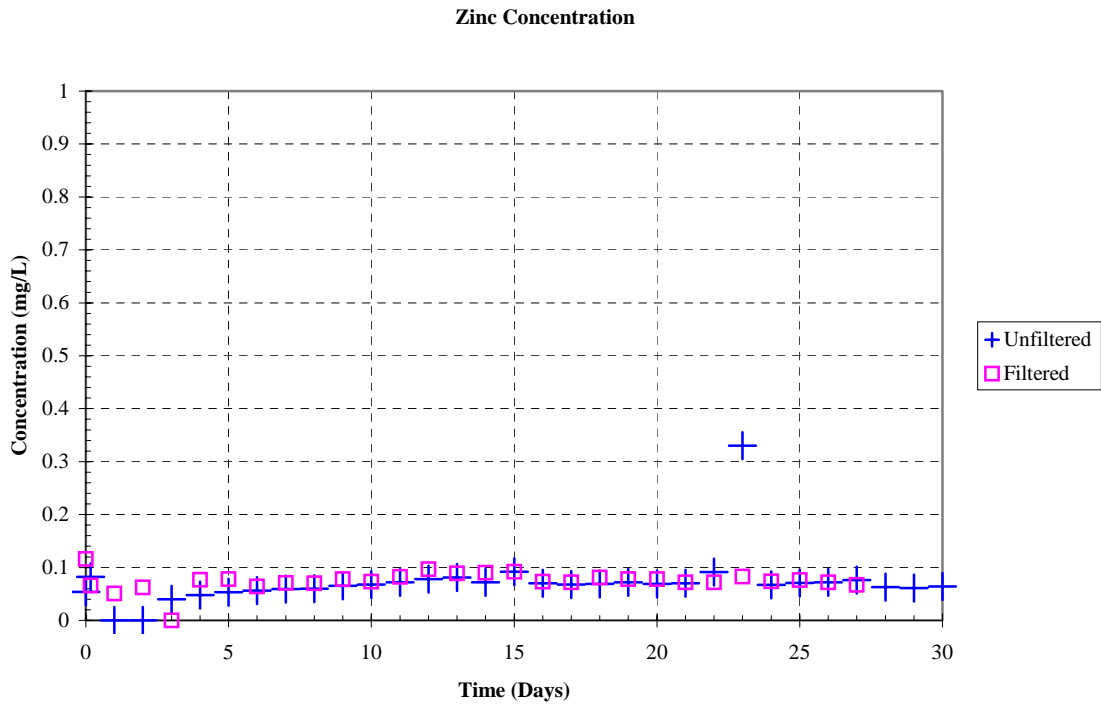


Figure 3-15. Zinc concentration.

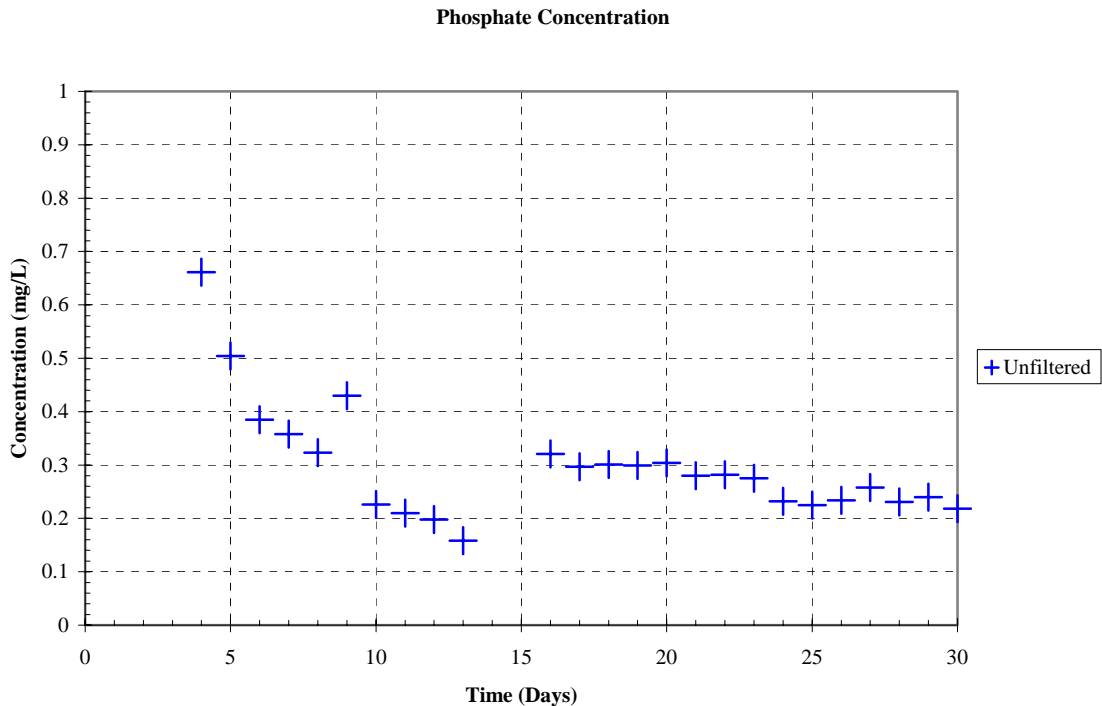


Figure 3-16. Phosphate concentration.

3.2.3. Optical/TEM Images from Filtered and Unfiltered Samples

TEM/EDS and diffraction patterns analysis were performed for Test #3 Day 4, Day 15, and Day 30 filtered and unfiltered solution samples. The filtered solution samples were passed through a 0.7- μm fiberglass filter at 60°C. The unfiltered solution samples were extracted from the tank directly. The results showed no significant diffraction pattern, due to the amorphous nature of the samples. In addition, no significant presence of colloidal particles was observed. Appendix J contains the TEM data.

3.3 Insulation

Test #3 was the first ICET test that included cal-sil insulation in addition to NUKON™ fiberglass samples. The fiberglass samples received more thorough investigations, with samples removed from the tank on Day 4, Day 15, and Day 30. The cal-sil was analyzed based on its Day 30 character. In addition, analyses were performed on the raw cal-sil, both baked and not baked.

3.3.1 Deposits in Fiberglass Samples

The fiberglass debris was contained in SS mesh bags to minimize migration of the fiberglass throughout the tank and piping. Small mesh envelopes, approximately 4 in. square, containing approximately 5 g of fiber, were pulled out of the tank periodically for SEM examination. These sample envelopes were placed in a range of water flow

conditions, but none experience direct water flow through the fiber. All were thoroughly immersed in the test solution until they were recovered from the tank.

After the fiberglass had been exposed in the test solution for some time, deposits have formed throughout the fiber matrix and appear to be chemically originated and/or physically retained or attached. Because there was no significant water flow directly through the fiber, the migration of particles into the fiberglass interior is likely insignificant. Therefore, the deposits found in the interior of the fiberglass samples were likely chemically originated, i.e., formed through precipitation. However, particulate deposits may have been physically retained or attached on the fiberglass exterior.

There were four fiberglass locations in the tank that were examined in this test, including the low-flow area, the high-flow area, the birdcage, and the drain collar. (See Subsection 2.4.1.1 for descriptions of the fiberglass samples.) Both the exterior and the interior of the fiberglass samples from each location were examined. Subsections 3.3.1.1 through 3.3.1.7 give the ESEM/SEM/EDS results according to the location of the fiberglass samples in the tank and the sampling date. The different samples include Day 4 low-flow, Day 15 low-flow, Day 15 high-flow, Day 30 low-flow, Day 30 high-flow, Day 30 drain collar, and Day 30 birdcage. The corresponding figures are Figures 3-17 through 3-77. Additional micrographs of fiberglass samples are presented in Appendices A, B, and C.

In general, the deposits appear to be more prevalent and/or to develop as the test proceeds. The particulate/flocculent deposits on Day 4 and Day 15 high- and low-flow fiberglass samples were likely originated through chemical precipitation during the drying process of the samples. The figures show that the deposits are pervasive throughout the fiber. Comparing probe SEM results with ESEM results reveals that much more significant flocculence was found with probe SEM analysis, possibly because ESEM samples were much moister than were probe SEM samples during the examination process. The drying process caused the formation of the flocculence through chemical precipitation.

Far more particulate deposits were found on Day 30 exterior samples, especially on the drain collar and the birdcage fiberglass samples, which showed the development of a continuous coating on their exteriors. The deposits on these samples include particulate deposits that were likely physically captured or attached. "Physically captured" means the deposits existed/formed in bulk solution first followed by attachment on the fiberglass. "Chemically originated" means the deposits formed directly in the fiberglass. Based on EDS analysis, the particulate deposits on the fiberglass exterior may be classified into two categories according to P and Si content. Particulate deposits of lower P and higher Si content were likely cal-sil particles; particulate deposits of high P and lower Si were likely composed of $\text{Ca}_3(\text{PO}_4)_2$ precipitates. Both kinds of deposits may be physically transported and/or deposited onto the fiberglass sample exterior. However, different from the exterior, the interior fiberglass samples were relatively clean. This result suggests that almost all of the particulate deposits were physically retained at the fiberglass exterior. The deposits in the fiberglass interior were probably formed by chemical precipitation during the sample drying process for ESEM/SEM analysis. EDS analysis indicates that

the flocculent deposits contained insignificant amounts of P, meaning that the deposits did not have a direct relation to the white gel (cream) that was seen forming during the injection of TSP on the first day of the test.

3.3.1.1 Day 4 Low-Flow Fiberglass Samples

Since there was no significant water flow through the fiberglass samples during the test, particle migration from the solution into the fiberglass interior is insignificant. Based on the ESEM/SEM results, deposits were found on both the exterior and the interior of the low-flow fiberglass samples after test Day 4. Because these deposits formed continuously among glass fibers and even coated the fibers, it is likely that these deposits are of chemical origin instead of being physically attached/retained. Comparing ESEM and SEM results for the same fiberglass sample reveals that some dark deposits were found with ESEM results only. However, when the fiberglass samples were totally dried for SEM analysis, only white flocculence deposits were found, possibly because the fiberglass samples were semidried (partially dehydrated) with ESEM analysis. It is likely that the dark deposits began to precipitate out when the fiberglass samples were partially dehydrated during ESEM analysis. However, these dark deposits were totally precipitated out and dehydrated for SEM analysis. As a result, a significant amount of the white flocculence were found with SEM results. EDS results show that the deposits were commonly composed of O, Si (possible), Na, Ca, and small amounts of Mg, Al, B, and P, whether they were found on the exterior or interior of the fiberglass samples. The uncertainty of Si is due to the fact that x-ray may be scattered and/or penetrate the deposits. As a result, the signal may be reflected to the detector by the fiberglass in addition to the deposits. Therefore, when Si peaks show up, the existence of Si in the deposits cannot be confirmed or excluded. In addition, it should be noted that the deposits contained insignificant amounts of P, which means that the deposits did not have a direct relation to the white particles observed in the tank during TSP injection on the first day of the test.

Comparing interior and exterior fiberglass samples reveals no significant difference in the amount of deposits, again probably because of a chemical origin for the deposits. Chemical precipitation occurs to the same degree on both exterior and the interior fiberglass samples. Figures 3-17 through 3-27 show the Day 4, low-flow fiberglass results.

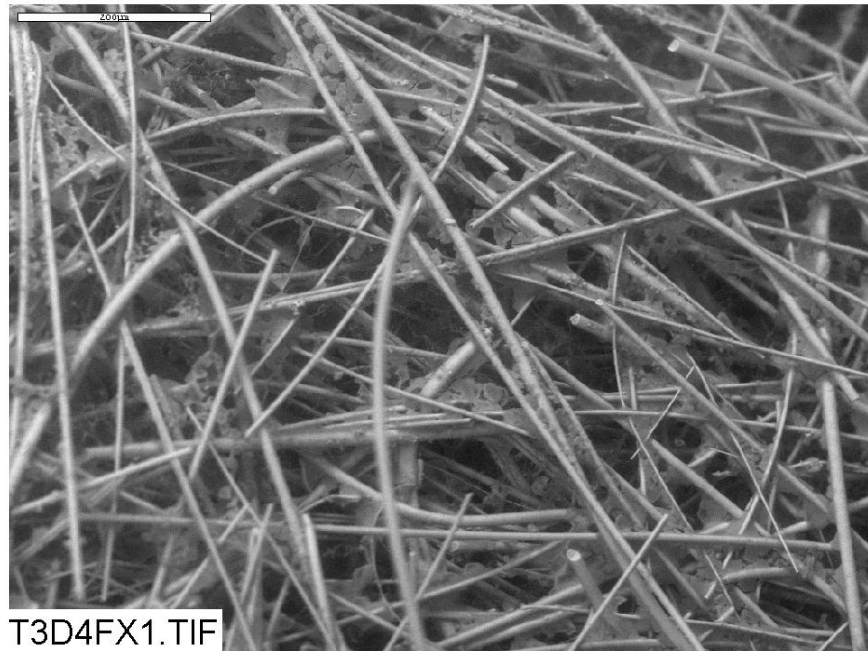


Figure 3-17. ESEM image of a Test #3 Day 4 low-flow exterior fiberglass sample, magnified 150 times. (T3D4FX1, 4/12/05)



Figure 3-18. ESEM image for a Test #3 Day 4 low-flow exterior fiberglass sample, magnified 1000 times. (T3D4FX2, 4/12/05)

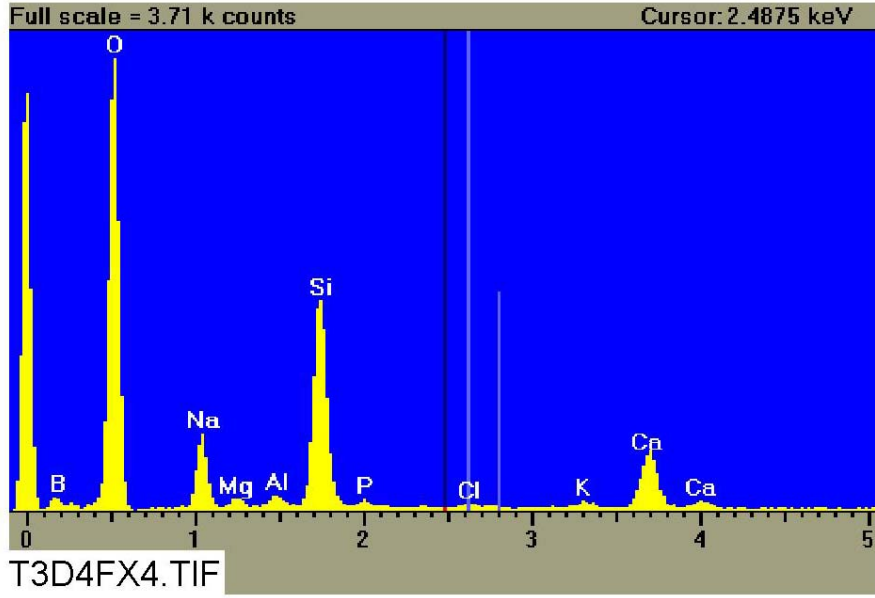


Figure 3-19. EDS counting spectrum (after calibration) for the deposits between the fibers on the ESEM image shown in Figure 3-18. (T3D4FX4, 4/12/05)

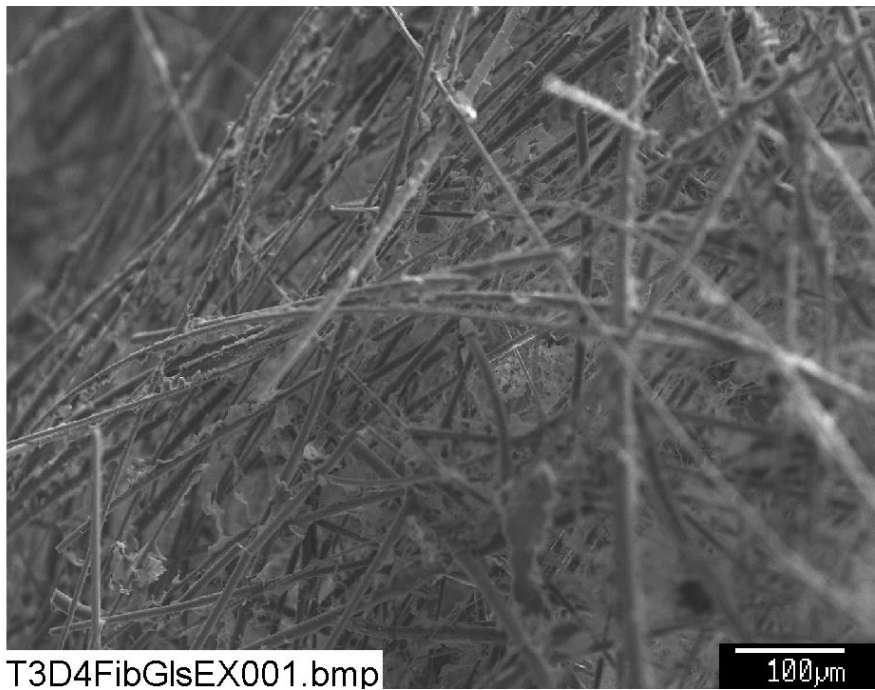


Figure 3-20. SEM image of a Test #3 Day 4 low-flow exterior fiberglass sample, magnified 150 times. (T3D4FibGlsEX001, 4/12/05)

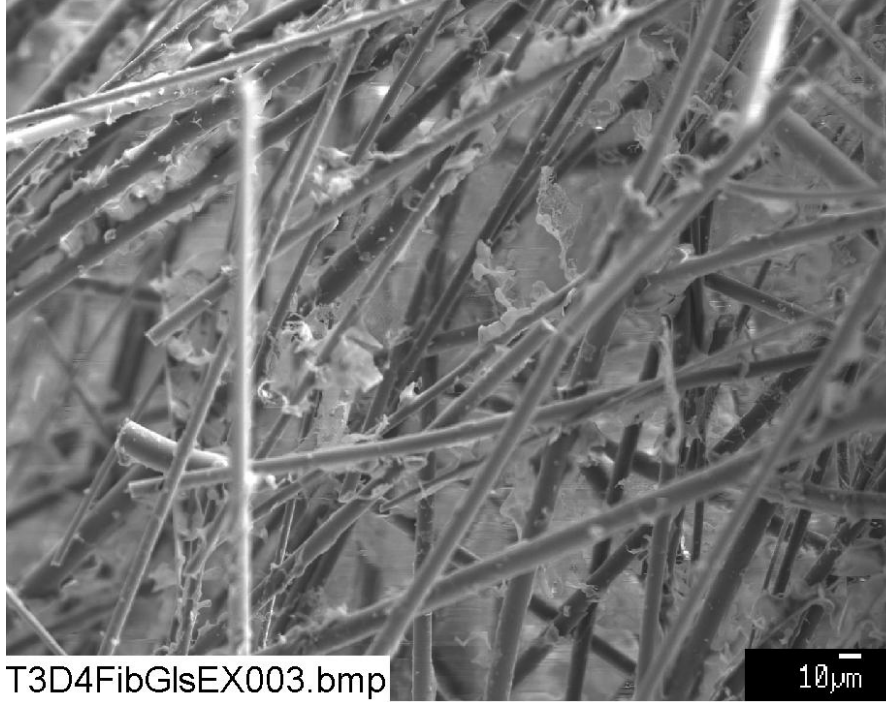


Figure 3-21. SEM image of a Test #3 Day 4 low-flow exterior fiberglass sample, magnified 300 times. (T3D4FibGlsEX003, 4/12/05)

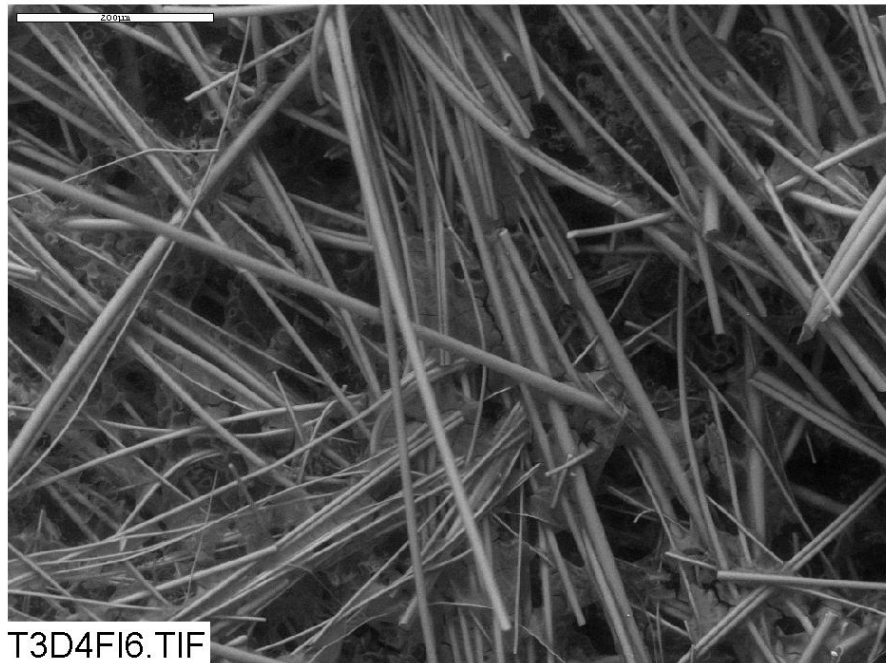


Figure 3-22. ESEM image of a Test #3 Day 4 low-flow interior fiberglass sample, magnified 150 times. (T3D4FI6, 4/12/05)

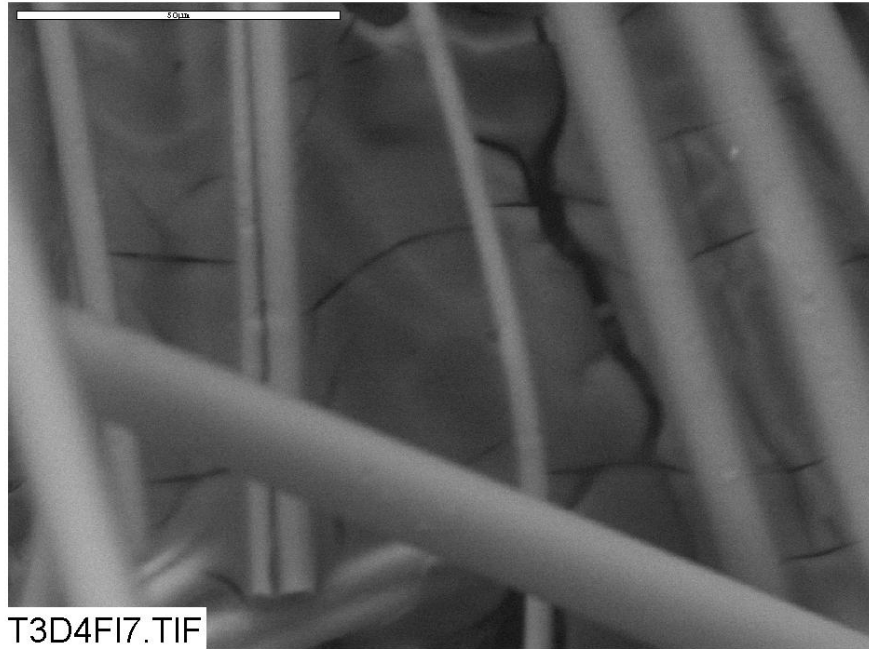


Figure 3-23. ESEM image of a Test #3 Day 4 low-flow interior fiberglass sample, magnified 1000 times. (T3D4FI7, 4/12/05)

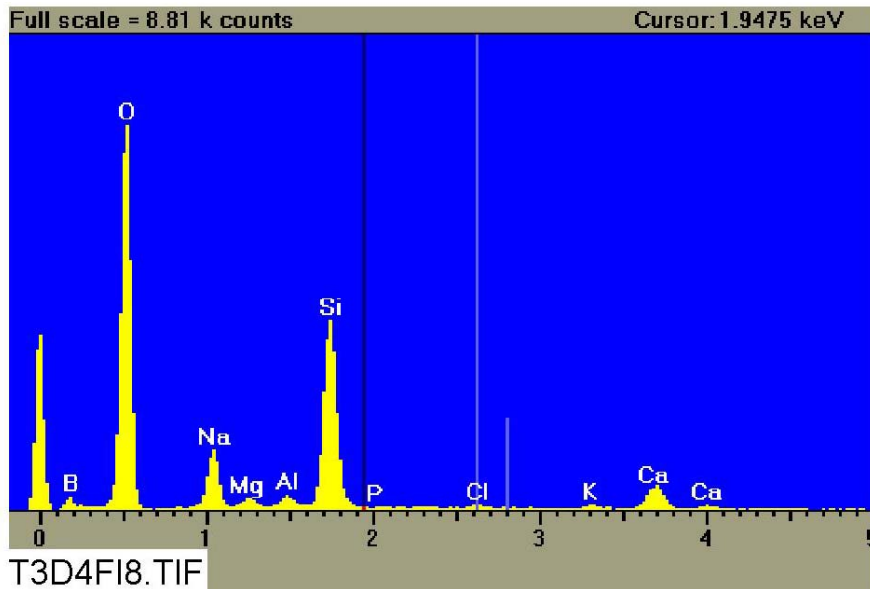


Figure 3-24. EDS counting spectrum (after calibration) for the deposits between the fibers on the ESEM image shown in Figure 3-23. (T3D4FI8, 4/12/05)

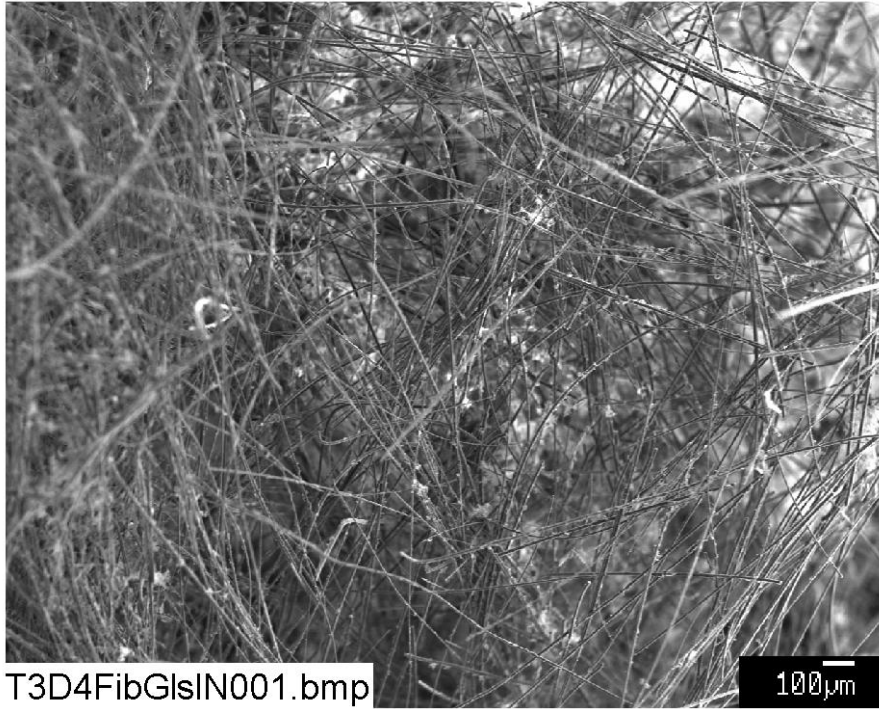


Figure 3-25. SEM image of a Test #3 Day 4 low-flow interior fiberglass sample, magnified 50 times. (T3D4FibGlsIN001, 4/12/05)

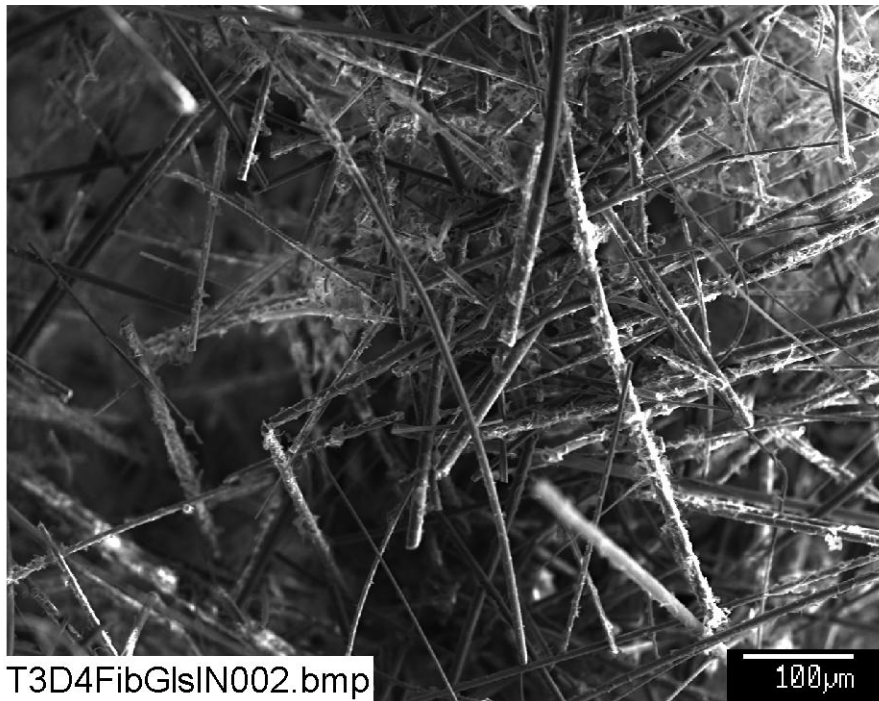


Figure 3-26. SEM image for a Test #3 Day 4 low-flow interior fiberglass sample, magnified 150 times. (T3D4FibGlsIN002, 4/12/05)

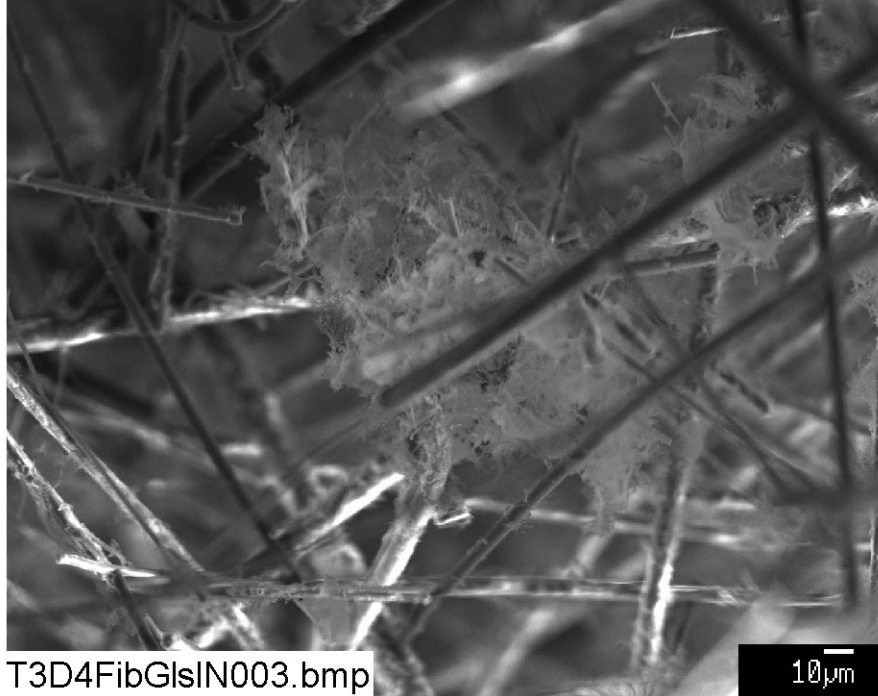


Figure 3-27. SEM image of a Test #3 Day 4 low-flow interior fiberglass sample, magnified 400 times. (T3D4FibGlsIN003, 4/12/05)

3.3.1.2 Day 15 Low-Flow Fiberglass Samples

As with Day 4 samples, dark deposits and white flocculence were found with ESEM and SEM results, respectively, on Day 15 low-flow fiberglass samples. There was no significant increase in the amount of deposits on Day 15 samples compared with Day 4 samples. Comparing the amount of deposits on the exterior and the interior Day 15 low-flow fiberglass samples revealed no significant difference. Again, EDS results show that the deposits on both of the exterior and the interior samples were commonly composed of O, Si (possible), Na, Ca, and small amounts of Mg, Al, B, and P, suggesting the deposits' likely chemical origin. Figures 3-28 through 3-38 show the Day 15 low-flow fiberglass results.

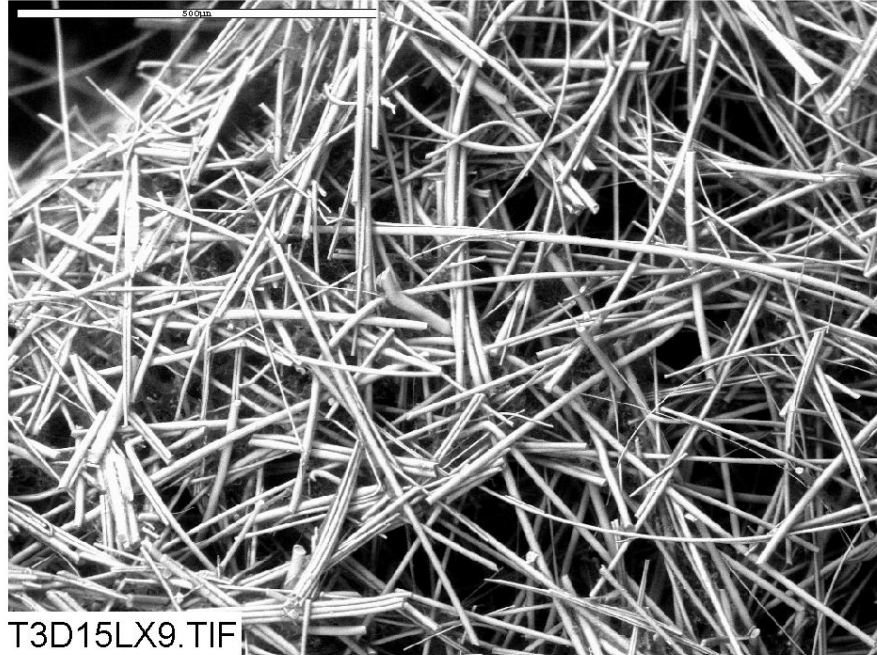


Figure 3-28. ESEM image of a Test #3 Day 15 low-flow exterior fiberglass sample, magnified 110 times. (T3D15LX9)

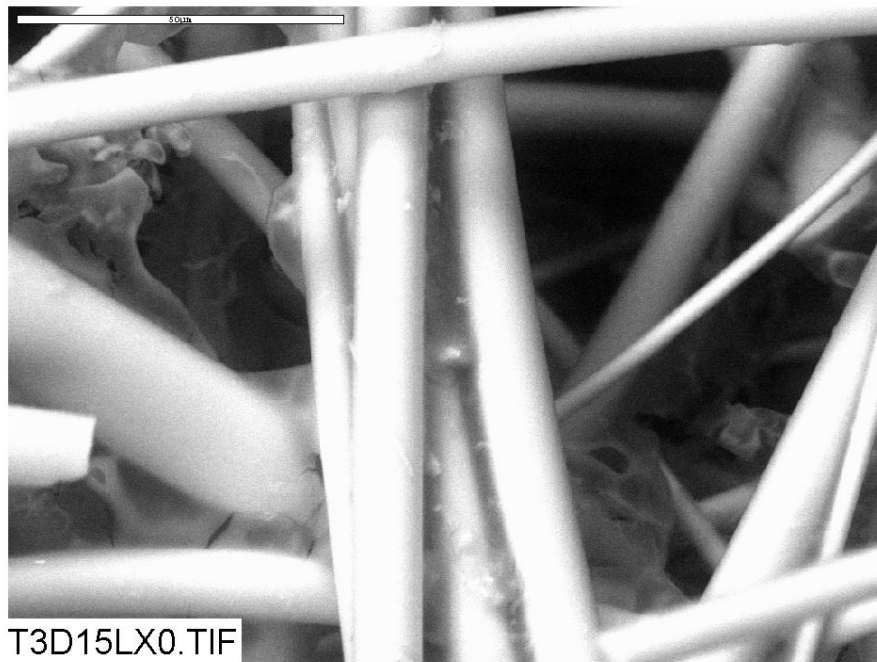


Figure 3-29. ESEM image of a Test #3 Day 15 low-flow exterior fiberglass sample, magnified 1000 times. (T3D15LX0)

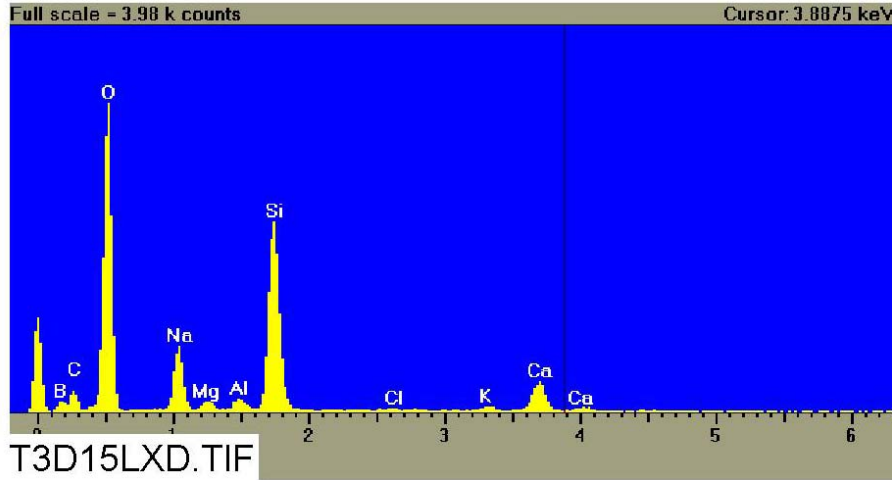


Figure 3-30. EDS counting spectrum for the deposits between the fibers on the ESEM image shown in Figure 3-29. (T3D15LXD)

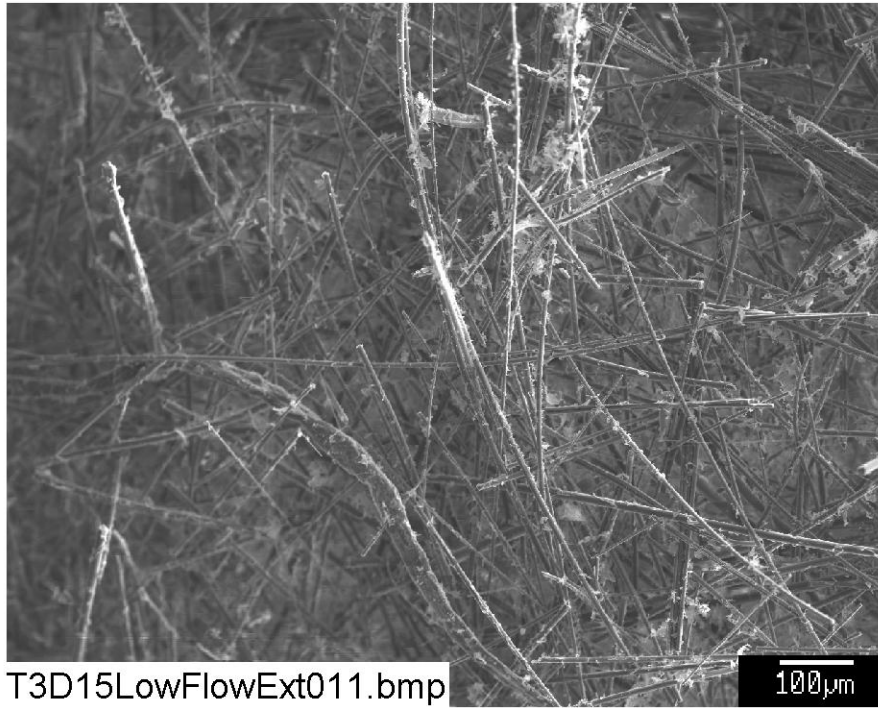


Figure 3-31. SEM image of a Test #3 Day 15 low-flow exterior fiberglass sample, magnified 100 times. (T3D15LowFlowExt011)



Figure 3-32. SEM image of a Test #3 Day 15 low-flow exterior fiberglass sample, magnified 1000 times. (T3D15LowFlowExt013)

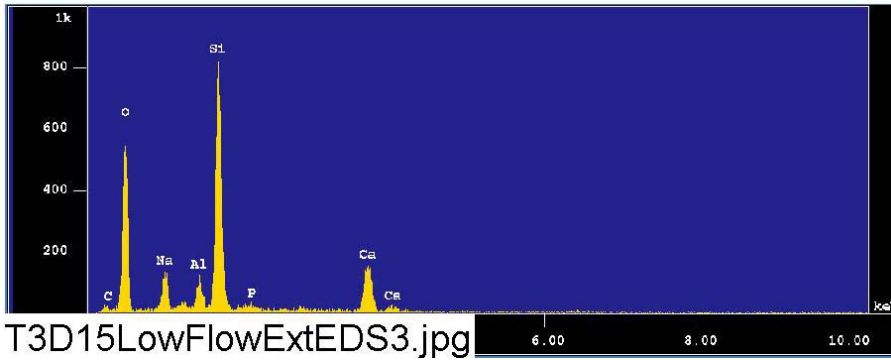


Figure 3-33. EDS counting spectrum for the flocculent deposits between the fibers on the SEM image shown in Figure 3-32. (T3D15LowFlowExtEDS3)

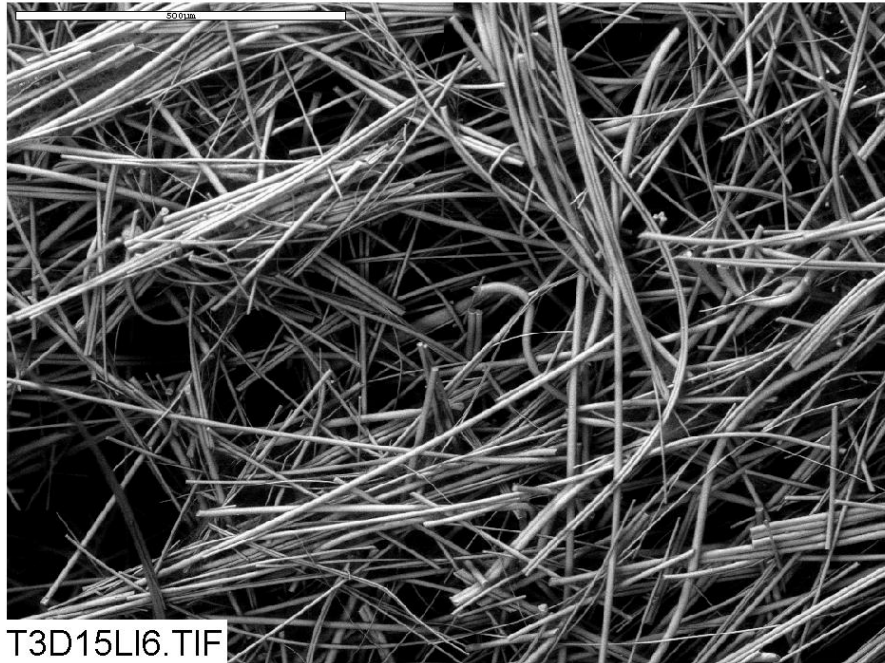


Figure 3-34. ESEM image of a Test #3 Day 15 low-flow interior fiberglass sample, magnified 100 times. (T3D15LI6)

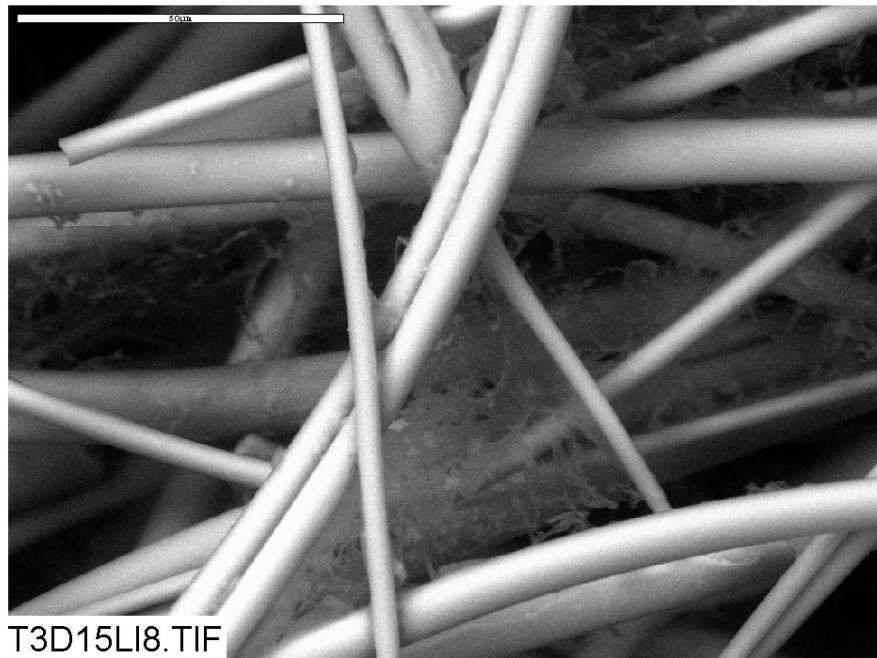


Figure 3-35. ESEM image of a Test# 3 Day 15 low-flow interior fiberglass sample, magnified 1000 times. (T3D15LI8)

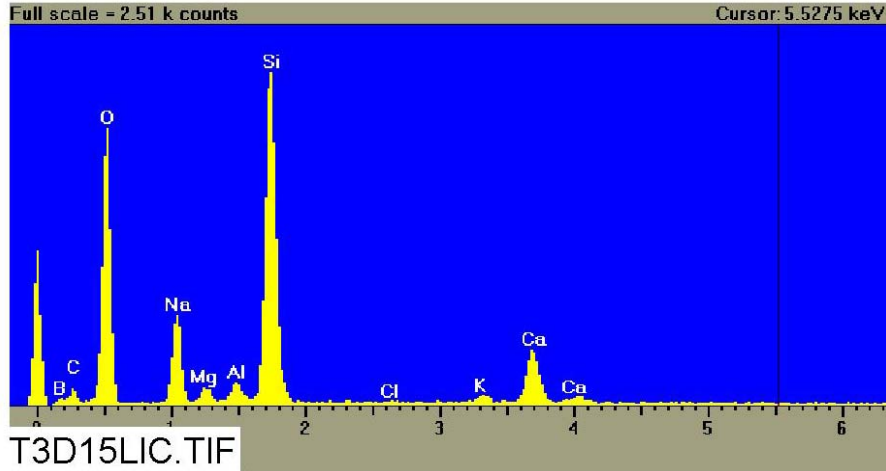


Figure 3-36. EDS counting spectrum for the flocculent deposits between the fibers on the ESEM image shown in Figure 3-35. (T3D15LIC)

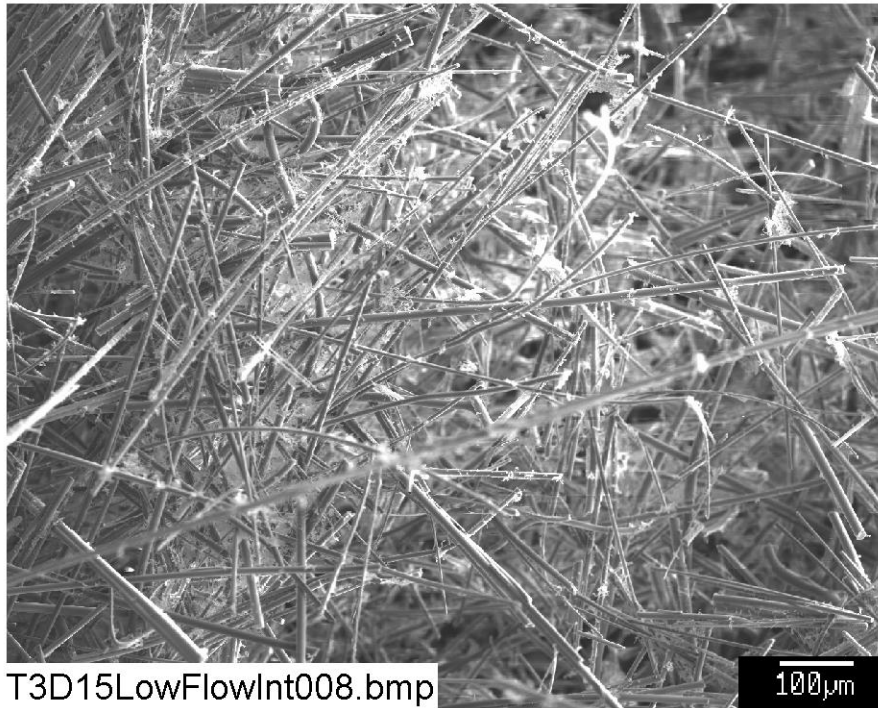


Figure 3-37. SEM image of a Test #3 Day 15 low-flow interior fiberglass sample, magnified 100 times. (T3D15LowFlowInt008)

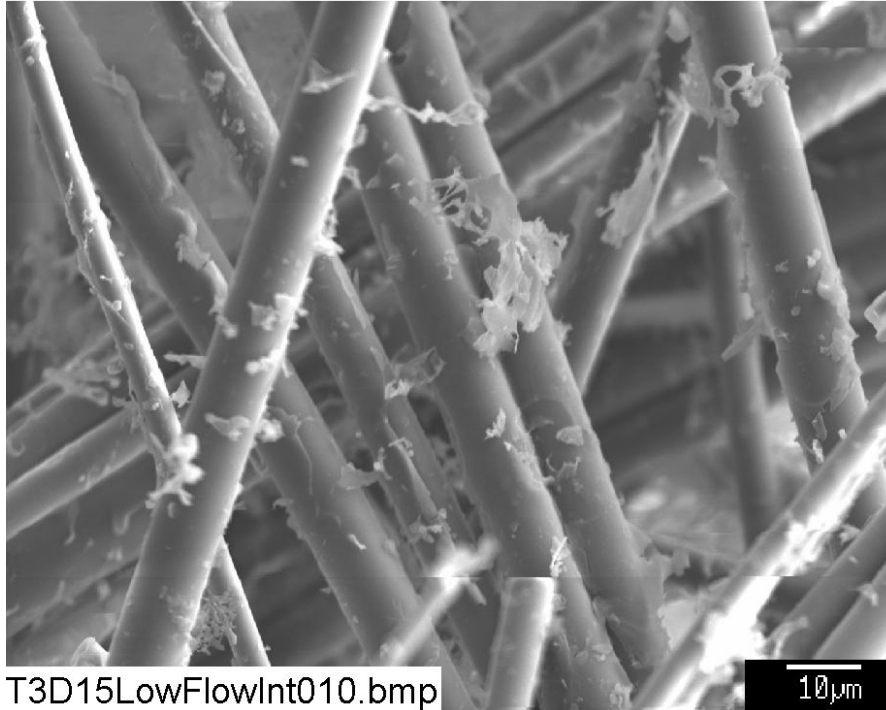


Figure 3-38. SEM image of a Test #3 Day 15 low-flow interior fiberglass sample, magnified 1000 times. (T3D15LowFlowInt010)

3.3.1.3 Day 15 High-Flow Fiberglass Samples

No significant difference was found between Day 15 high-flow and low-flow fiberglass samples, except for some large flat fibers found on the Day 15 high-flow exterior fiberglass samples (see lower left corner of Figure 3-39). These large flat fibers, which were likely from the submerged cal-sil samples (see Appendix H), were physically attached/retained on the exterior of the fiberglass samples. No large flat fibers were found in the interior of the fiberglass samples. Again, dark deposits and white flocculence were found with ESEM and SEM results, respectively, on Day 15 high-flow fiberglass samples. There was no significant difference in the amount of deposits on the exterior and interior fiberglass samples. Similarly, EDS results verified that the deposits on the exterior and interior samples were commonly composed of O, Si (possible), Na, Ca, and small amount of Mg, Al, B, and P, suggesting the deposits' likely chemical origin. Figures 3-39 through 3-50 show the Day 15 high-flow fiberglass results.

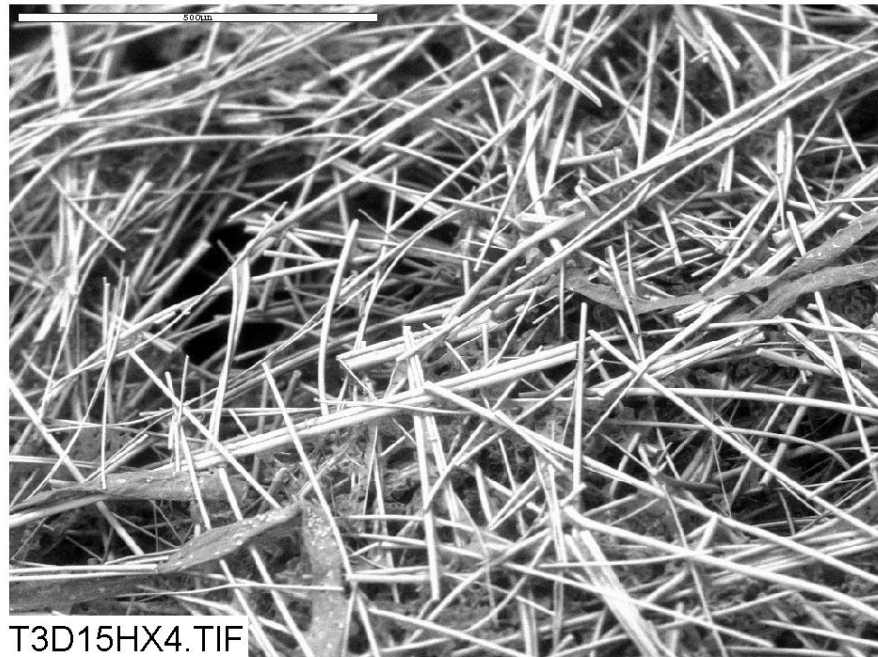


Figure 3-39. ESEM image of a Test #3 Day 15 high-flow exterior fiberglass sample, magnified 110 times. (T3D15HX4, 4/22/05)

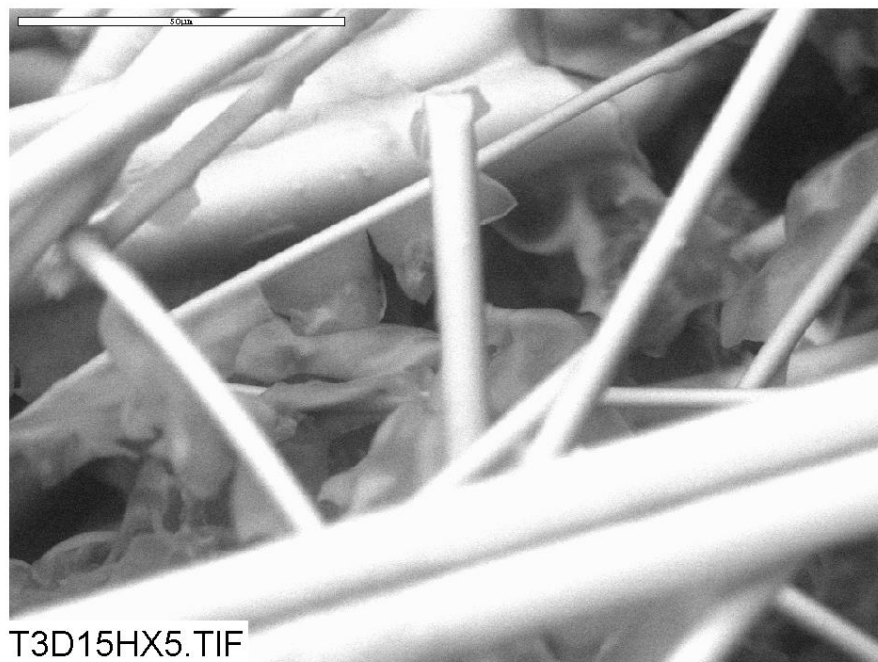


Figure 3-40. ESEM image of a Test #3 Day 15 high-flow exterior fiberglass sample, magnified 1000 times. (T3D15HX5, 4/22/05)

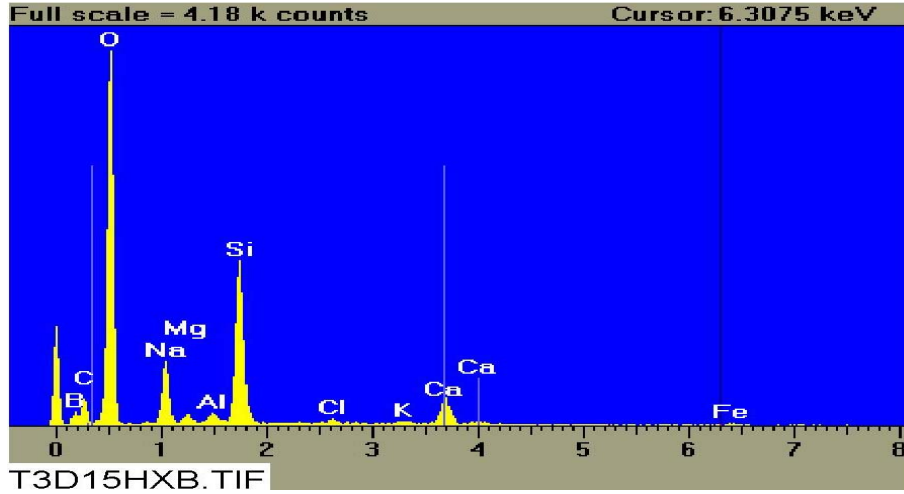


Figure 3-41. EDS counting spectrum for the deposits between the fibers on the ESEM image shown in Figure 3-40. (T3D15HIB, 4/22/05)

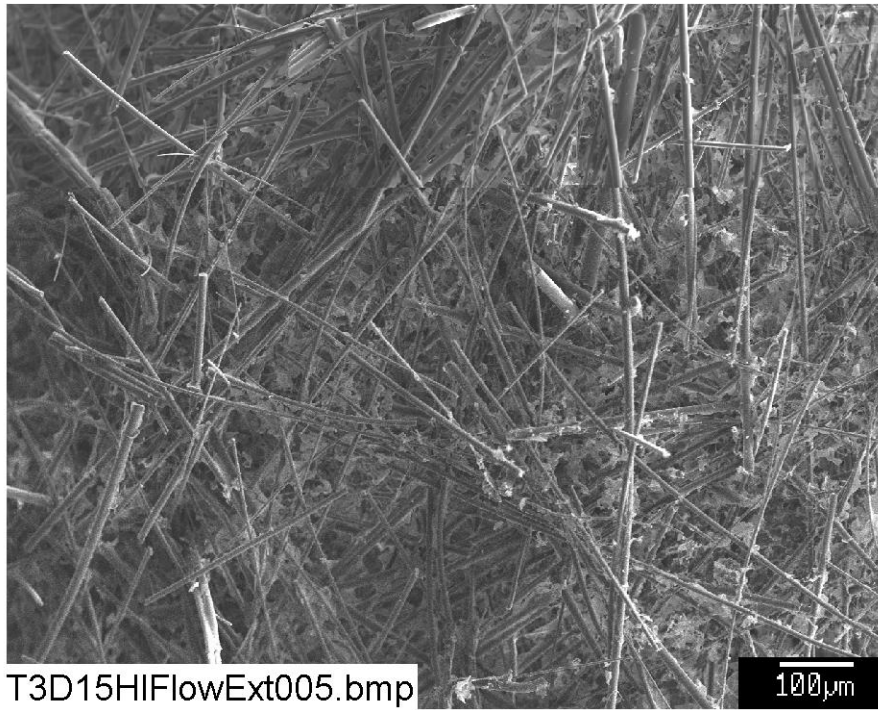


Figure 3-42. SEM image of a Test #3 Day 15 high-flow exterior fiberglass sample, magnified 100 times. (T3D15HIFlowExt005, 4/22/05)

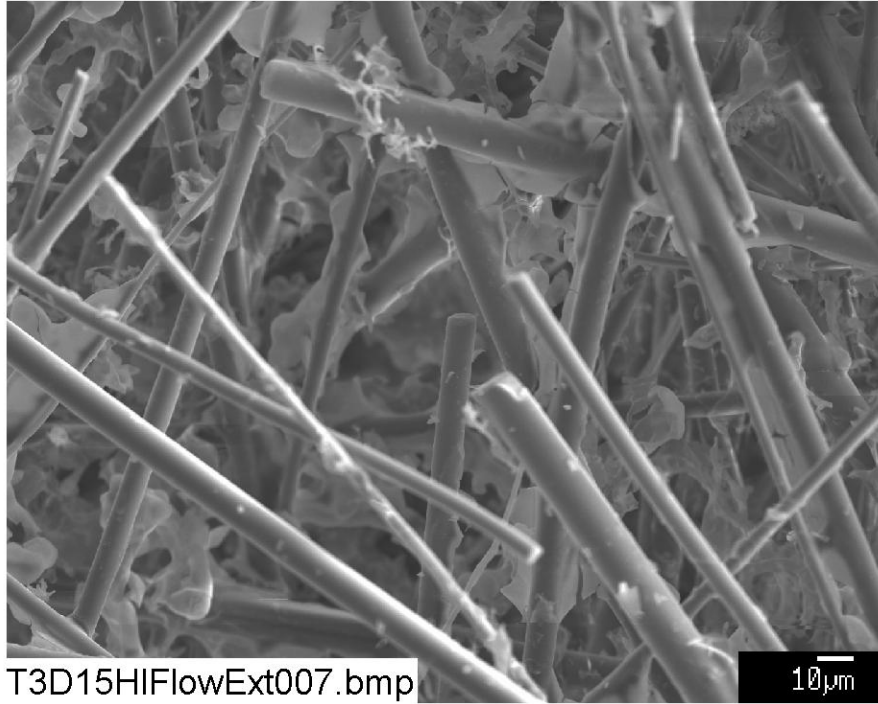


Figure 3-43. SEM image of a Test #3 Day 15 high-flow exterior fiberglass sample, magnified 500 times. (T3D15HiFlowExt007, 4/22/05)

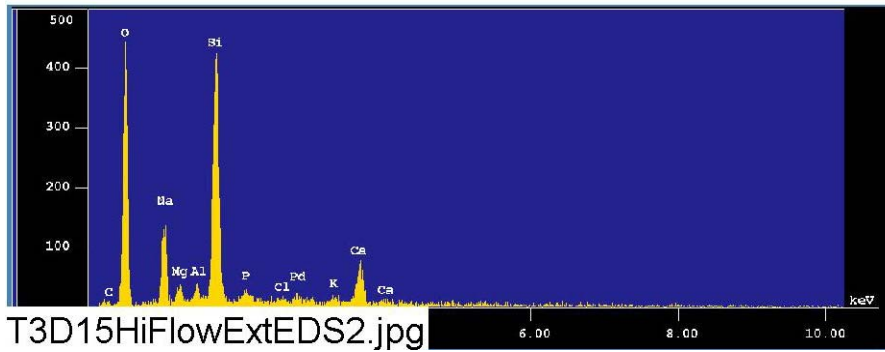


Figure 3-44. EDS counting spectrum for the flocculent deposits between the fibers on the SEM image shown in Figure 3-43. (T3D15HiFlowExtEDS2, 4/22/05)

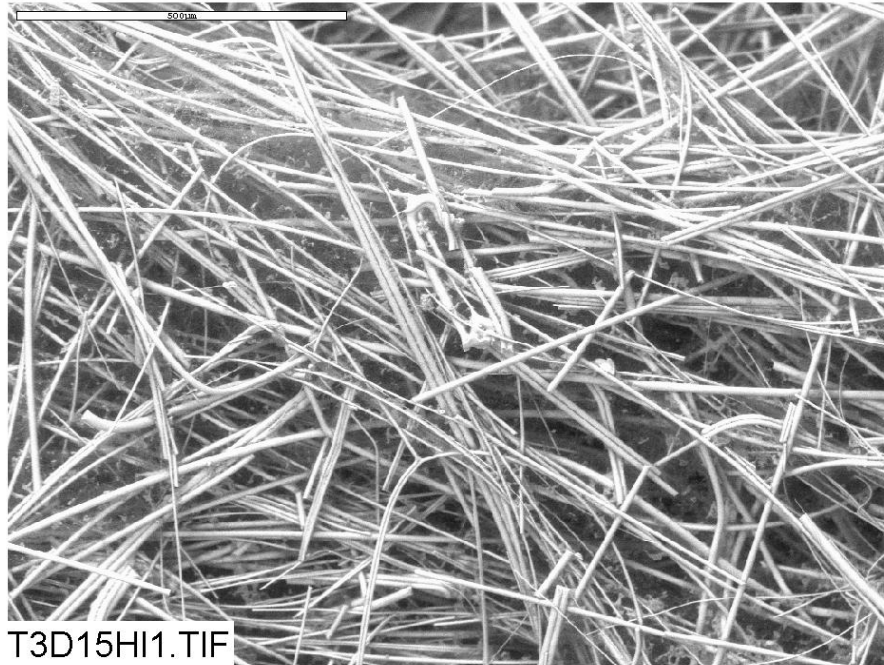


Figure 3-45. ESEM image of a Test #3 Day 15 high-flow interior fiberglass sample, magnified 100 times. (T3D15HI1, 4/22/05)

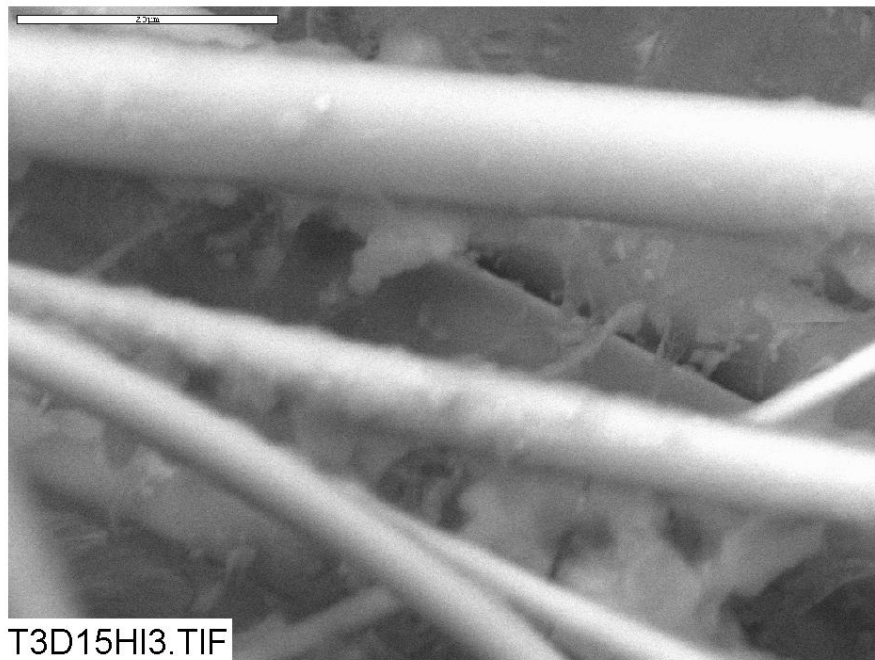


Figure 3-46. ESEM image of a Test #3 Day 15 high-flow interior fiberglass sample, magnified 2000 times. (T3D15HI3, 4/22/05)

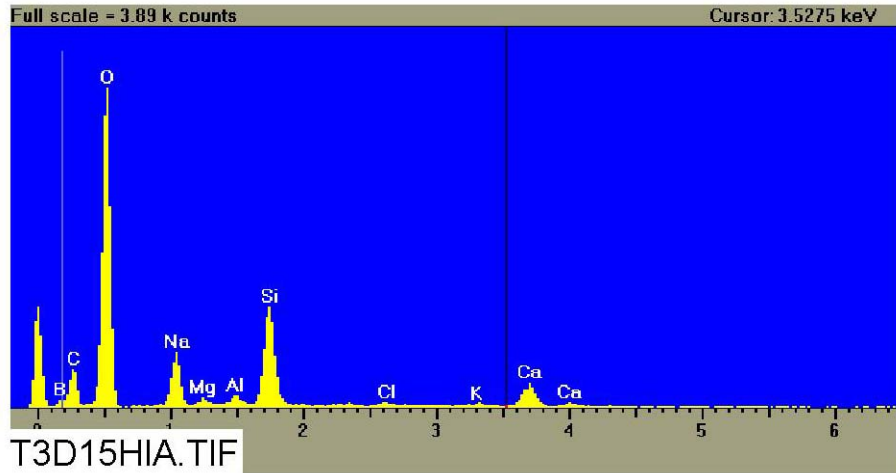


Figure 3-47. EDS counting spectrum for the flocculent deposits between the fibers on the ESEM image shown in Figure 3-46. (T3D15HIA, 4/22/05)

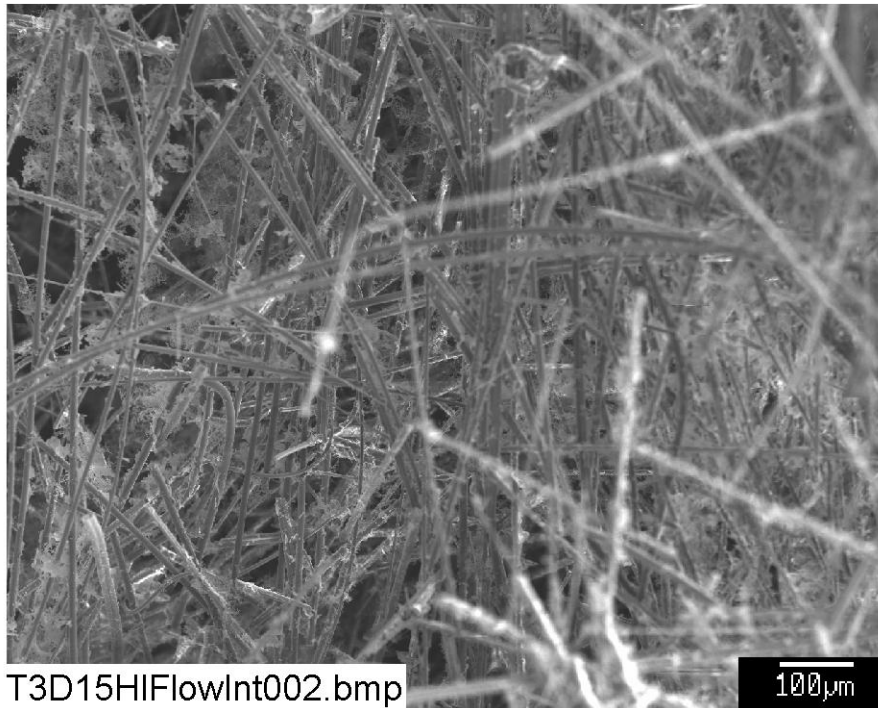


Figure 3-48. SEM image of a Test #3 Day 15 high-flow interior fiberglass sample, magnified 100 times. (T3D15HIFlowInt002, 4/22/05)

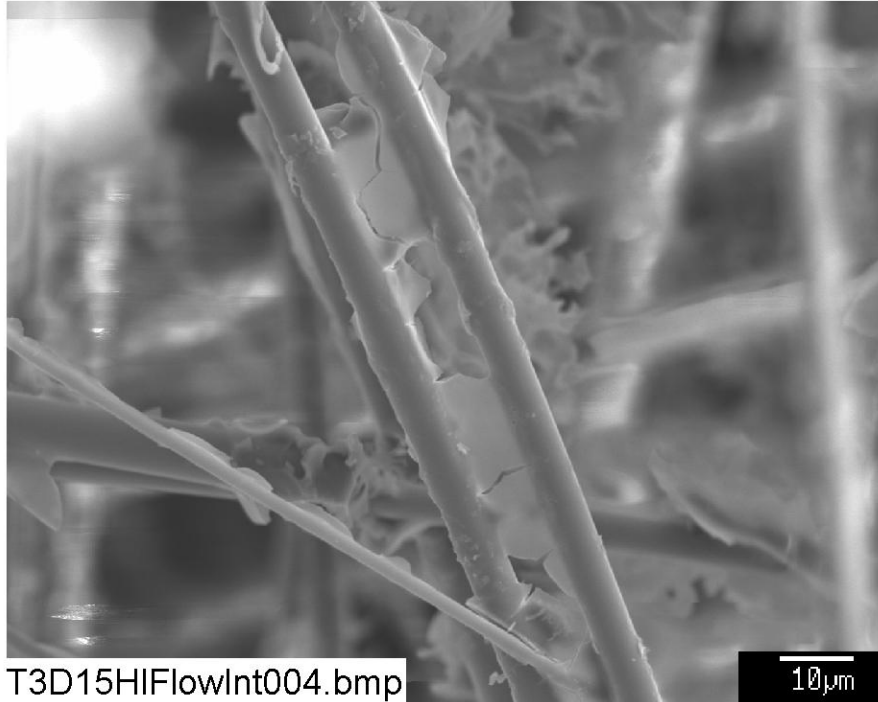


Figure 3-49. SEM image of a Test #3 Day 15 high-flow interior fiberglass sample, magnified 1000 times. (T3D15HiFlowInt004, 4/22/05)

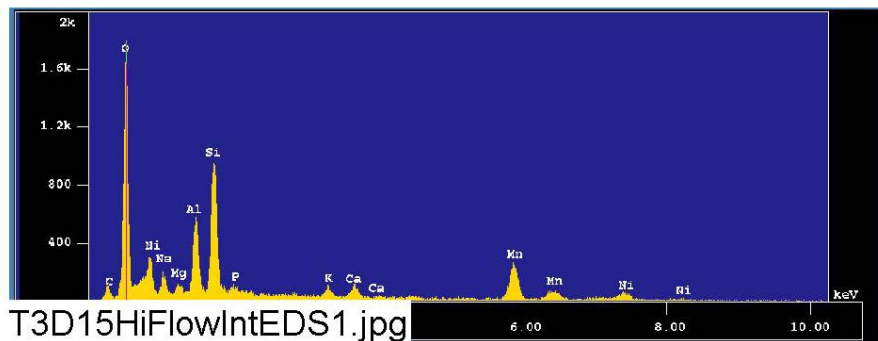


Figure 3-50. EDS counting spectrum for the flocculent deposits between the fibers on the SEM image shown in Figure 3-49. (T3D15HiFlowIntEDS1, 4/22/05)

3.3.1.4 Day 30 Low-Flow Fiberglass Samples

Comparing Day 30 low-flow fiberglass samples with Day 4 and Day 15 low-flow fiberglass samples revealed deposits that are similar in property and amount. In addition, there was no significant difference in the amount of deposits found in exterior and interior Day 30 low-flow fiberglass samples. Figures 3-51 through 3-54 show the Day 30 low-flow fiberglass results.

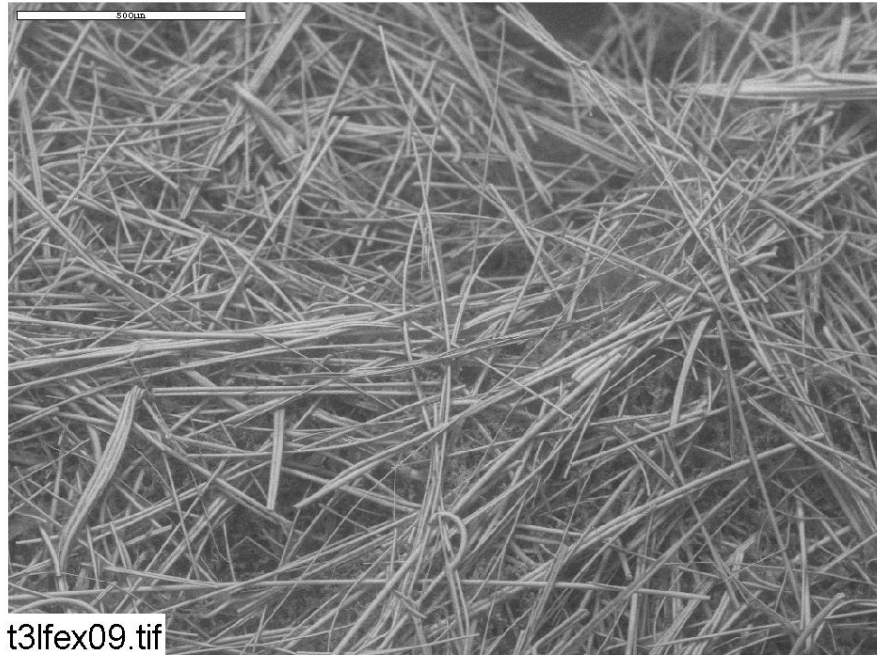


Figure 3-51. ESEM image of a Test #3 Day 30 exterior low-flow fiberglass sample, magnified 70 times. (t3lfex09, 5/6/05)

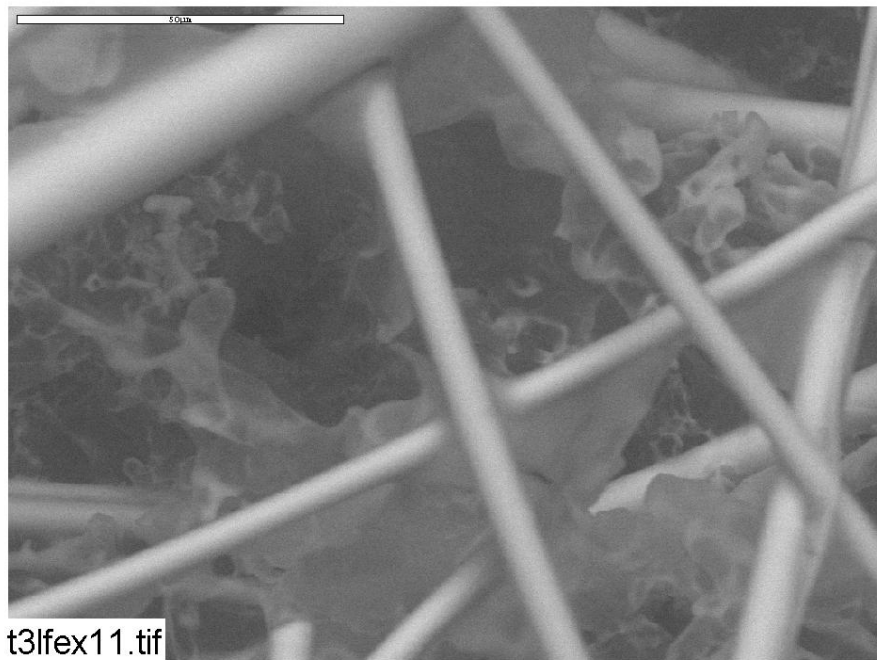


Figure 3-52. ESEM image of a Test #3 Day 30 exterior low-low fiberglass sample, magnified 1000 times. (t3lfex11, 5/6/05)

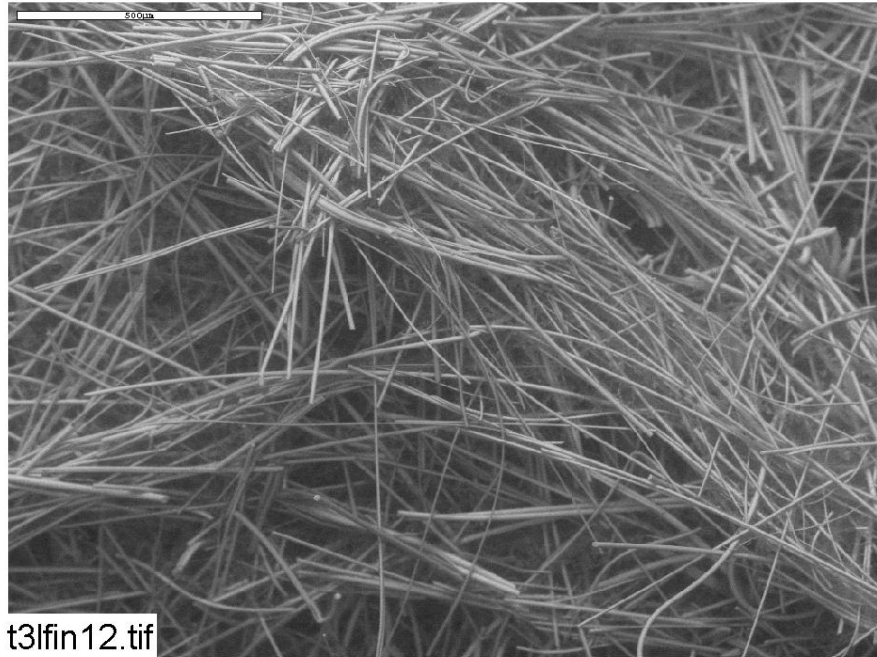


Figure 3-53. ESEM image of a Test #3 Day 30 interior low-flow fiberglass sample, magnified 70 times. (t3lfin12, 5/6/05)

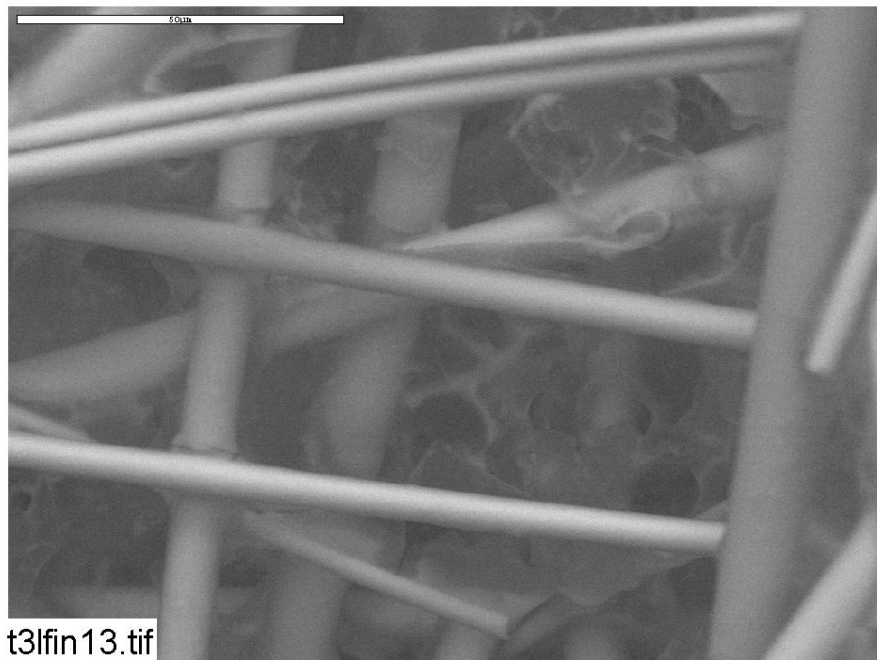


Figure 3-54. ESEM image of a Test #3 Day 30 interior low-flow fiberglass sample, magnified 1000 times. (t3lfin13, 5/6/05)

3.3.1.5 Day 30 High-Flow Fiberglass Samples

Compared with other high- and low-flow fiberglass samples, Day 30 high-flow exterior samples contained a significant amount of particulates. As opposed to the exterior samples, the interior samples were relatively clean, suggesting that the particulate deposits were physically attached/retained on the fiberglass exterior. EDS results show that the particulate deposits were composed of a significant amount of P, which is different from the previous fiberglass samples. The deposits' high P, Ca, and O content suggests that the deposits were $\text{Ca}_3(\text{PO}_4)_2$, which relates to the white gel (cream) formed during the injection of TSP. That $\text{Ca}_3(\text{PO}_4)_2$ was likely precipitated out from the testing solution, followed by sedimentation/transportation onto the Day 30 high-flow fiberglass exterior. Figures 3-55 through 3-59 show the Day 30 high-flow fiberglass results.

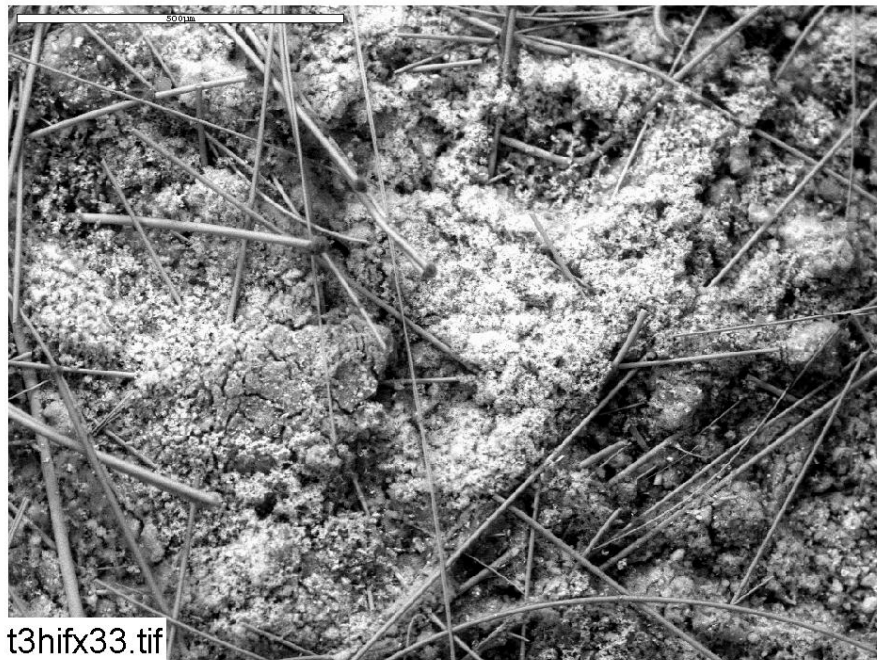


Figure 3-55. ESEM image of a Test #3 Day 30 exterior high-flow fiberglass sample, magnified 100 times. (t3hifx33, 5/11/05)

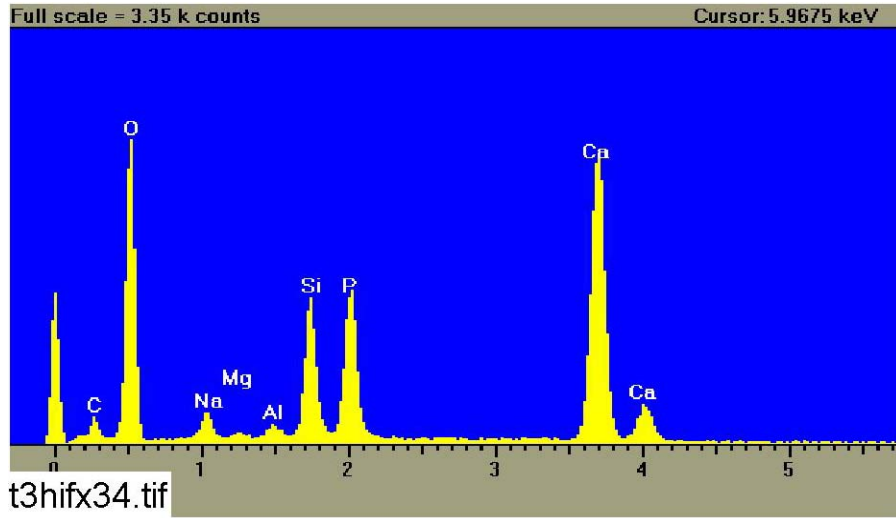


Figure 3-56. EDS counting spectrum for the large masses of particulate deposits shown in Figure 3-55. (t3hifx34, 5/11/05)



Figure 3-57. ESEM image of a Test #3 Day 30 exterior high-flow fiberglass sample, magnified 600 times. (t3hifx35, 5/11/05)

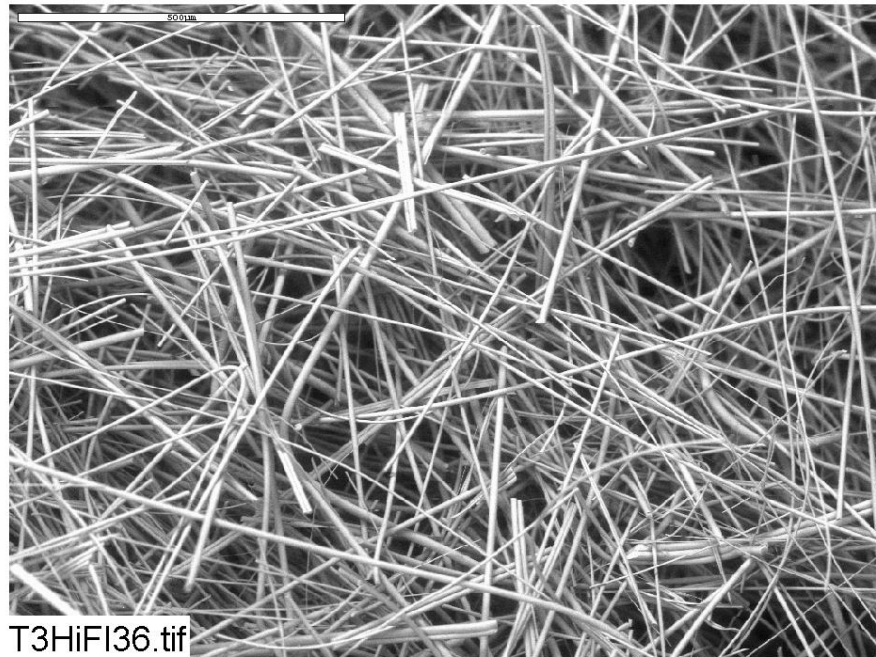


Figure 3-58. ESEM image of a Test #3 Day 30 interior high-flow fiberglass sample, magnified 100 times. (T3HiF136, 5/11/05)

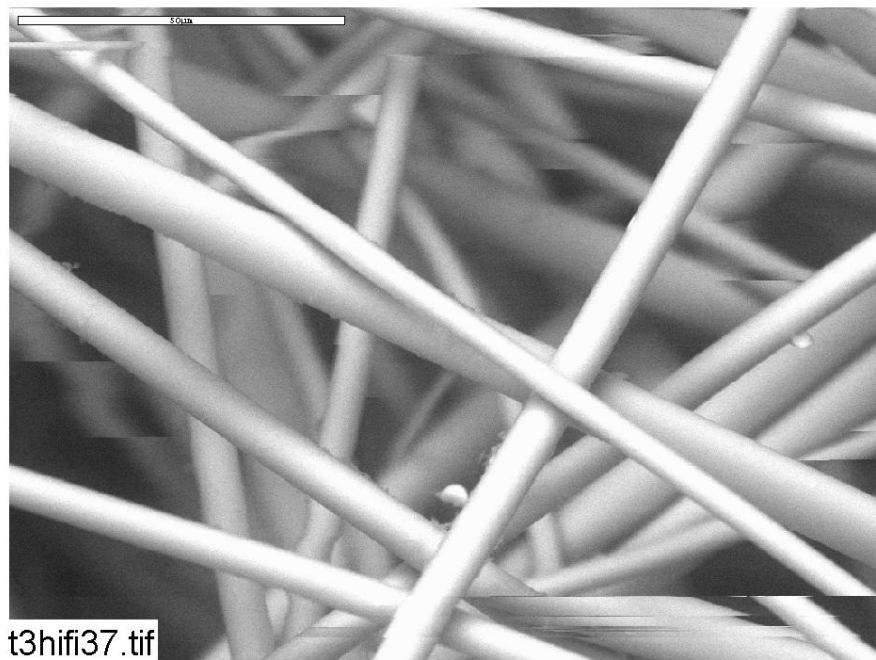


Figure 3-59. ESEM image of a Test #3 Day 30 interior high-flow fiberglass sample, magnified 1000 times. (t3hifi37, 5/11/05)

3.3.1.6 Day 30 Drain Collar Fiberglass Samples

Figure 3-60 shows the drain collar after it was removed from the tank. When the tank was drained, the drain collar was totally surrounded by sediment. Both the exterior fiberglass sample that was farthest from the drain screen and the exterior sample that was next to the drain screen have very significant amounts of particulate deposits. Inspection revealed the development of a continuous coating on the drain collar exterior, including particulate deposits that were likely physically retained or attached. The amount of deposits on the drain collar exterior was greater than on high- and low-flow fiberglass samples. The ESEM images showed that two types of material were retained; an amorphous material that appeared darker in the ESEM images and a lighter granular material. The EDS results indicate that these materials had different P and Si content. The lighter particulate deposits (see Figure 3-62) have a higher percentage of P and a lower percentage of Si than the dark deposits, suggesting that light particulate deposits are likely composed of $\text{Ca}_3(\text{PO}_4)_2$ precipitates and dark deposits of cal-sil particles. Both kinds of deposits could have been transported and/or deposited/retained on the drain collar fiberglass exterior. As opposed to what was found on the exterior sample, no significant deposits were found in the drain collar interior sample, suggesting that that almost all of the particulate deposits were physically retained at the fiberglass exterior. The result is consistent with findings for the Day 30 high-flow fiberglass samples. Figures 3-61 through 3-70 show the drain Day 30 drain collar fiberglass results.



Figure 3-60. Drain screen collar removed from the tank.

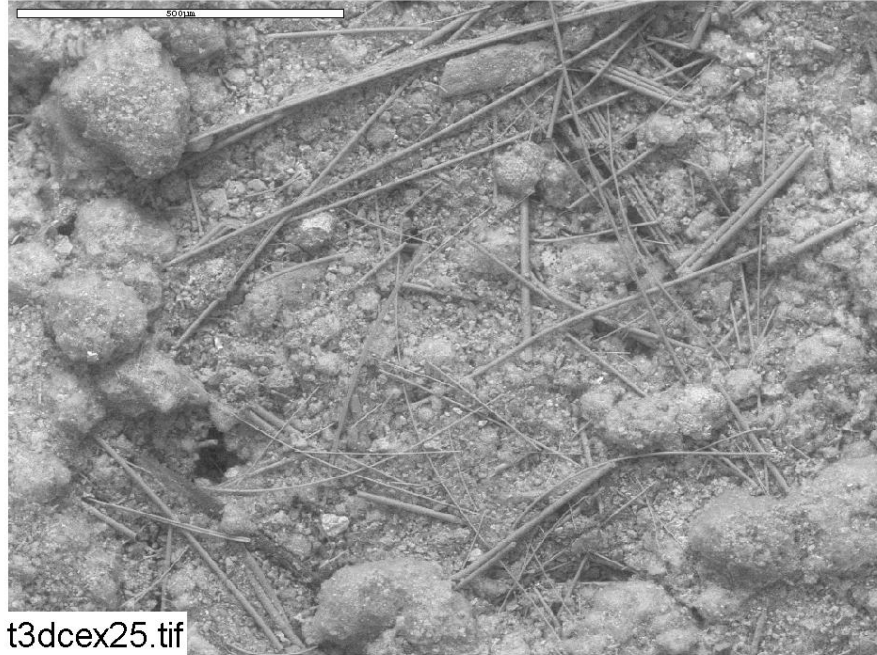


Figure 3-61. ESEM image of a Test #3 Day 30 exterior fiberglass sample on the drain collar (away from the drain screen), magnified 100 times. (t3dcex25, 5/6/05)

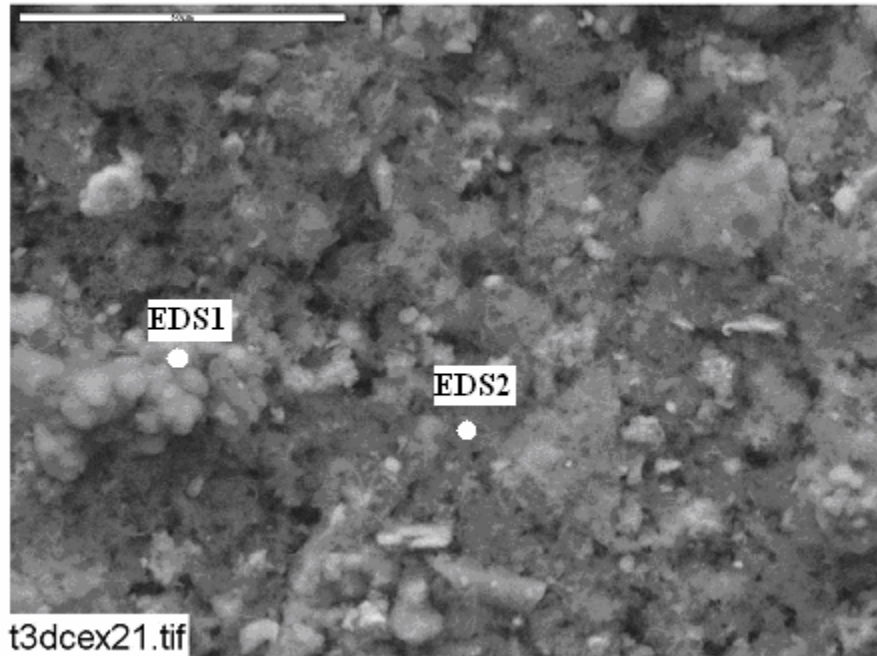


Figure 3-62. ESEM image of a Test #3 Day 30 exterior fiberglass sample on the drain collar (away from the drain screen), magnified 1000 times. (t3dcex21, 5/6/05)

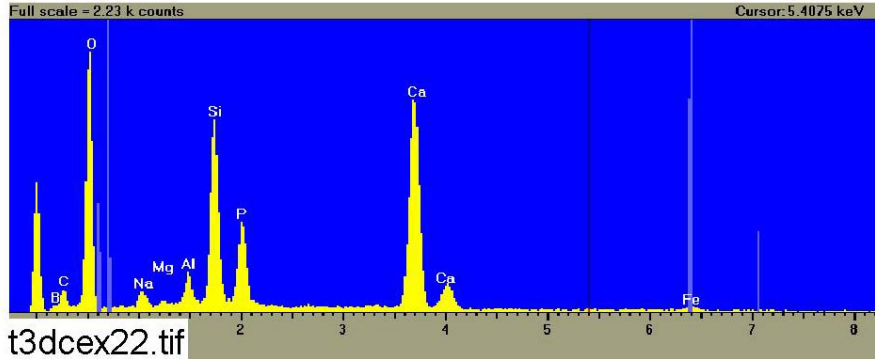


Figure 3-63. EDS counting spectrum for the light particulate deposits (EDS1) shown in Figure 3-62. (t3dcex22, 5/6/05)

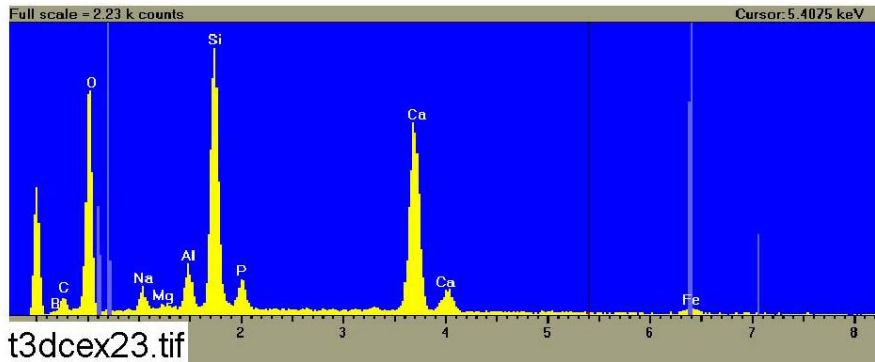


Figure 3-64. EDS counting spectrum for the dark deposits (EDS2) shown in Figure 3-62. (t3dcex23, 5/6/05)

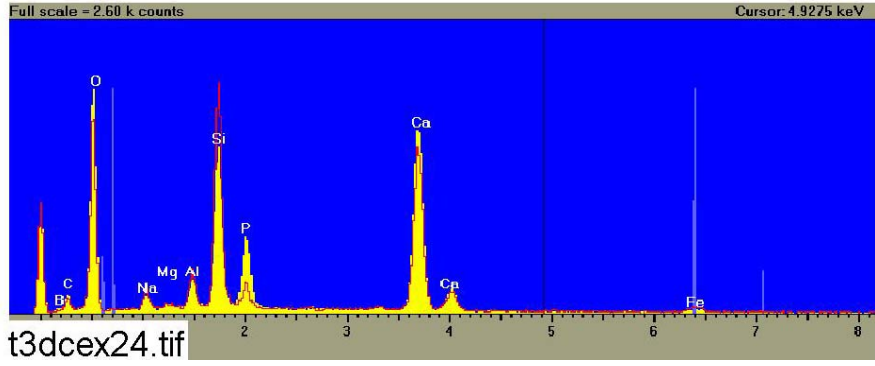


Figure 3-65. Comparison of EDS counting spectra between Figure 3-63 (yellow) and Figure 3-64 (red). (t3dcex24, 5/6/05)



Figure 3-66. ESEM image of a Test #3 Day 30 exterior fiberglass sample on the drain collar (adjacent to the drain screen), magnified 100 times. (t3DCSC16, 5/6/05)

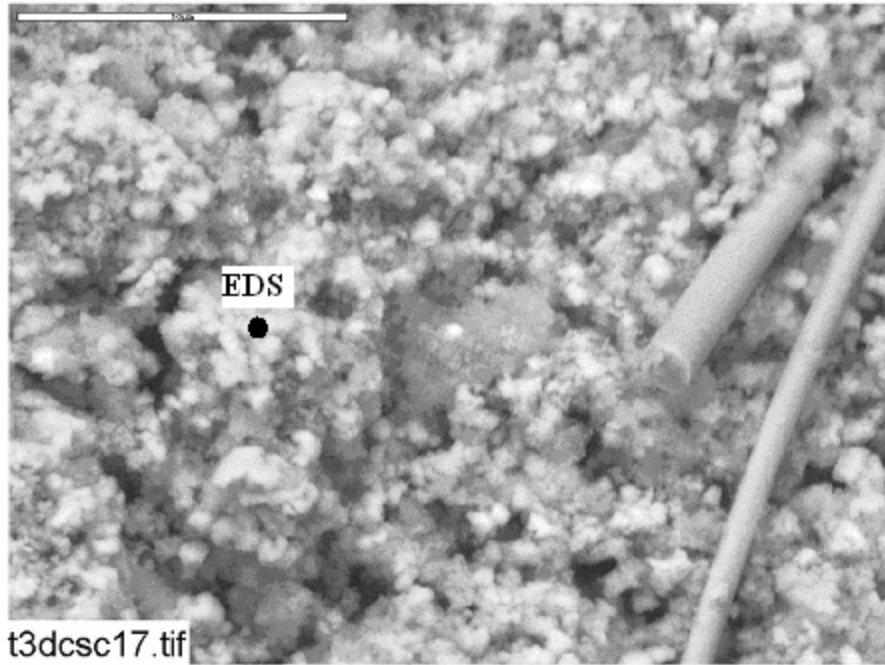


Figure 3-67. ESEM image of a Test #3 Day 30 exterior fiberglass sample on the drain collar (adjacent to the drain screen), magnified 1000 times. (t3dcsc17, 5/6/05)

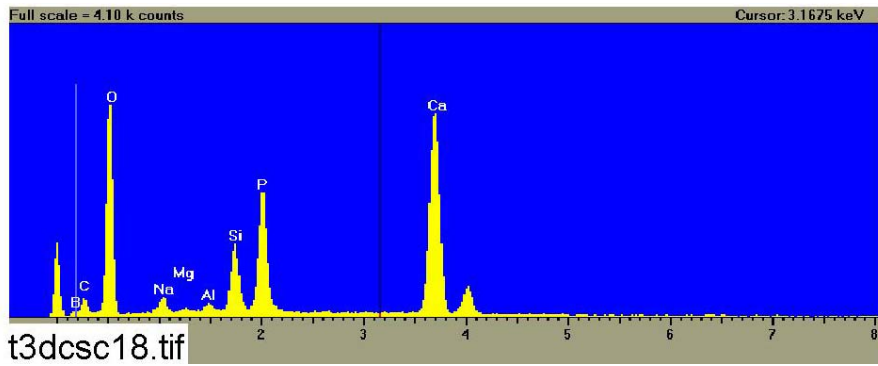


Figure 3-68. EDS counting spectrum for the particulate deposits shown in Figure 3-67. (t3dcsc18, 5/6/05)

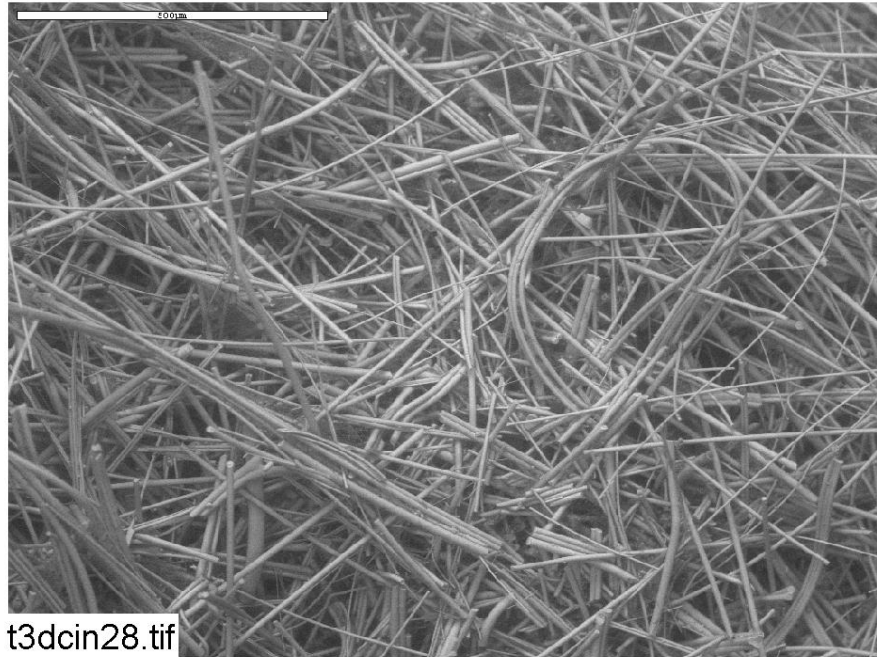


Figure 3-69. ESEM image of a Test #3 Day 30 interior fiberglass sample on the drain collar, magnified 100 times. (t3dcin28, 5/6/05)

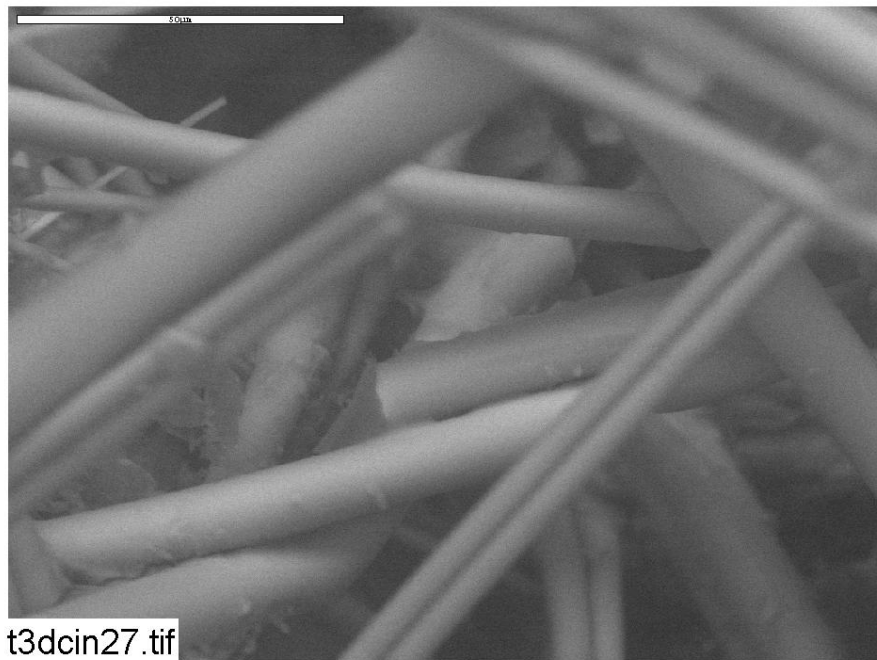


Figure 3-70. ESEM image of a Test #3 Day 30 interior fiberglass sample on the drain collar, magnified 1000 times. (t3dcin27, 5/6/05)

3.3.1.7 Day 30 Fiberglass Sample within the Birdcage

The test fluid was drained from the tank at the end of the 30-day test. Figure 3-71 shows the bottom of the tank after the tank was emptied. The birdcage is the cube in the center bottom of the figure, covered on its top with and sitting in light-colored gel-like material. For the Day 30 fiberglass sample within the birdcage, SEM images indicate large deposits (Figure 3-72) as well as a continuous coating (Figure 3-74) over the exterior of the fiberglass. The amount of particulate deposits within the birdcage was greater than on high- and low-flow fiberglass samples. The EDS result shows that the large particulate deposits had higher P and lower Si percentages than did the continuous coating shown in Figure 3-74. As with the particulate deposits on the drain collar, the large deposits are likely composed of $\text{Ca}_3(\text{PO}_4)_2$ precipitates, while the continuous coating was likely cal-sil particles. Both kinds of deposits were physically transported and/or deposited/retained on the birdcage fiberglass exterior. Compared with the exterior sample, the interior sample was relatively clean. Only small amounts of deposits were found. These deposits were similar to the deposits observed on high- and low-flow interior samples, which were likely caused by chemical precipitation during the drying process. Again, this result suggests that almost all of the particulate deposits were physically retained at the fiberglass exterior, consistent with conditions on the Day 30 high-flow and drain-collar fiberglass samples. Figures 3-72 through 3-79 show the Day 30 birdcage fiberglass results.



Figure 3-71. Tank bottom after the test fluid was drained.

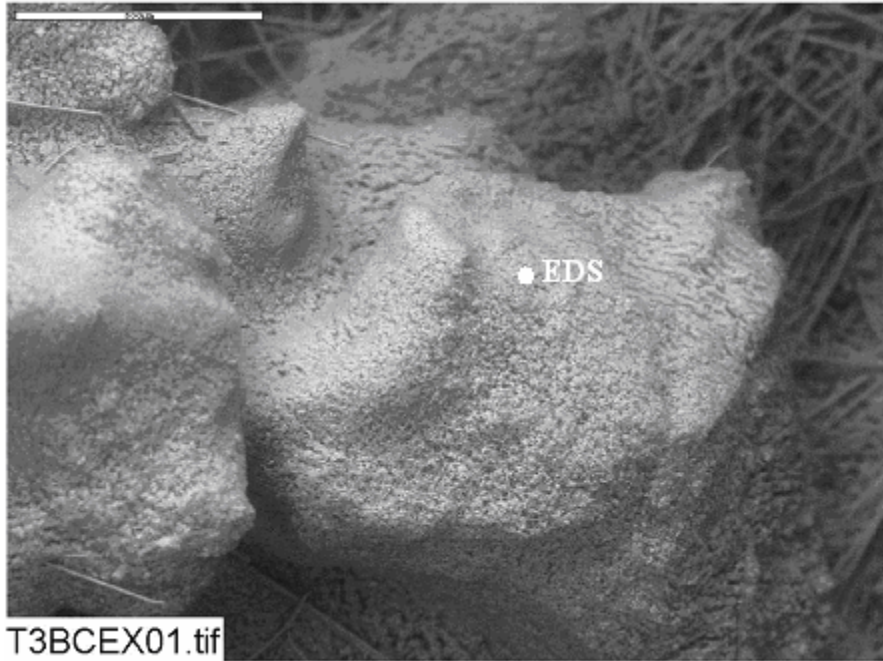


Figure 3-72. ESEM image of a Test #3 Day 30 exterior fiberglass sample within the birdcage, magnified 80 times. (T3BCEX01, 5/6/05)

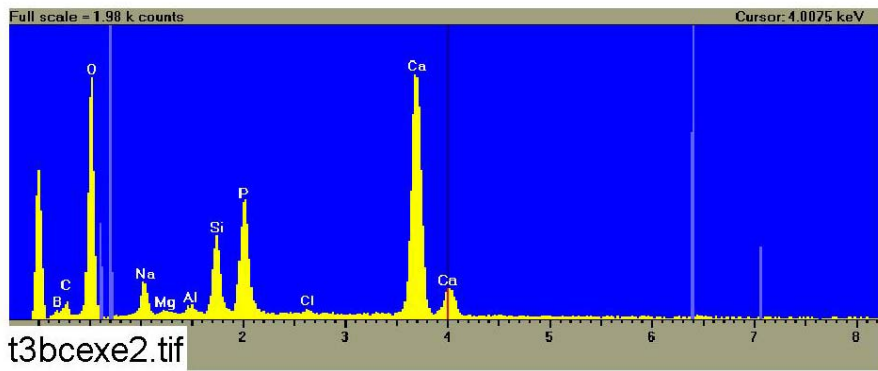


Figure 3-73. EDS counting spectrum for the large deposits shown in Figure 3-72. (t3bcexe2, 5/6/05)

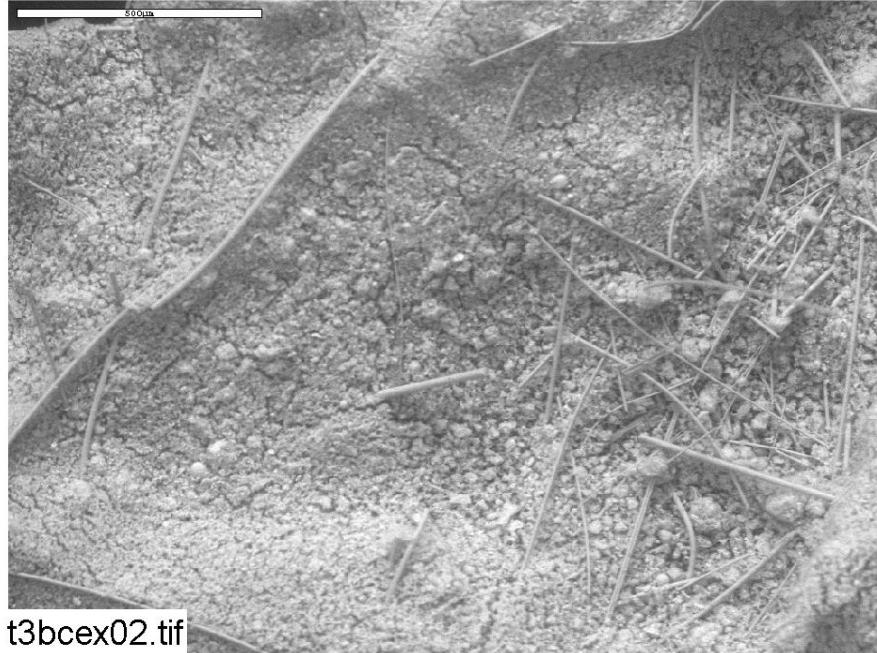


Figure 3-74. ESEM image of a Test #3 Day 30 exterior fiberglass sample within the birdcage, magnified 80 times. (t3bcex02, 5/6/05)

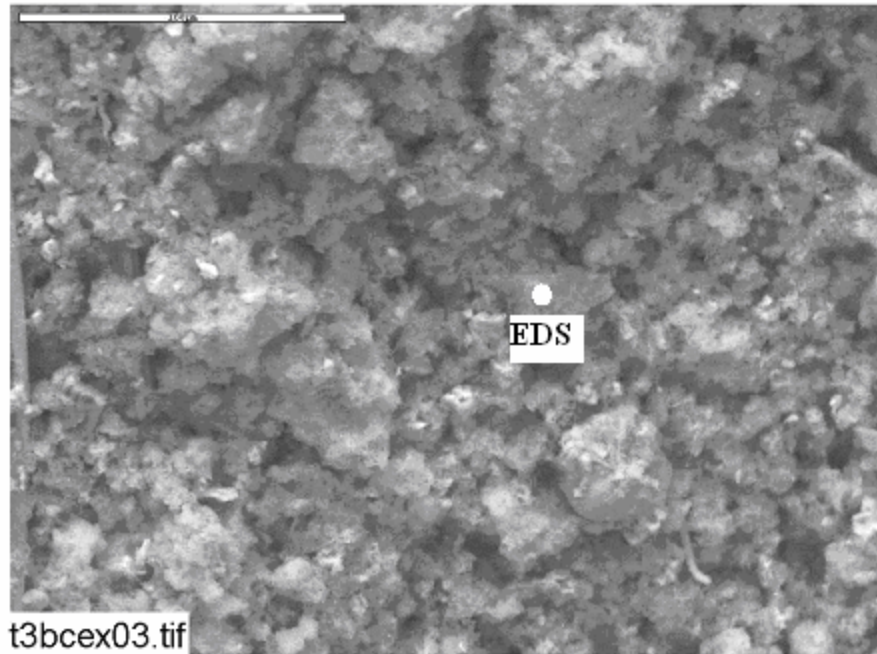


Figure 3-75. ESEM image of a Test #3 Day 30 exterior fiberglass sample within the birdcage, magnified 500 times. (t3bcex03, 5/6/05)

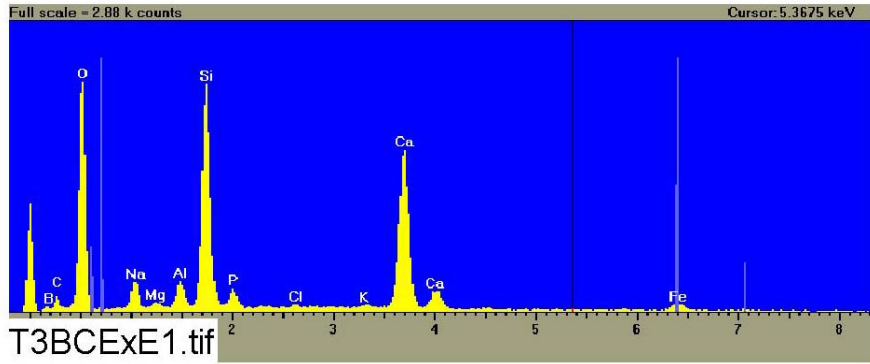


Figure 3-76. EDS counting spectrum for the deposits shown in Figure 3-75. (T3BCExE1, 5/6/05)

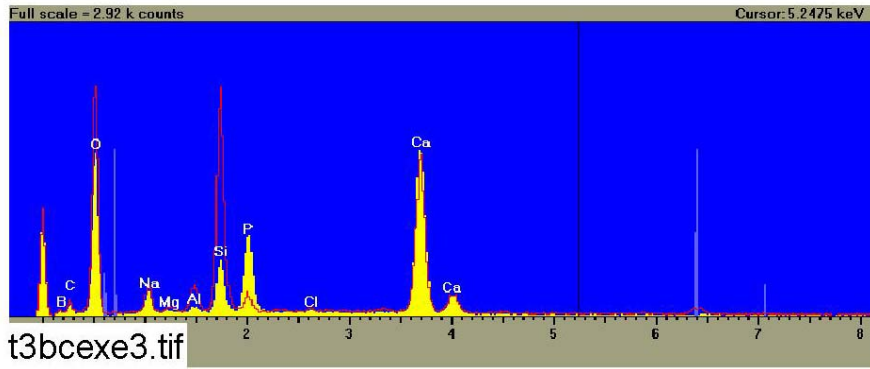


Figure 3-77. Comparison of EDS counting spectra of Figure 3-76 (red) and Figure 3-73 (yellow). (t3bcexe3, 5/6/05)

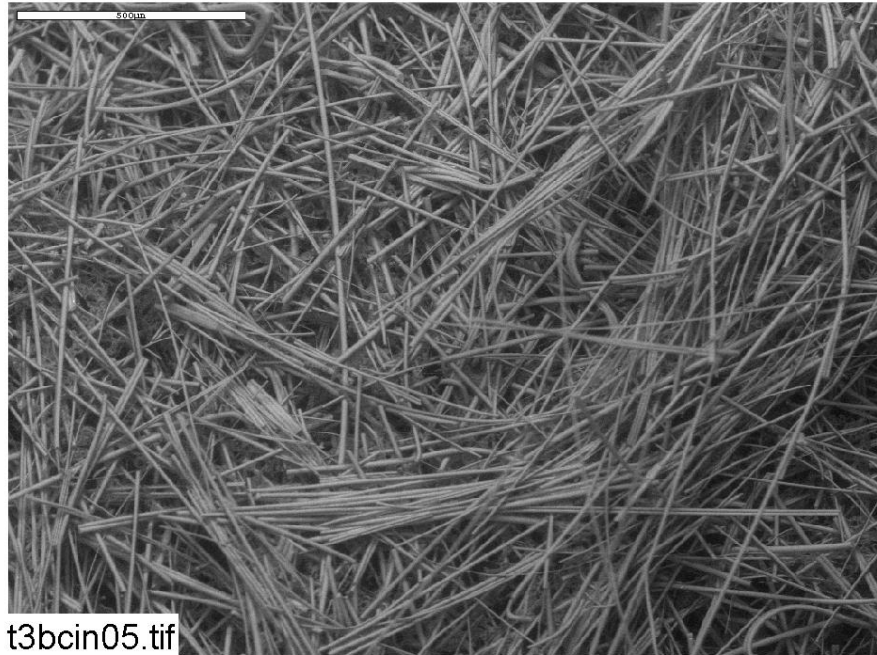


Figure 3-78. ESEM image of a Test #3 Day 30 interior fiberglass sample within the birdcage, magnified 80 times. (t3bcin05, 5/6/05)

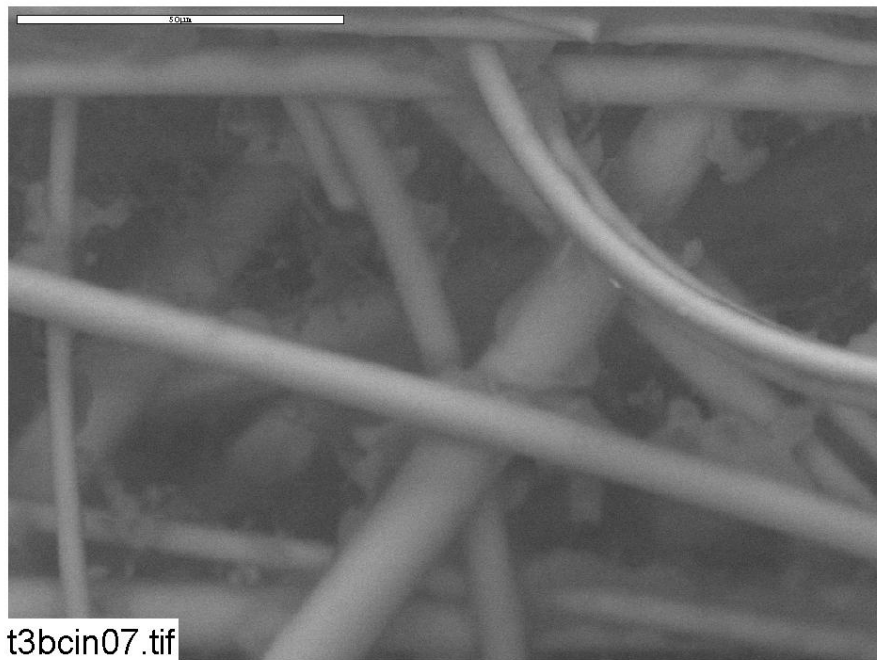


Figure 3-79. ESEM image of a Test #3 Day 30 interior fiberglass sample within the birdcage, magnified 1000 times. (t3bcin07, 5/6/05)

3.3.2 Calcium Silicate Samples

Test #3 was the first ICET test that included cal-sil in addition to fiberglass samples. XRD/XRF results show the crystal structure and the chemical composition of the unused raw and unused baked cal-sil samples. Based on XRD results, both unused raw and unused baked cal-sil samples contained crystalline substances of tobermorite ($\text{Ca}_{2.25}(\text{Si}_3\text{O}_{7.5}(\text{OH})_{1.5})(\text{H}_2\text{O})$) and calcite (CaCO_3). XRF results indicated that the dominant elemental compositions of cal-sil include Si and Ca and small amount of Al, Fe, Na, and Mg. There was no significant difference in elemental composition between raw and baked unused cal-sil. After being baked in a laboratory oven at 260°C for 72 hours, the raw cal-sil color changed from yellow to pink. The possible property changes of cal-sil after being baked include loss of water and oxidation of reductive species such as organic carbon, Fe(0), and Fe(II), as well as possible mineral and crystal structural changes. Specifically, oxidation of Fe(0) and Fe(II) into Fe_2O_3 is likely responsible for the baked cal-sil's turning pink.

ESEM/SEM/EDS examined a Day 30 unbaked cal-sil sample that had been submerged in the birdcage and a Day 30 baked cal-sil sample that had been submerged in the high-flow zone. EDS results show a significant amount of P on the exterior of the submerged cal-sil samples, both baked and unbaked; almost no P was present in the interior of the submerged cal-sil. (The interior cal-sil sample was obtained by breaking a chunk of cal-sil in half, and the interior sample was examined with SEM.) This result may be explained by the cal-sil exterior surface's being exposed to the testing solution, likely causing phosphate to complex with Ca at the exterior surface. However, because of limited phosphate diffusion into the cal-sil interior, no P was found in the interior cal-sil samples. In addition, unlike fiberglass, cal-sil is granular, making it difficult to distinguish cal-sil particles from the foreign deposits/debris attached on the cal-sil samples. Appendix H includes ESEM and SEM/EDS data for the cal-sil.

3.4 Metallic and Concrete Samples

3.4.1 Weights and Visual Descriptions

3.4.1.1 Submerged Coupons

Examination of the 40 submerged coupons provides valuable insight into the nature of the chemical kinetics that occurred during this 30-day test. The physical change that these coupons experienced is determined through both visual evidence and weight measurement of each coupon before and after the test. Pre-test pictures were taken of the coupons when they were received and prior to insertion in the racks. Post-test pictures were taken several days after the racks had been removed from the tank. All racks with coupons still inserted were staged to allow complete drying of the coupons prior to the post-test pictures. The coupons were placed in a low-humidity room and allowed to air dry. All coupons were also weighed before they were inserted into the tank and after the 30-day test was completed. Generally, the submerged coupons experienced more dramatic changes in both appearance and weight.

There are three submerged aluminum coupons in each test. Figures 3-80 through 3-85 display the pre- and post-test pictures of those coupons that were in Test #3. Each post-test aluminum coupon exhibits a pattern of white particulate deposition. In addition, each post-test coupon is a light reddish-brown, which may be attributable to copper's leaching into the test solution. The particulate deposition patterns for post-test aluminum coupons 155 and 156 are similar. However, the deposition pattern for the post-test Al-157 possesses a grayish tint, and a stream of white deposition runs from the rack contact point at the top to the bottom of the coupon. The relative spatial location of these coupons, given in order from the west side of the tank to the east side of the tank, is as follows: Al-155, Al-156, and Al-157. The concentration of particles increases slightly from the western-most coupon to the eastern-most coupon.



Figure 3-80. Al-155, submerged, pre-test.



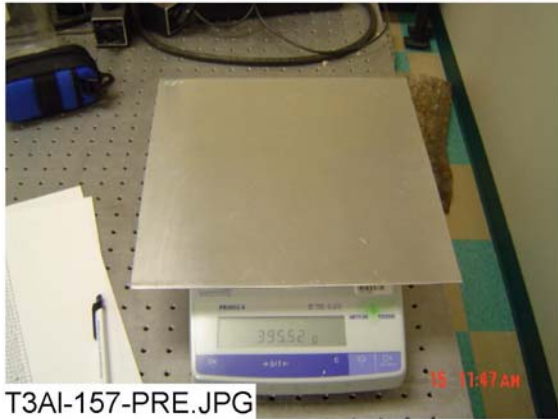
Figure 3-81. Al-155, submerged, post-test.



Figure 3-82. Al-156, submerged, pre-test.



Figure 3-83. Al-156 submerged, post-test.



T3AI-157-PRE.JPG

Figure 3-84. Al-157, submerged, pre-test.



T3AI-157-POST.JPG

Figure 3-85. Al-157, submerged, post-test.

The galvanized steel coupons exhibited nearly identical patterns of dense gray particle deposition. Figures 3-86 and 3-87 present the pre- and post-test pictures of one submerged galvanized steel coupon. There were no observable differences in post-test appearance based on the coupon's location in the rack.



T3GS-468-PRE.JPG

Figure 3-86. GS-468, submerged, pre-test.



T3GS-468-POST.JPG

Figure 3-87. GS-468, submerged, post-test.

Figures 3-88 and 3-89 present the pre- and post-test pictures of a typical submerged IOZ-coated steel coupon. Each post-test coated steel coupon exhibited a similar pattern of white particle deposition.

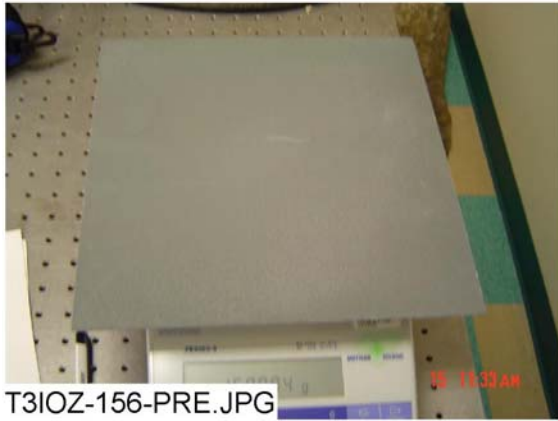


Figure 3-88. IOZ-156, submerged, pre-test.



Figure 3-89. IOZ-156, submerged, post-test.

Figures 3-90 through 3-93 present the pre- and post-test pictures of two submerged copper coupons. The patterns of white deposition are different for these post-test coupons. The CU-207 post-test coupon is almost completely covered with a dense collection of white deposits. The CU-225 post-test coupon, in contrast, exhibits faint horizontal streak-lines of white deposits. The CU-207 coupon was located on the west side of the tank in relation to the CU-225 coupon. The CU-207 coupon gained 1.2 g, while the CU-225 coupon lost 0.1 g.

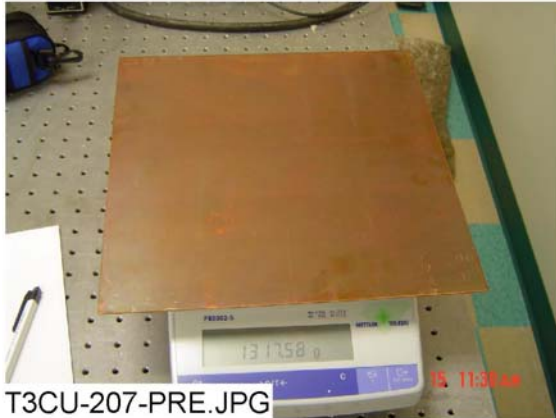


Figure 3-90. CU-207 submerged, pre-test.



Figure 3-91. CU-207, submerged, post-test.

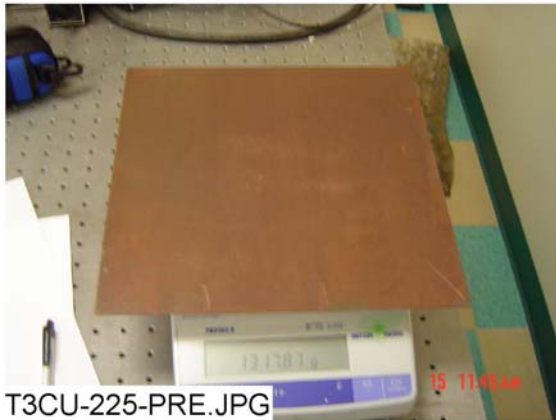


Figure 3-92. CU-225, submerged, pre-test.



Figure 3-93. CU-225, submerged, post-test.

Figures 3-94 and 3-95 present the pre- and post-test pictures of the single submerged carbon steel coupon. It has a light coating of white deposits over a large portion of the surface area. Also, there is observable rust along the bottom edge of the coupon. The rust deposits are mainly congregated near the lower corners of the coupon, near the rack's contact points. Differences in corrosion or deposits at the location of the coupon rack contact points may have been due to stagnant solution conditions that may have limited mass transfer to or from the surface and caused local differences in solution composition. Coupon US-11 lost 1.1 g.



Figure 3-94. US-11, submerged, pre-test.



Figure 3-95. US-11, submerged, post-test.

Figures 3-96 and 3-97 present the pre- and post-test pictures of the submerged concrete coupon. The post-test concrete coupon exhibits an enhanced gray compared with the pre-test coupon. The concrete coupon gained 180.5 g, which is estimated to be primarily water absorption.



Figure 3-96. Conc-005, submerged, pre-test.



Figure 3-97. Conc-005, submerged, post-test.

Table 3-2 presents the pre- and post-test weight data for each representative submerged coupon shown above.

Table 3-2. Weight Data for Submerged Coupons

Type	Coupon No.	Pre-Test Wt. (g)	Post-Test Wt. (g)	Net Gain/Loss
AI	155	393.0	398.7	5.7
AI	156	391.2	392.2	1.0
AI	157	395.5	390.8	-4.7
GS	468	1058.1	1074.0	15.9
IOZ	156	1600.9	1602.4	1.5
CU	207	1317.6	1318.8	1.2
CU	225	1317.9	1317.8	-0.1
US	11	1026.8	1025.7	-1.1
Conc	5	8020.0	8200.5	180.5

Table 3-3 shows the mean weight gain/loss summary in grams for all of the submerged coupons.

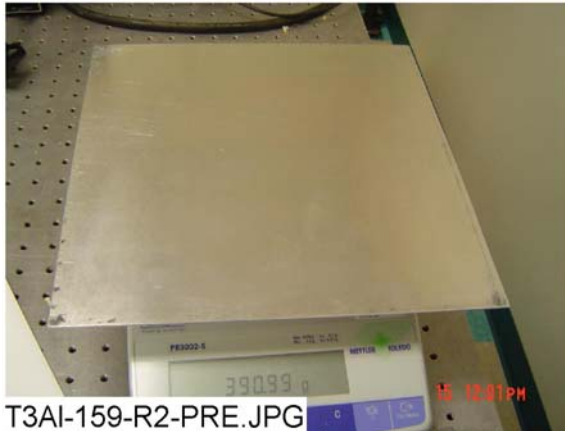
**Table 3-3. Mean Weight Gain/Loss (g)
Data for Submerged Coupons**

Coupon Type	Mean Gain - Loss (g)
AL	0.6
GS	15.0
CU	0.3
IOZ	1.8
US	-1.1
Concrete	180.5

3.4.1.2 Unsubmerged Coupons

Compared with the submerged Test #3 coupons, unsubmerged Test #3 coupons were effected less by their 30-day exposure. While they experienced some changes, those changes were far less significant than the changes seen in submerged coupons.

Figures 3-98 and 3-99 show the pre- and post-test pictures of a typical unsubmerged aluminum coupon. The coupons exhibit a light pattern of deposition. Also, each post-test coupon has coarser texture and a less-lustrous surface.



T3AI-159-R2-PRE.JPG

Figure 3-98. Al-159, unsubmerged, pre-test.



T3AI-159-R2-POST.JPG

Figure 3-99. Al-159, unsubmerged, post-test.

Figures 3-100 and 3-101 show the pre- and post-test pictures of a typical unsubmerged galvanized steel coupon. Each post-test galvanized steel coupon exhibited a similar light deposition.



T3GS-503-R3-PRE.JPG

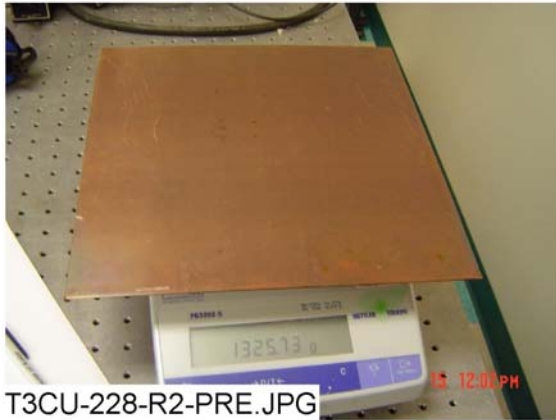
Figure 3-100. GS-503, unsubmerged, pre-test.



T3GS-503-R3-POST.JPG

Figure 3-101. GS-503, unsubmerged, post-test.

Figures 3-101 and 3-102 present the pre- and post-test pictures of a typical unsubmerged copper coupon. Each post-test copper coupon exhibited a similar pattern of streak-like deposition.



T3CU-228-R2-PRE.JPG

Figure 3-102. CU-228, unsubmerged, pre-test.



T3CU-228-R2-POST.JPG

Figure 3-103. CU-228 unsubmerged, post-test.

Figures 3-104 and 3-105 present the pre- and post-test pictures of a typical unsubmerged IOZ-coated steel coupon. Each post-test coated steel coupon exhibited a similar pattern of deposition.



T3IOZ-187-R4-PRE.JPG

Figure 3-104. IOZ-187, unsubmerged, pre-test.



T3IOZ-187-R4-POST.JPG

Figure 3-105. IOZ-187, unsubmerged, post-test.

Figures 3-106 and 3-107 present the pre- and post-test pictures of a typical unsubmerged carbon steel coupon. The post-test carbon steel coupons turned reddish-brown and exhibited slight corrosion around the edges.

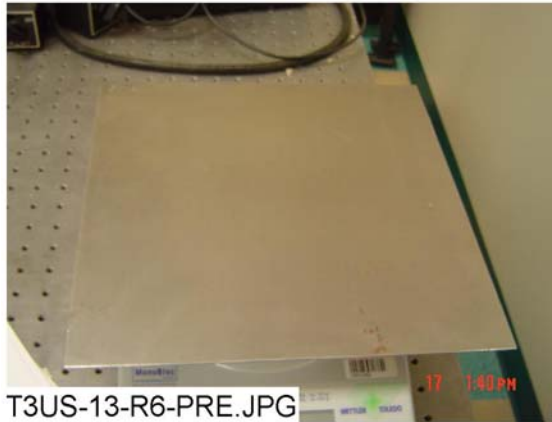


Figure 3-106. US-13, unsubmerged, pre-test.

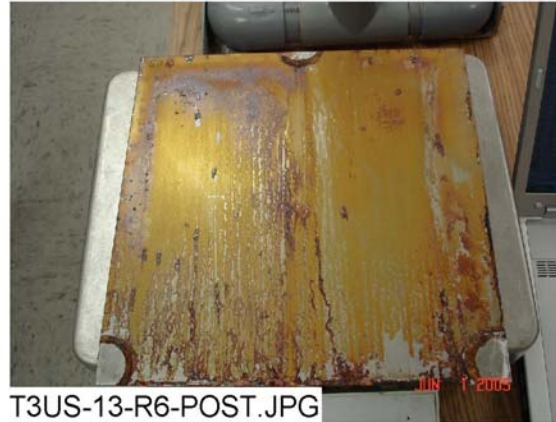


Figure 3-107. US-13, unsubmerged, post-test.

Table 3-4 presents the pre- and post-test weight data for each representative unsubmerged coupon.

Table 3-4. Weight Data for Unsubmerged Coupons

Type	Coupon No.	Pre-Test Wt. (g)	Post-Test Wt. (g)	Net Gain/Loss
Al	159	391.0	391.6	0.6
GS	503	1049.0	1049.1	0.1
IOZ	187	1628.2	1630.4	2.2
CU	228	1325.7	1325.7	0.0
US	13	1023.2	1023.7	0.5

Table 3-5 presents the mean weight gain/loss summary in grams for all of the unsubmerged coupons.

Table 3-5. Mean Gain/Loss (g) Data for Unsubmerged Coupons

	Mean Gain-Loss Per Coupon Type (g)				
	AL	GS	CU	IOZ	US
2	0.5	0.1	0.3	1.6	n/a
3	0.0	0.1	0.0	1.4	n/a
4	0.2	0.3	0.0	2.1	1.4
5	0.6	0.1	0.1	2.4	n/a
6	0.6	0.3	0.3	2.3	0.5
7	0.4	0.1	0.3	2.3	n/a
Overall	0.4	0.2	0.2	2.0	1.0

3.4.2 SEM Analyses

3.4.2.1 Submerged Coupons

During the ICET tests, trace metal cations may be released from the submerged metal coupon surfaces due to corrosion effects. Subsequently, the released metal cations may complex with the anions from the solution through electrostatic interactions, resulting in, for example, OH^- , PO_4^{3-} , SiO_3^{2-} , and CO_3^{2-} . In turn, the complexed anions may attract other cations from the solution, such as Ca^{2+} , Mg^{2+} , Al^{3+} , Cu^{2+} , Zn^{2+} , and H^+ . As a result, corrosion products (deposits) are formed and may continuously grow on the metal coupon surfaces. The thickness of the deposits is in the millimeter range. The adherence between the metal coupons and the deposits is through chemical bonds, which are a much stronger connection than van der Waals forces. Due to the vertical placement of the metal coupons in the tank (with a small horizontal cross-sectional area), the deposits on the metal coupon surface are likely of chemical origin rather than being the result of particles settling on the surface.

According to SEM/EDS results, the dominant corrosion products on the submerged Al coupons are likely aluminum hydroxide with other substances containing Si, Ca, and O. For submerged Cu coupons, the possible corrosion products include CuO, $\text{Cu}_2(\text{CO}_3)(\text{OH})_2$, and substances containing Ca, Si, and O. For the submerged galvanized steel coupons, the possible corrosion products are phosphate, silicate, and carbonate compounds of Zn and Ca. For the submerged steel coupons, the possible corrosion products include phosphate, silicate, and carbonate compounds of Fe and Ca and compounds composed of Fe, Al, Si, Ca, P, and O.

3.4.2.2 Unsubmerged Coupons

The physical and chemical changes that the unsubmerged coupons experienced during Test #3 are less significant than the changes seen on the submerged coupons. The unsubmerged coupons were affected by the testing solution only during the 4-hour spraying period on the first day of the test and, following that, were affected by water vapor throughout the test.

According to SEM/EDS results, the dominant corrosion products on the unsubmerged Al coupons are likely aluminum hydroxide and/or aluminum oxide. For unsubmerged Cu, the corrosion products on the coupon surface are likely CuO and $\text{Cu}_2(\text{CO}_3)(\text{OH})_2$. ZnO and ZnCO_3 are likely the dominant corrosion products on the unsubmerged galvanized steel coupon surface. For the unsubmerged steel coupon, the likely corrosion products are Fe_2O_3 , $\text{Fe}(\text{OH})_3$, and $\text{Fe}_2(\text{CO}_3)_3$.

Appendix E contains the SEM data for the coupons.

3.5 Sedimentation

Sediment was collected from the tank bottom after the test solution was drained. It consisted of two main macroscopic quantities, a particulate sediment on the bottom covered in many places with a whitish-pink gel-like material. Figure 3-108 shows this sediment. In addition, Figure 3-109 shows SS mesh holding insulation samples after it was pulled from the tank bottom. The pink and yellow particulate sediment covers much of the mesh, and the gel-like material is seen above it and is being pointed to in the figure.

The particulate sediment samples were identified and classified by their color: pink or yellow. The yellow or pink sediments were large enough (pea-sized or larger) to be visually seen and picked up from the bulk sediment. The pink sediment likely originated from baked cal-sil debris and the yellow sediment from unbaked cal-sil debris. ESEM/EDS and XRD/XRF analysis provided the information on the morphology and composition of these sediments. EDS results show that there is no significant compositional difference between the yellow and pink sediments. Both contain significant amounts of Si, Ca, and O. XRF results consistently show that Si and Ca are the major elements in the mixed sediments. However, P (present in phosphorus pentoxide, P_2O_5) is less than 2% of the total mass, possibly because Test #3 precipitates containing P make up a smaller portion of the total debris than do particles originating from cal-sil.

Based on XRD results, a sediment sample recovered from the bottom of the test tank contained crystalline substances of tobermorite ($Ca_{2.25}(Si_3O_{7.5}(OH)_{1.5})(H_2O)$) and calcite ($CaCO_3$), which are the same as unused baked or unbaked cal-sil samples. XRD results are consistent with the ESEM/EDS analysis, i.e., most of the sediments in the test tank were generated from the baked and unbaked cal-sil debris. However, other debris such as corrosion products, white gel-like precipitates, and fiberglass may also contribute to the sediments. Figures 3-110 through 3-117 and Table 3-6 provide ESEM/EDS and XRD/XRF analysis results. A comparison of Figures 3-113 and 3-114 shows that the surface morphology of the deposits was consistent even in locations where the thickness or ruggedness of the deposits varied. The complete Day 30 sediment analysis is contained in Appendix I.



Figure 3-108. Sediment removed from the tank. Some gel appears on the top.



Figure 3-109. Samples removed from the tank bottom.

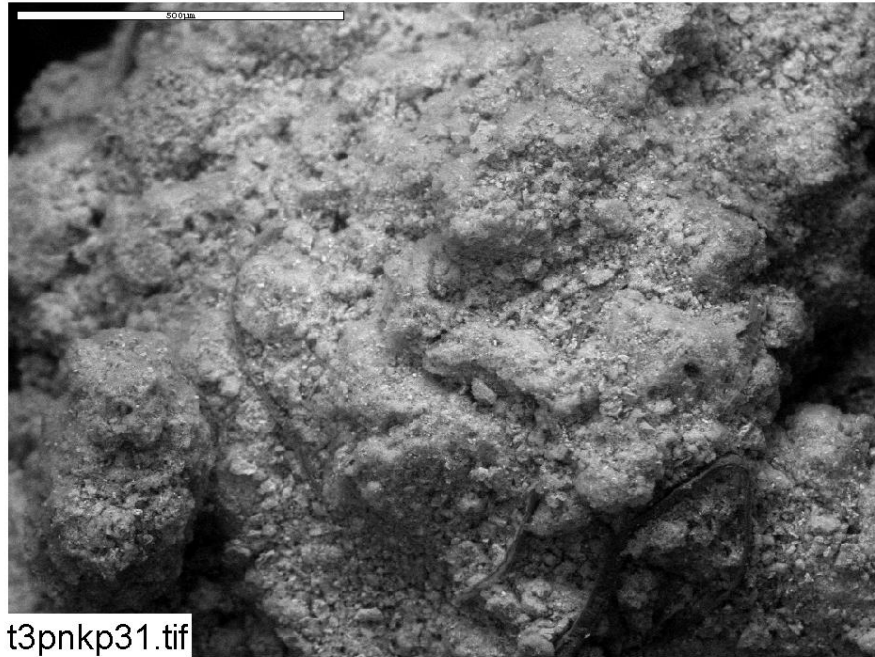


Figure 3-110. ESEM image of a Test #3 Day 30 pink sediment, magnified 100 times. (t3pnkp31, 5/6/05)

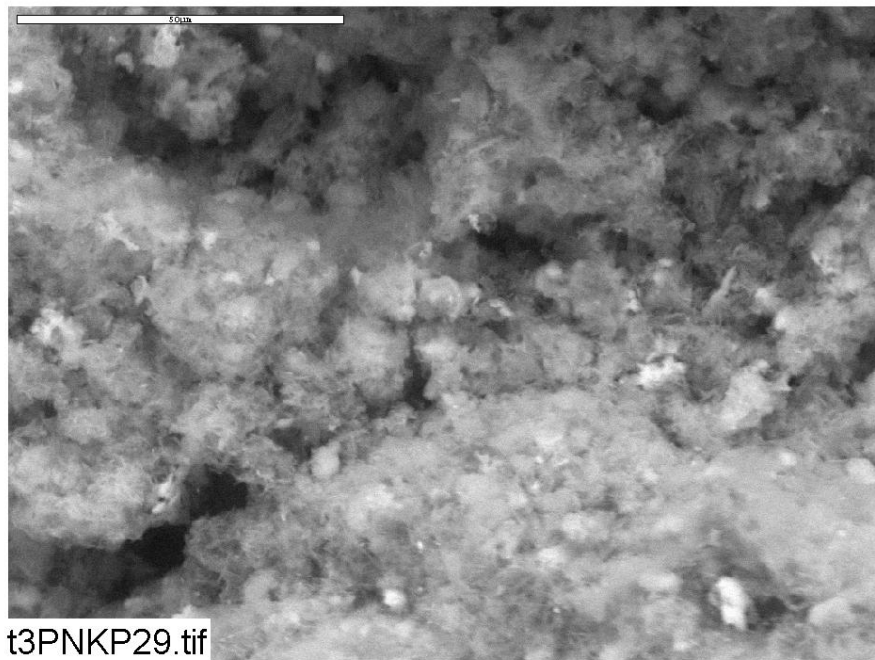


Table 3-111. ESEM image of a Test #3 Day 30 pink sediment, magnified 1000 times. (t3PNKP29, 5/6/05)

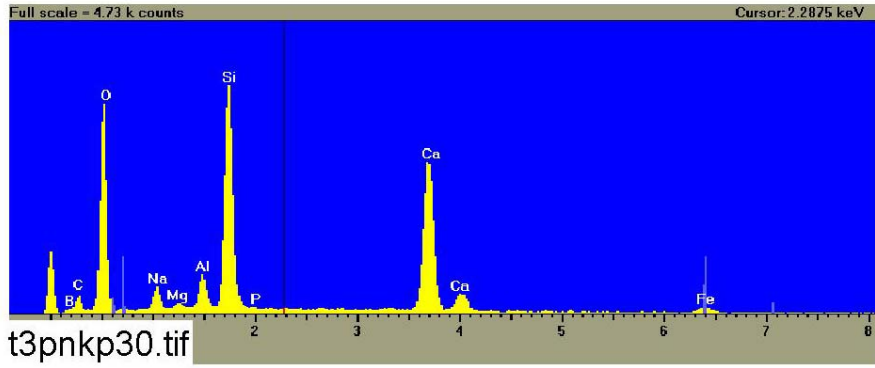


Table 3-112. EDS counting spectrum for the sediment shown in Figure 3-111. (t3pnkp30, 5/6/05)

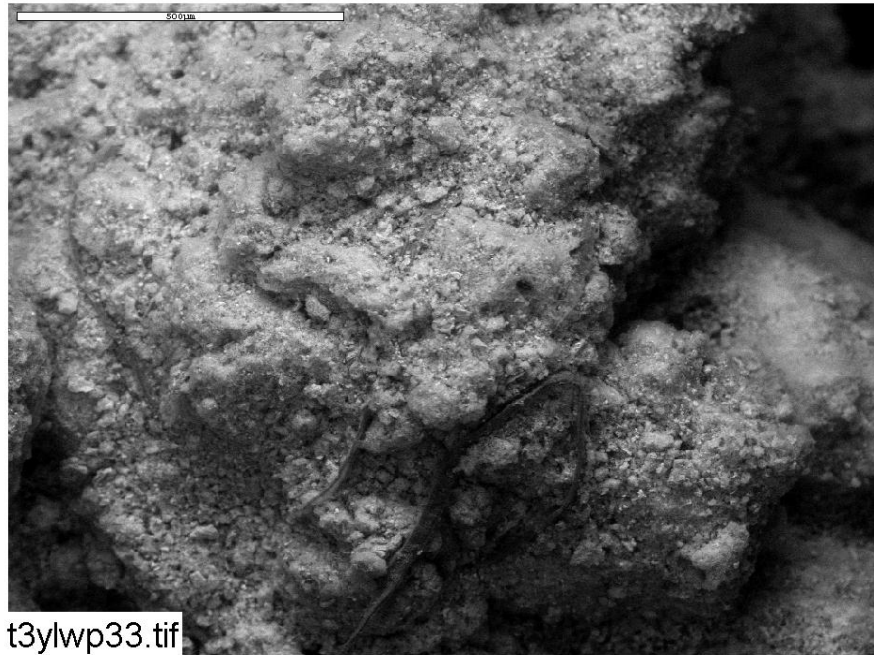


Figure 3-113. ESEM image of a Test #3 Day 30 yellow sediment, magnified 100 times. (t3ylwp33, 5/6/05)

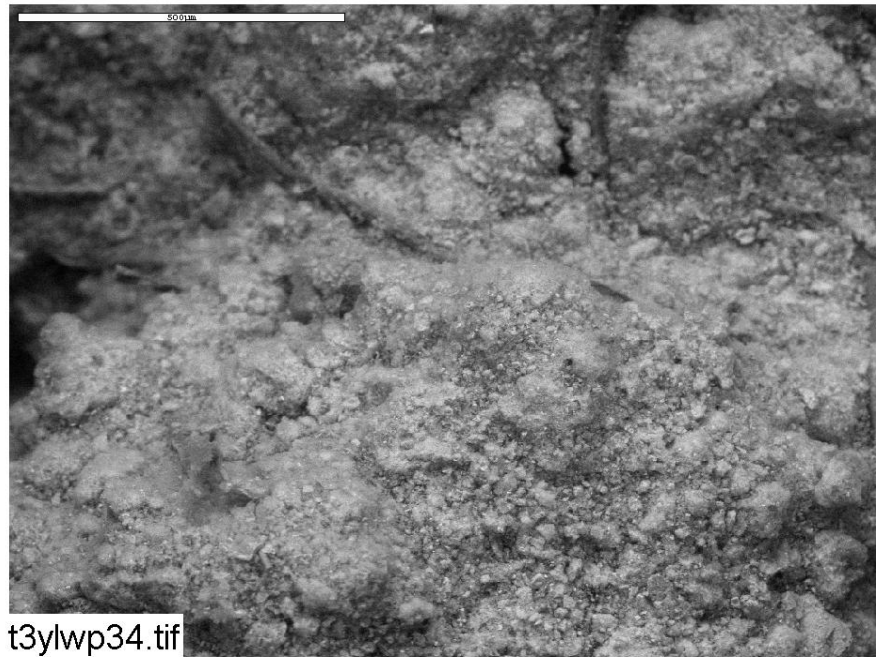


Figure 3-114. ESEM image of a Test #3 Day 30 yellow sediment, magnified 100 times. (t3ylwp34, 5/6/05)

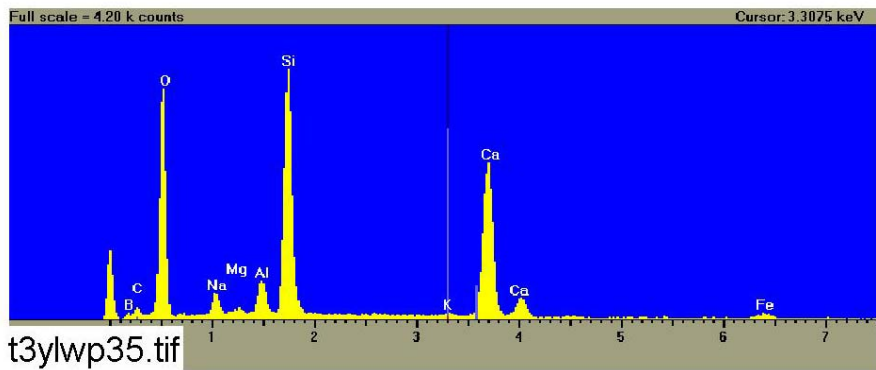


Figure 3-115. EDS counting spectrum for the particles shown in Figure 3-114. (t3ylwp35, 5/6/05)

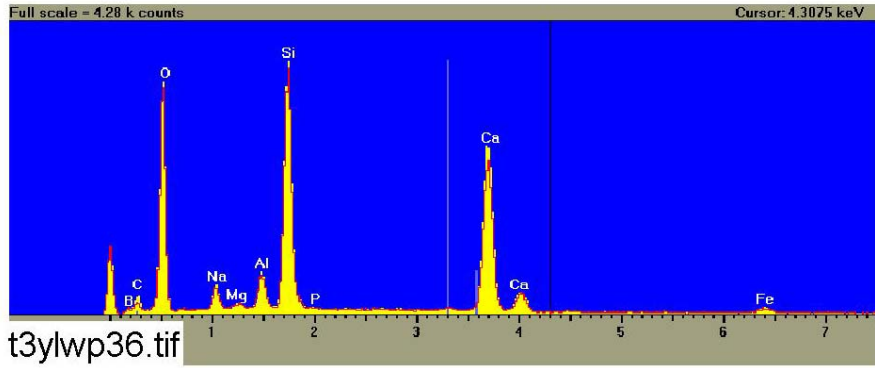


Figure 3-116. Comparison of EDS counting spectra for pink sediment (yellow, t3pnkp30) and yellow sediment (red, t3ylwp35). (t3ylwp36, 5/6/05)

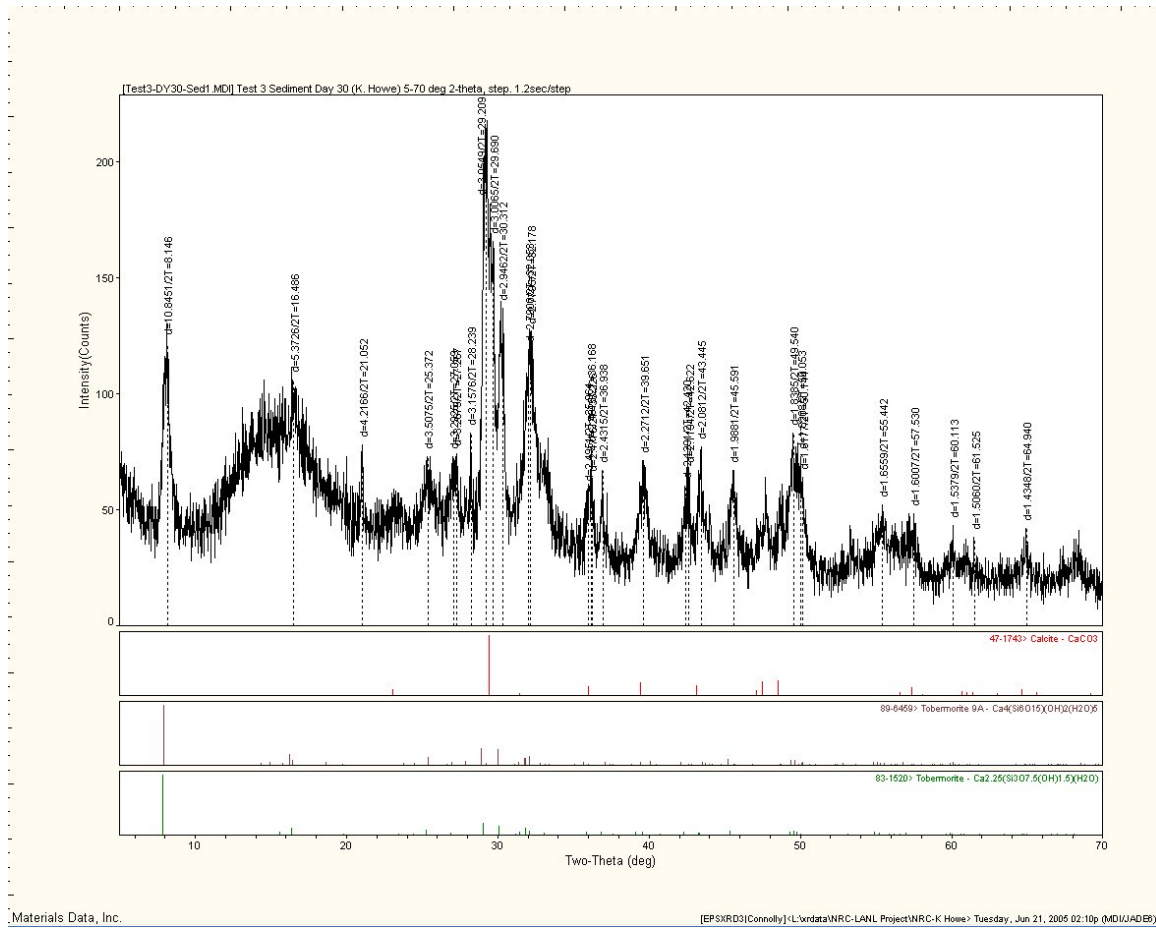


Figure 3-117. XRD results for Test #3 Day 30 mixed sediment.

Table 3-6. Dry Mass Compositions of Test #3 Day 30 Sediment by XRF Analysis

The first row is the chemical component; the second row is the mass composition (%).														
SiO ₂	TiO ₂	Al ₂ O ₃	Fe ₂ O ₃	FeO	MnO	MgO	CaO	Na ₂ O	K ₂ O	H ₂ O(-)	H ₂ O(+) CO ₂	P ₂ O ₅	Total	H ₂ O(+) CO ₂ /DF (10) & Cover. To %
36.29	0.20	4.92	2.24	0.00	0.06	0.62	27.16	2.19	0.45	0.58	20.65	3.05	98.42	1.0211

3.6 Precipitates

Test #3 was markedly different from Test #1 in that no precipitate was found in the test solution, even after it cooled to room temperature. Based on a series of bench-top controlled experiments, the white precipitate observed in Test #1 contained a significant amount of aluminum. The aluminum concentration of the Test #1 solution was as high as 350 mg/L. However, the aluminum in the Test #3 solution occurred only in trace amounts.

3.7 Corrosion Products

Powder samples were collected from five different locations in the tank on Day 30. These samples included (1) fine powders on a piece of the submerged chlorinated polyvinyl chloride [CPVC] rack, (2) corrosion products on a submerged galvanized steel coupon, (3) corrosion products on a submerged copper coupon, (4) corrosion products on a submerged aluminum coupon, and (5) corrosion products on the submerged concrete coupon.

These corrosion products were collected by directly adhering onto double-sided carbon tape for probe SEM/EDS examination. After the samples were dried in air, Au/Pd coating was applied to enhance the surface conductivity for SEM examination. ESEM and SEM/EDS results indicated that the fine powders collected from the submerged CPVC rack are composed mainly of O, Ca, and P, which make up 95% of the composition of the powder. Therefore, the powders are likely Ca₃(PO₄)₂, which precipitated out of the testing solution and became sediment on the submerged rack. The corrosion products collected from the submerged galvanized steel coupon are composed mainly of O, Zn, Si, and Ca. The possible substances are silicate compounds of Zn and Ca. The corrosion products on the surface of the submerged copper coupon are rich in O, Ca, P, and Si. Therefore, they are likely phosphate and silicate compounds of Ca. The corrosion products on the surface of the submerged aluminum coupon are composed mainly of O, Si, Al, Ca, and B. As a result, the possible substances include silicate and boric compounds of Al and Ca. The corrosion/reaction products on the submerged concrete coupon are rich in Ca, O, P, and Si. So, they are likely phosphate and silicate compounds of Ca.

It should be noted that the corrosion/reaction products analysis is not exactly the same as the coupon surface examination because the corrosion/reaction products reflect just the substances on the very top surface of the coupons, while coupon examination gives more details of the compounds on the subsurface and on the coupon itself (see Subsection 3.4).

Appendix D contains the ESEM and SEM/EDS data for the corrosion products.

3.8 Gel Analysis

3.8.1 Visual Description

In ICET Test #3, one significant phenomenon is the presence of white gel-like precipitates in the test solution, especially during and after the injection of TSP on the first day of the test. When Test #3 was shut down, deposits of the pinkish-white gel-like precipitates were observed on the top of the birdcage and on other objects on the tank's bottom. Figures 3-118 and 3-119 show the gel-like precipitates.



Figure 3-118. Gel-like material covering stainless steel mesh on the bottom of the test tank.



Figure 3-119. Gel-like material recovered from the bottom of the test tank.

3.8.2 ESEM and SEM/EDS Analyses

ESEM/SEM/EDS and XRD/XRF analyses were used to characterize the white gel-like precipitates. EDS results show that 92% of the gel-like precipitate is composed of Ca, O, and P. Consistently, XRF results indicate that the gel-like precipitates contain significant amounts of Ca and P. Therefore, it is likely that the white gel-like precipitate is $\text{Ca}_3(\text{PO}_4)_2$. In addition, EDS and XRF results also indicate that the gel-like precipitates have a small amount of C, which is possibly from carbonate (CO_3^{2-}) and/or organic carbon from the testing solution.

Based on the XRD results, the white gel-like precipitates contained crystalline substances of sodium calcium hydrogen carbonate phosphate hydrate ($\text{Ca}_8\text{H}_2(\text{PO}_4)_6 \cdot \text{H}_2\text{O} \cdot \text{NaHCO}_3 \cdot \text{H}_2\text{O}$) and lithium calcium hydrogen carbonate phosphate hydrate ($\text{Ca}_8\text{H}_2(\text{PO}_4)_6 \cdot \text{H}_2\text{O} \cdot \text{Li}_2\text{CO}_3 \cdot \text{H}_2\text{O}$). It should be noted that XRD can detect only crystalline substances. If the formed $\text{Ca}_3(\text{PO}_4)_2$ is amorphous, it cannot be reflected by XRD results.

In Test #3, significant amounts of the white gel-like precipitates were deposited on the top of the birdcage. EDS analysis was performed to compare the white gel-like precipitates on the bottom of the tank with the particulate deposits on exterior fiberglass samples taken from the birdcage. That analysis shows that their compositions are not exactly the same. The gel-like precipitates from the bottom of the tank contain higher amounts of P and lower amounts of Si than do the particulate deposits on samples from the birdcage exterior. This result suggests that some cal-sil debris were deposited on the

birdcage exterior in addition to the white gel-like precipitates. As with any SEM sample, the gel-like precipitates were dried prior to analyses. Because they were a thick slurry and a mostly solid sample, the drying process is unlikely to affect the major solid composition of the sample. Other precipitates with high P content have chemical similarity with the dried gel-like precipitates.

Figures 3-120 through 3-126, Table 3-7, and Table 3-8 provide SEM/ESEM/EDS and XRD/XRF analysis results. The complete set of Day 30 gel analyses is contained in Appendix G.

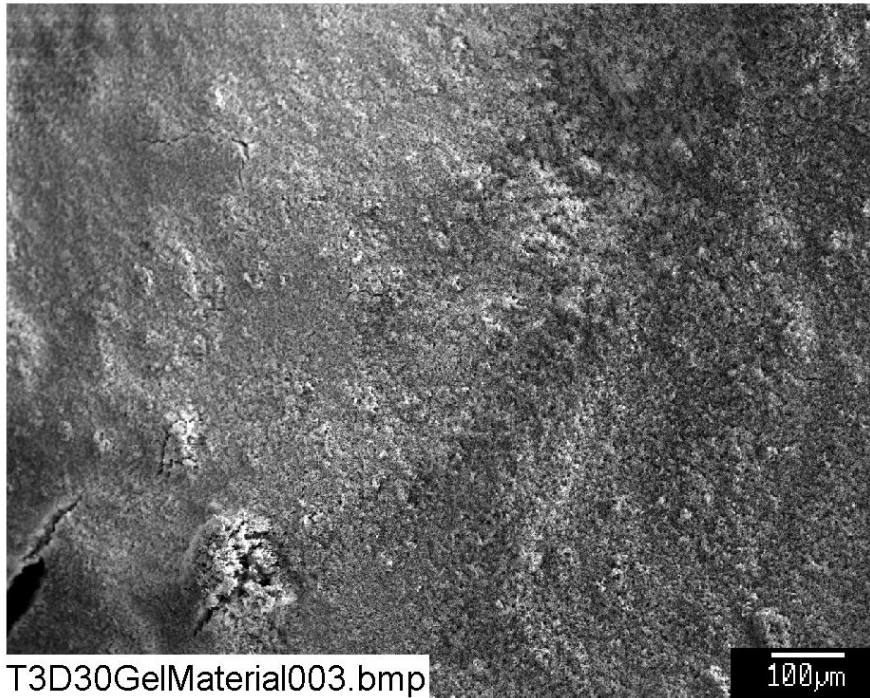


Figure 3-120. SEM image of a Test #3 Day 30 white gel-like material from the top of the birdcage, magnified 100 times. (T3D30GelMaterial003, 5/9/05)

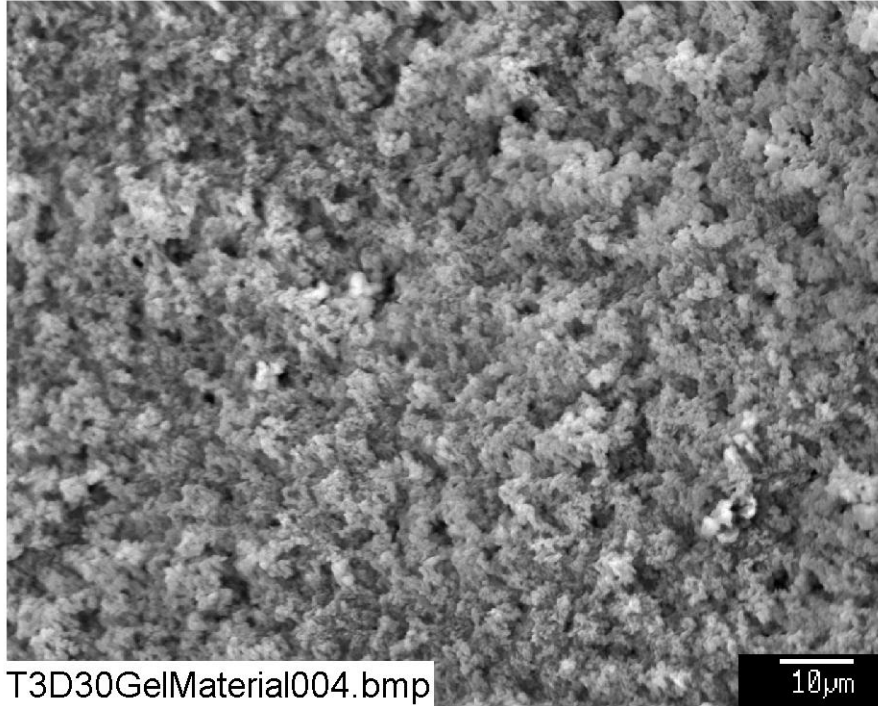


Figure 3-121. SEM image of a Test #3 Day 30 white gel-like material from the top of the birdcage, magnified 1000 times. (T3D30GelMaterial004, 5/9/05)

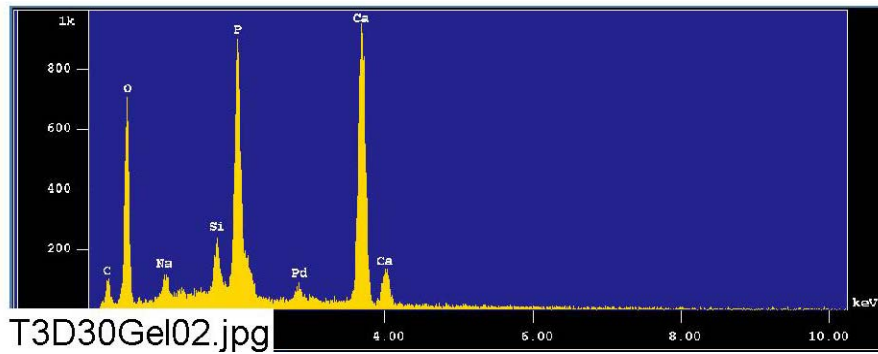


Figure 3-122. EDS counting spectrum for the white, gel-like material (whole image) shown in Figure 3-121. (T3D30Gel02, 5/9/05)

The results from the chemical composition analysis for Figure 3-122 are given in Table 3-7.

Table 3-7. The Chemical Compositions for Figure 3-122

May 9

2005

```

Group       : NRC
Sample      : T3D30 ID# : 2
Comment     : GelMaterial
Condition   : Full Scale : 20KeV(10eV/ch,2Kch)
              Live Time  : 60.000 sec   Aperture #   : 1
              Acc. Volt   : 15.0 KV      Probe Current : 1.606E-09 A
              Stage Point : X=79.625 Y=59.260 Z=11.424
              Acq. Date   : Mon May 9 11:42:11 2005
    
```

Element	Mode	ROI (KeV)	K-ratio(%)	+/-	Net/Background
C K	Normal	0.09- 0.46	0.6057	0.0005	338 / 119
O K	Normal	0.25- 0.77	12.2043	0.0032	4587 / 68
Na K	Normal	0.81- 1.27	0.5675	0.0010	613 / 50
Si K	Normal	1.50- 2.05	0.9391	0.0005	1366 / 271
P K	Normal	1.75- 2.38	8.4975	0.0055	7628 / 107
Ca K	Normal	3.39- 4.30	17.1295	0.0038	12109 / 26

 Chi_square = 42.7915

Element	Mass%	Atomic%	ZAF	Z	A	F
C	4.355	7.8616	3.7318	1.0194	3.6611	0.9999
O	45.521	61.6928	1.9361	0.9721	1.9917	1.0000
Na	1.639	1.5456	1.4989	1.0256	1.4614	1.0000
Si	2.072	1.5994	1.1451	0.9756	1.1812	0.9937
P	13.776	9.6435	0.8415	1.1708	0.7203	0.9978
Ca	32.638	17.6571	0.9890	0.9947	0.9943	1.0000

 Total 100.000 100.0000
 Normalization factor = 1.9265
 total 100.000 100.0000
 Normalization factor = 2.1120

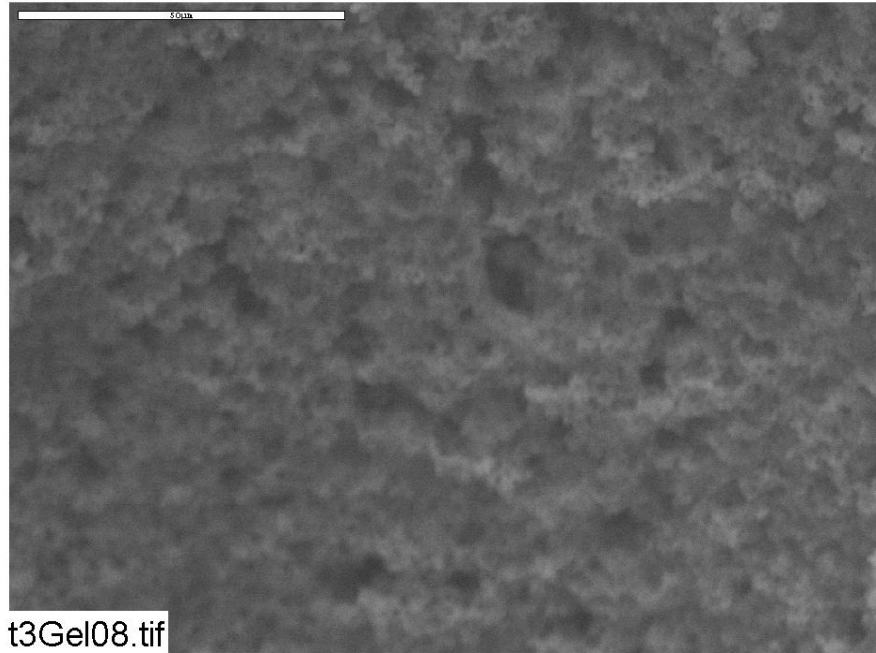


Figure 3-123. ESEM image of a Test #3 Day 30 white gel-like material from the top of the birdcage, magnified 1000 times. (t3Gel08, 5/6/05)

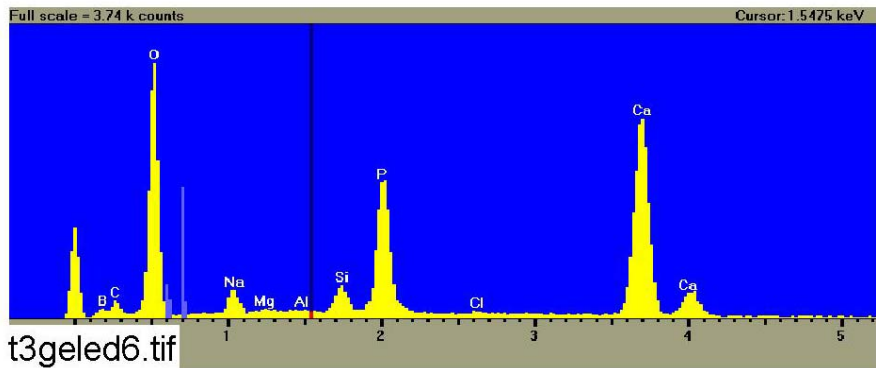


Figure 3-124. EDS counting spectrum for the white, gel-like material shown in Figure 3-123. (t3geled6, 5/6/05)

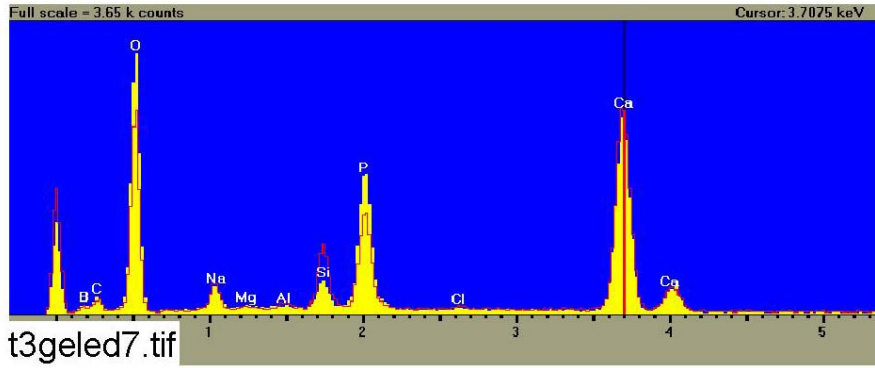


Figure 3-125. Comparison of EDS counting spectra for Figure 3-124 (yellow: the gel-like materials shown in figure 3-123) and Figure 3-73 (red: the large deposits taken from the birdcage exterior shown in Figure 3-72). (t3geled7, 5/6/05)

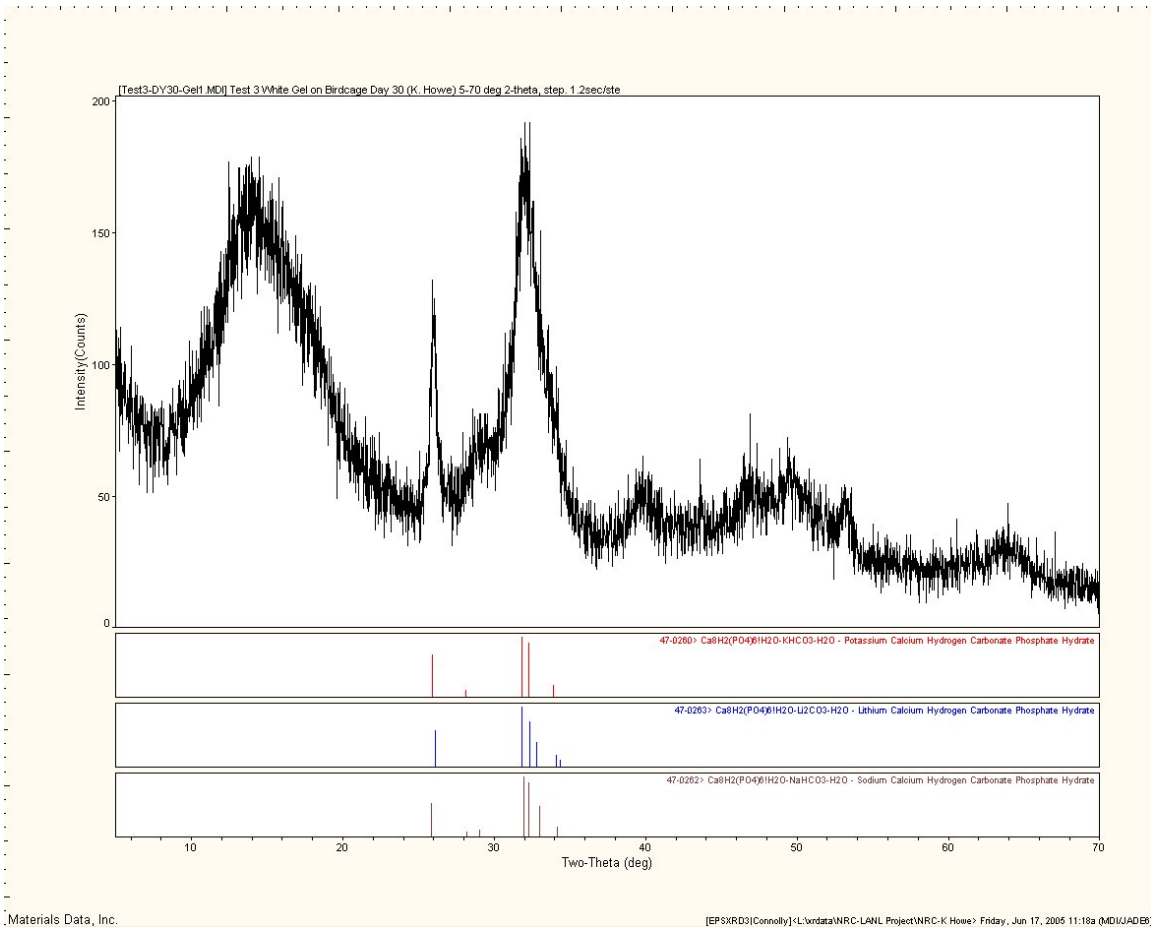


Figure 3-126. XRD results for a Test #3 Day 30 white, gel-like sample.

Table 3-8. Dry Mass Composition of a Test #3 Day-30 White Gel-like Sample by XRF Analysis

The first row is the chemical component; the second row is the mass composition (%).																	
SiO ₂	TiO ₂	Al ₂ O ₃	Fe ₂ O ₃	FeO	MnO	MgO	CaO	Na ₂ O	K ₂ O	H ₂ O(-)	H ₂ O(+)	CO ₂	P ₂ O ₅	Total	H ₂ O(+)	CO ₂	/DF (10) & Cover. To %
5.26	0.02	0.63	0.07	0.00	0.00	0.25	35.01	2.39	0.06	4.75	19.24		27.09	94.77			1.0196

4 SUMMARY OF KEY OBSERVATIONS

ICET Test #3 was conducted successfully, maintaining the critical physical and chemical parameters called out in the Test Plan. The test ran uninterrupted for 30 days. The solution chemistry behaved as expected, with the turbidity declining from its early values to steady numbers from Day 1 until the end of the test. TSS was relatively steady near its baseline value, with some increases during the test. The kinematic viscosity was steady for the entire test; and the pH was steady, averaging a value of 8.0.

Samples of the solution were taken daily. The chemical elements present were calcium, magnesium, silica, and sodium. Aluminum, copper, iron, zinc, and nickel were present in trace amounts. Strain-rate viscosity measurements indicated that the solution remained Newtonian throughout the test. No precipitates were observed in the solution, even after it had cooled to room temperature.

The submerged aluminum, IOZ-coated steel, copper, and uncoated steel coupons developed significant amounts of white particulate deposits. The aluminum coupons gained an average of 0.6 g, the IOZ-coated steel coupons 1.8 g, the copper 0.3 g, and the uncoated steel coupon lost 1.1 g. The submerged galvanized steel coupons were covered with a dense, gray particulate deposition, and they gained an average of 15.0 g.

The unsubmerged coupons exhibited light patterns of deposition, and they all experienced uniform weight gains. The aluminum coupons gained an average of 0.4 g, the galvanized steel 0.2 g, the copper 0.2 g, the IOZ-coated steel 2.0 g, and the uncoated steel 1.0 g.

Deposits on the fiberglass samples increased over time, and the deposits appeared to be chemically originated for the samples not lying on the tank bottom. These deposits covered individual fiberglass strands and in some cases formed webs between strands. Based on the SEM and ESEM results, the deposits likely originated from chemical precipitation during the sample-drying process. Comparing Days 4, 15, and 30 fiberglass samples showed deposits that were similar in property and amount. There was no significant difference in the amount of deposits found in the exterior and interior samples. Deposits found on the drain collar fiberglass were likely physically attached, and the exterior samples had significantly more deposits than the interior samples. Two different deposits were identified with EDS, one with a higher percentage of P and one with a higher percentage of Si. The former is likely calcium phosphate particles and the latter cal-sil particles. Deposits on and in the birdcage fiberglass similarly had the two different particulate deposits present. In addition, a pinkish-white gel-like precipitate covered the birdcage and much of the sediment. This gel had a consistency much like face cream, and it was composed primarily of Ca, O, and P, making it likely calcium phosphate.

Sediment on the tank bottom was prevalent, accumulating to depths of over 8 in. The sediment contained crystalline substances and calcite, making it primarily cal-sil, although some fugitive fiberglass was also present.

REFERENCES

1. "Test Plan: Characterization of Chemical and Corrosion Effects Potentially Occurring Inside a PWR Containment Following a LOCA, Rev. 12c," March 30, 2005.
2. J. Dallman, J. Garcia, B. Letellier, and K. Howe, "Integrated Chemical Effects Tests: Data Compilation for Test 1," LA-UR-05-0124, July 2005.
3. "Pre-Test Operations, Test #3," ICET-PI-012, Rev. 1, April 1, 2005.
4. "Test Operations, Test #3 (cal-sil and fiberglass, with TSP)," ICET-PI-014, Rev. 0, April 5, 2005.
5. "Post-Test Operations, Test #3," ICET-PI-008, Rev. 3, May 2, 2005.